Université de Montréal

The regulatory roles of APE1 and Prdx1 interaction

par

Zhiqiang Wang

Département de Microbiologie, Infectiologie et Immunologie
Faculté de Médecine

Thèse présentée à la Faculté des études supérieures
en vue de l'obtention du grade de Philosophiae Doctor (Ph.D)
en Microbiologie et Immunologie

July 2014

Résumé

L'apurinic/apyrimidic endonuclease 1 (APE1) est une protéine multifonctionnelle qui joue un rôle important dans la voie de réparation de l'ADN par excision de base. Elle sert également de coactivateur de transcription et est aussi impliquée dans le métabolisme de l'ARN et la régulation redox. APE1 peut cliver les sites AP ainsi que retirer des groupements, sur des extrémités 3' créées suite à des bris simple brin, qui bloquent les autres enzymes de réparation, permettant de poursuivre la réparation de l'ADN, puisqu'elle possède plusieurs activités de réparation de l'ADN comme une activité phosphodiestérase 3' et une activité exonucléase 3'→5'. Les cellules de mammifères ayant subi un knockdown d'APE1 présentent une grande sensibilité face à de nombreux agents génotoxiques. APE1 ne possède qu'une seule cystéine située au 65^{e} acide aminé. Celle-ci est nécessaire pour maintenir l'état de réduction de nombreux activateurs de transcription tels que p53, NF-κB, AP-1, c-Jun at c-Fos. Ainsi, elle se retrouve impliquée dans la régulation de l'expression génique. APE1 passe également à travers au moins 4 types de modifications post-traductionnelles : l'acétylation, la désacétylation, la phosphorylation et l'ubiquitylation. La façon dont APE1 est recrutée pour accomplir ses différentes fonctions biologiques demeure un mystère, bien que cela puisse être relié à sa capacité d'interaction avec de multiples partenaires différents. Sous des conditions de croissance normales, il a été démontré qu'APE1 interagit avec de nombreux partenaires impliqués dans de multiples fonctions. Nous émettons l'hypothèse que l'état d'oxydation d'APE1 est ce qui contrôle les partenaires avec lesquels la protéine interagira, lui permettant d'accomplir des fonctions précises. Dans cette étude nous démontrons que le peroxyde d'hydrogène altère le réseau d'interactions d'APE1. Un nouveau partenaire d'interaction d'APE1, Prdx1, un membre de la famille des peroxirédoxines responsable de récupérer le

peroxyde d'hydrogène, est caractérisé. Nous démontrons qu'un knockdown de Prdx1 n'affecte pas l'activité de réparation de l'ADN d'APE1, mais altère sa détection et sa distribution cellulaire à l'intérieur des cellules HepG2 conduisant à une induction accrue de l'interleukine 8 (IL-8). L'IL8 est une chimiokine impliquée dans le stress cellulaire en conditions physiologiques et en cas de stress oxydatif. Il a été démontré que l'induction de l'IL-8 est dépendante d'APE1 indiquant que Prdx1 pourrait réguler l'activité transcriptionnelle d'APE1.

Il a été découvert que Prdx1 est impliquée dans la régulation redox suite à une réponse initiée par le peroxyde d'hydrogène. Ce dernier possède un rôle important comme molécule de signalisation dans de nombreux processus biologiques. Nous montrons que Prdx1 est nécessaire pour réduire APE1 dans le cytoplasme en réponse à la présence de H_2O_2. En présence de Prdx1, la fraction d'APE1 présent dans le cytoplasme est réduite suite à une exposition au peroxyde d'hydrogène, et Prdx1 est hyperoxydé suite à l'interaction entre les deux molécules. Cela suggère que le signal, que produit le peroxyde d'hydrogène, sur APE1 passe par Prdx1. Un knockdown d'APE1 diminue la conversion de la forme dimérique de Prdx1 vers la forme monomérique. Cette observation implique qu'APE1 pourrait être impliquée dans la régulation de l'activité catalytique de Prdx1 en accélérant son hyperoxydation.

Mots-clés : APE1, Prdx1, IL-8, peroxyde d'hydrogène, signalisation cellulaire

Abstract

Apurinic/apyrimidinic endonuclease 1 (APE1) is a multifunctional protein, which play important roles in base excision repair (BER) pathway and serve as transcriptional co-activator. APE1 is also involved in RNA metabolism and redox regulation. APE1 can cleave abasic sites and process 3'-blocking termini into 3'-OH for DNA repair replication as it posseses several DNA repair activities including AP endonuclease, 3'-phosphodiesterase and 3' to 5'-exonuclease. Mammalian cells knockdown for APE1 are very sensitive to various DNA damaging agents. APE1 has a unique cysteine C65, which is required to maintain the reduced state of several transcriptional activators such as p53, NF-κB, AP-1, c-Jun, and c-Fos and therefore is involved in the regulation of gene expression. APE1 also undergoes at least four types of post-translational modifications that include acetylation, deacetylation, phosphorylation and ubiquitylation. How APE1 is being recruited to execute the various biological functions remains a challenge, although this could be directly related to its ability to interact with multiple different partners. Under normal growth conditions, APE1 has been shown to interact with a number of proteins that are involved in various functions. We propose that the oxidative state of APE1 governs its interacting partners thereby allowing the protein to perform specific functions. In this study we find that APE1 interactome alters in response to hydrogen peroxide. One novel APE1 interacting partner Prdx1, a member of the peroxiredoxin family that can scavenge hydrogen peroxide is characterized. We demonstrate that knockdown of Prdx1 did not impair APE1 DNA repair activity, but alters APE1 detection, and subcellular distribution in HepG2 cells leading to the induction of interleukin 8 (IL-8). IL-8 is a pro-inflammatory chemokine involved in cellular stress, under physiological and

oxidative stress conditions. It has been shown that the induction of IL-8 is dependent on APE1 indicating Prdx1 may regulate APE1 transcriptional activity.

Prdx1 has been discovered to be involved in the redox regulation of cell signaling initiated by hydrogen peroxide, which has important roles as a signaling molecule in the regulation of a variety of biological processes. Prdx1 exists as a dimer in the cells and we show that Prdx1 is required to reduce APE1 in the cytoplasm in response to H_2O_2. During this process, the dimeric form of Prdx1 is converted to the oxidized monomeric form. Interestingly, the H_2O_2-induced conversion of Prdx1 to the monomeric form is dependent upon the presence of APE1. These observations imply that there is a tight regulatory network existing between APE1 and Prdx1.

Keywords: APE1, Prdx1, IL-8, hydrogen peroxide, cell signaling

Table of contents

List of tables

.

List of figures

List of Abbreviations:

AP site	Apurinic/apyrimidinic site
AP-1	Activating Protein-1
APE1	Apurinic/ apyrimidinic endonuclease 1
ATR	Ataxia telangiectasia and Rad3-related
ATM	Ataxia telangiectasia mutated
BER	Base excision repair
CdKs	Cyclin-dependent kinases
CKI and CKII	Casein kinase I and II
CSR	Class switch recombination
CS	Cockayne syndrome
DNA	Deoxyribonucleic acid
DDR	DNA damage response
DSB	Double strand breaks
DNA-PKcs	DNA-dependent kinase catalytic subunit

DR	direct repair
dRP	Deoxyribophosphate
dRPase	Deoxyribophosphodiesterase
Egr-1	Early growth response protein-1
ERCC1	Excision repair cross-complementation group 1
ERCC4	Excision repair cross-complementation group 4
8-OHG	8-Hydroxyguanine
FEN1	Flap endonuclease I
H_2O_2	Hydrogenperoxide
HR	Homologous recombination
HIF-1	Hypoxia-inducible factor-1
HIF-1α	Hypoxia-inducible factor-1 alpha
hnRNPL	Heterogeneous ribonucleoprotein L
HADCs	Histone deacetylases
IL-8	Interleukin 8
IR	Ionizing radiation
Lys6	Lysine 2

Lys7	Lysine 7
mRNA	messenger ribonucleic acids
MMR	Mismatch repair
MLH1	MutL homolog 1
MMR	Mismatch repair
MMS	Methyl methane sulfonate
MPG	N-methylpurine DNA glycosylase
MYH	MutY glycosylase homolog
MRN	Mre11/Rad50/Nbs1
MSH2	MutS homolog 2
MSH3	MutS homolog 3
MSH6	MutS homolog 6
NADPH	Nicotinamide adenine dinucleotide phosphate
NHEJ	Non-homologous end joining
NER	Nucleotide excision repair
NEIL	Nei-like proteins
NF-κB	Nuclear factor kappa B

NTH	homolog of E. coli endonuclease III (nth)
nCaRE	Negative calcium responsive elements
NLS	Nuclear localization signal
NPM1	Nucleophosmin 1
MPG	Methyl- purine glycosylase
N^7-meG	N^7-methylguanine
OGG1	8-Oxoguanine glycosylase
PARP	poly (ADP-ribose) polymerase
Pax	Paired box-containing proteins
PCNA	Proliferating cell nuclear antigen
PKC	Protein kinase C
PTEN	Phosphatase and tensin homolog
PTH	Parathyroid hormone
PTM	Post-translational modification
Pol β	DNA polymerase beta
Pol δ	DNA polymerase delta
Pol ε	DNA polymerase epsilon

RFC	Replication factor C
ROS	Reactive oxygen species
RNS	Reactive nitrogen species
shRNAs	short hairpin RNA
SSB	Single strand breaks
SCAN1	Spinocerebellar ataxia with axonal neuropathy
ssDNA	single-strand DNA
TCR	Transcription-coupled repair
TDG	Thymine-DNA glycosylase
TFIIH	Transcription factor IIH
TNF-α	Tumor necrosis factor alpha
Trx	Thioredoxin
TrxR	Thioredoxin reductase
Tg	5, 6-dihydroxy-5, 6-dihydrothymine
UV	Ultraviolet
UDG	Uracil-DNA glycosylase
XP	Xeroderma pigmentosum

XPB	Xeroderma pigmentosum complementary group B protein
XPC	Xeroderma pigmentosum complementary group C protein
XPD	Xeroderma pigmentosum complementary group D protein
XPF1	Xeroderma pigmentosum complementary group F protein
XPG	Xerodermapigmentosum group G protein
XRCC1	X-ray repair complementing defective repair in Chinese hamster cells 1
XRCC4	X-ray repair complementing defective repair in Chinese hamster cells 4

DEDICATION

This thesis is dedicated to my parents, who sacrificed a lot for me and never stopped offering me their selfless love throughout my life, and their relentless support throughout the course of my studies and until now. From great distance, their patience, assistance and support throughout all these years have made this thesis possible.

Acknowledgments

It is my pleasure to take this great opportunity to thank all those who made this work possible. Firstly I owe a big debt of gratitude to my supervisor, Dr. Dindial Ramotar, for his trust in me and giving me an opportunity to pursue my Ph.D. study in his laboratory. His constant guidance, great patience, humour and sincere advices always impressed me. His enthusiasm, dedication to sciences inspired me in exploring the scientific black hole. I would like to thank him for the time he invested in my training, in helping me with studentship applications, oral presentations and manuscript preparations. I have learnt a lot under his supervision.

Besides, special thanks go to Xiaoming Yang and Taramatti Harihar (Rad). They not only always tried to create humorous and comfortable climates for our lab, but also helped us preparing experiments. I am deeply grateful to them for their technical support, encouragements and for their enthusiastic discussions about science, life and religions.

I would like to greatly acknowledge the financial support from University of Montreal and also China Scholarship Council.

I felt happy to work with so many colleagues who I think of as good friends and good scientists: Sammy Ayachi, Ousmane Male, Abdelghani Mazouzi, Saalman Hasgarally, Emil Andreev and Nicolas Brosseau: thank you all for your helpful advices, efforts, and constructive comments on my presentations and for your friendship.

I would like to sincerely thank Dr. El Bachir Affar, for his valuable help and advices and his important support throughout my studies and research work. I also give great thanks to his team including Helen Yu, Helen Pak, Salima Daou and Diana Adjaoud for their help.

I would like to thank everyone from Maisonneuve Rosemont Hospital research center including Dr. Janos G. Filep, Dr.Elliot Drobetsky, Dr Éric Milot, and Dr. Hugo Wurtele along with their lab teams, for their kind help and support in any way possible.

I also want to say thanks to my jury members for your critical comment and advices on my work.

Last but not least, I would like to thank my family especially my parents and my wife. They always give me their generous love, care, encouragements and supports.

1. General Introduction

1.1 ROS and antioxidants

Reactive oxygen species (ROS) and reactive nitrogen species (RNS) represent the most abundant free radicals in living organisms. Free radicals are highly reactive molecules with one or more unpaired electrons. ROS includes many forms of oxygen radicals such as hydroxyl radical ($^{\bullet}OH$), peroxyl ($RO_2^{\bullet}$), superoxide radical ($O_2^{\bullet}$), singlet oxygen (O_2) and alkoxyl ($RO^{\bullet}$) and certain nonradicals such as ozone (O_3), hypochlorous acid (HOCl), peroxynitrite ($ONOO^{-}$), and hydrogen peroxide (H_2O_2), but these can be easily converted into radicals. RNS also is consisted of various molecules, for example, nitric oxide radical ($NO^{\bullet}$), peroxynitrite (ONOO−), nitrogen dioxide radical ($NO_2^{\bullet}$), other derivatives from the reactions between $NO^{\bullet}$ and ROS ($O_2^{\bullet}$, $RO^{\bullet}$ and $RO_2^{\bullet}$) (1). Besides unusual circumstances such as high energy exposure (ionising radiation, ultraviolet light) and toxic chemicals exposure, in vivo free radicals are generated generally via enzymatically mediated or non-enzymatically mediated electron transfer reactions. Cellular superoxide generation can occur in several different subcellular compartmentalization including mitochondria, endoplasmic reticulum, lysosomes, microsomes and peroxysomes. Under physiological circumstances the majority of free radicals are from the electron leakage in electron transport chains to molecular oxygen, which produces superoxide, in the mitochondria and endoplasmic reticulum (2). Hydroxyl radicals are highly reactive with a half-life of less than 1 ns in aqueous solution. So once produced in vivo they react locally and immediately. They can be generated in different ways. Ionizing radiation triggers the decomposition of H_2O, leading to formation of •OH and hydrogen atoms. Photolytic decomposition of alkylhydroperoxides also can produce •OH.

Hydroxyl radicals generated *in vivo* mostly arise from the metal catalyzed breakup of hydrogen peroxide (2). For instance, the Fenton reaction also can decompose hydrogen peroxide in Fe^{2+}-dependent manner (3). Activated NAD(P)H oxidase can take NAD(P)H from the cytoplasm and transfer electrons to O_2 to generate superoxide on the inner and outer surface of the plasma membrane through the reaction: $2O^2 + NAD(P)H \rightarrow 2O_2^{\bullet -} + NADP^+ + H^+$ (4, 5). Peroxyl radical (ROO•) production is prevalent as well in every facets of life as high-energy species, which can be generated chemically, physically or enzymatically by various ways, with a reduction potential from +0.77 to +1.44 V, depending on the R group (6). Nitric oxide, a gaseous radical produced by macrophages, reacts with superoxide to form peroxynitrite (7).

While cells produce diverse ROS, there are antioxidant systems to defend cells from deleterious effects caused by ROS. These antioxidants belong to two classes: one contains several organic substances comprising vitamins C, E and A (β-carotene derivatives), selenium (a mineral), and carotenoids (CAR) (7-9); the other class consists of enzymes that include superoxide dismutase (SOD), catalase, glutathione peroxidase, thioredoxin, peroxiredoxin (10-13). The former class can directly or indirectly donate protons to ROS to convert them into less reactive species; the latter can scavenge ROS by catalyzing the reactions relevant to ROS and pro-oxidants to nontoxic substances to mitigate the elevation of ROS. It has been recently reported that noncanonical antioxidants such as 17-beta-estradiol and vitamin K also can prevent neuronal death induced by ROS (14, 15). Sulfiredoxin can reduce cysteine-sulfinic acid as a specific phosphotransferase and a thioltransferase that formed in the peroxiredoxins PRDX1, PRDX2, PRDX3 and PRDX4 upon exposure to oxidants, but not in the case of PRDX5 or PRDX6 (16). Sulfiredoxin contributes to antioxidation because it can

catalyze the reduction in a multi-step process via the reaction: Peroxiredoxin-(S-hydroxy-S-oxocysteine) + ATP+2R-SH=peroxiredoxin-(S-hydroxycysteine)+ADP+ phosphate + R-S-S-R (16-18).

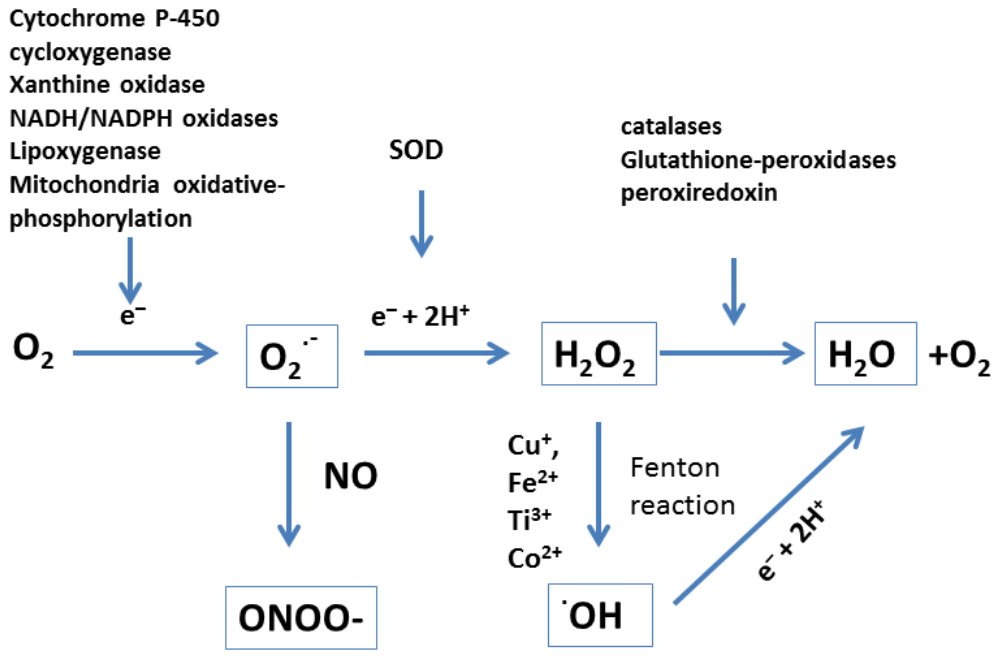

Figure 1 Endogenous sources of reactive oxygen species (ROS) [modified from (19)]

Overall, no matter what efforts antioxidants and reductases do to control ROS production, ROS production seems to be an inevitable event of life because they are natural concomitant products of metabolite while they are also deleterious mediators of cellular stress response at the same time. It is noteworthy that ROS also serve as second messengers to trigger and/or regulate important cellular signaling pathways (20). If we assume ROS as

"fires" in the cells and antioxidation system as "firefighters", these "firefighters" are unfortunately never able to extinguish these "fires", what they can do is just to keep the fires at manageable level.

1.1.1 Peroxiredoxin 1 and its functions

Peroxiredoxins (Prdxs) are a family of peroxidases with a small (22–27 kDa) molecular weight. six isoforms are found in mammalian. They all can catalyze peroxide reduction of H_2O_2, and peroxynitrite. Peroxiredoxin1 (Prdx1) is a typical 2-cysteine peroxiredoxin . As a peroxidase, Prdx1 N-terminal Cys^{52} is oxidized by H_2O_2 to cysteine-sulfenic acid (Cys^{52}-SOH) and reacts with Cys^{173}-SH of the other molecule to produce an intermolecular disulfide (head to tail dimer). Given the fact that thiol (Cys–SH) group, even at a neutral pH, to the thiolate anion ($Cys–S^-$), which is more readily oxidized to sulfenic acid (Cys–SOH) than is Cys–SH, so Prdx1 is a compulsory dimer in vivo (21, 22). Prdx1 dimer can only be reduced by thioredoxin (Trx), but not by GSH or glutaredoxin. Thus, the reducing equivalents stem from NADPH via thioredoxin reductase (TrxR) and Trx (11). Nevertheless, more and more studies show Prdx1 is more than just a peroxidase. Myc boxII is critically important for transformation and transcriptional activity. Prdx1binds to Myc boxII and causes a broad but selective loss of c-Myc target gene regulation (23) and the inhibitory effect of Prdx1 on Myc was highlighted by the evidence that c-Myc activates in $Prdx1^{-/-}$MEFs (24). Prdx1 is also shown to interact with the androgen receptor (AR), enhancing its transactivation independent of Prdx1 peroxidase activity (25). Prdx1 associates with nuclear factor NF-κB and both proteins are bound together to the cyclooxygenase (COX)-2 upstream promoter region in ER- but not in ER+ breast cancer cells via its chaperon function (26). All these suggest Prdx1 could regulate gene expression by interacting with transcription factors regardless of its

peroxidase activity. In addition Prdx1 can bind to DNA and RNA (27), its implication to maintain genomic stability were supported by the observations that Prdx1 deficiency brings more inclination to cancer (28) and human Prdx1 can prevent genomic instability in its orthologue Tsa1 depleted *Saccharomyces cerevisiae* (29).

1.2 DNA integrity is very important

Genomic deoxyribonucleic acid (DNA) is the genetic material that carries the information needed to constitute all the components of a living cell. Generally, genetic information can transfer to messenger ribonucleic acids (mRNA) by transcription and subsequently produce proteins. Given the diversity of protein function, one important event is the coordination of many proteins to verify the genome by checkpoint mechanisms to guarantee DNA replication fidelity before mitosis. So maintenance of genomic integrity is the essential and pivotal event for cells.

1.3 DNA damage

The cellular genome is always confronted with many kinds of insults from endogenous as well as exogenous sources, such as reactive free radical species, ultraviolet (UV), ionizing radiation (IR), and chemical DNA-damaging agents. These insults could cause various DNA lesions on the sugar backbone or bases of DNA directly or indirectly. These lesions include DNA double strand breaks (DSB), single strand breaks (SSB), apurinic/apyrimidinic (AP) sites, also called abasic sites, and damages to bases including oxidation, alkylation and deamination products.

1.3.1 DNA Base Damages

Base damages are referred to a large collection of damages occurring to the bases of DNA (Fig.2), e.g. 8-oxoguanine, O^6-methylguanine, thymine glycols, and other oxidized,

alkylated, deaminated or fragmented bases in DNA. Most damages are oxidation, methylation, depurination and deamination of the base. These damages can be generated by reactive oxygen/nitrogen species or by ionizing radiation. RNS such as nitric oxide radicals ($NO^{\bullet}$), peroxynitrite (ONOO−), nitrogen dioxide radicals ($NO_2^{\bullet}$), N_2O_3 and HNO_2, are potential mutagenic agents reacting with the bases of DNA and lead to nitrosation, nitration, and deamination of DNA bases (30). DNA cytosine methylation also accounts for the regulation of gene expression and carcinogenesis (31-33). ROS often convert guanine to 8-hydroxyguanine (34) and are also able to affect the enzyme-catalysed methylation of adjacent cytosines (33), thus suggesting a possible link between methylation profile and oxidative DNA damage.

ROS (ONOO−, •OH, O_2•, RO• and RO_2•) can cause many kinds of DNA base damages in different ways. •OH is exquisitely toxic and reactive. The high reactivity of •OH often randomly abstracts carbon-bound hydrogen atoms, e.g. from the sugar moeity. •OH reacts with guanine and generates 8-oxo-7, 8-dihydro-2-deoxyguanosine (8-oxo-dG) and 2, 6-diamino-5-formamido-4-hydroxypyrimidine (FAPy-G) (35, 36). Adenine likewise reacts with •OH, although this reaction occurs rarely in DNA damage (37). In cooperation with the Fe(III) or Fe(III)–EDTA complex, endogenous reductants such as ascorbate, GSH, NADH, can make damages on all types of nucleotides with a slight preference for guanine (38). Specifically, NADH reacts with Fe (III)–EDTA and H_2O_2 to generate •OH by which guanine is oxidized to 8-oxo-dG (39). Contrary to high reactivity of hydroxyl radicals, H_2O_2 cannot react with the bases of DNA at all (40, 41). 8-hydroxyguanine (8-OHG) is the most frequent DNA base lesion, therefore it is measured as a “biomarker” for oxidative DNA damage and even some

diseases including cancer and aging that can be performed using patients' DNA and urine by High Performance Liquid Chromatography (HPLC)-Tandem Mass Spectrometry (37, 42-44).

As one of the powerful agents ultraviolet radiation (UVR) (mainly UV-B:280–315 nm) also gives rise to a variety of mutagenic and cytotoxic DNA base lesions such as cyclobutane-pyrimidine dimers (CPDs), 6-4 pyrimidine pyrimidone photoproducts (6-4PPs), and their Dewar valence isomers (Figure 3) (45-50).

Chemically-induced base adducts are either large polycyclic hydrocarbons, bulky adducts or simple alkyl adducts induced by alkylating agents. Chemotherapeutic drugs, including cisplatin, nitrogen mustard, mitomycin C, psoralen, and adriamycin, can form base adducts, and the challenge for chemotherapy is to discover drugs that can damage DNA but cannot provoke DNA repair or checkpoint responses in tumor cells.

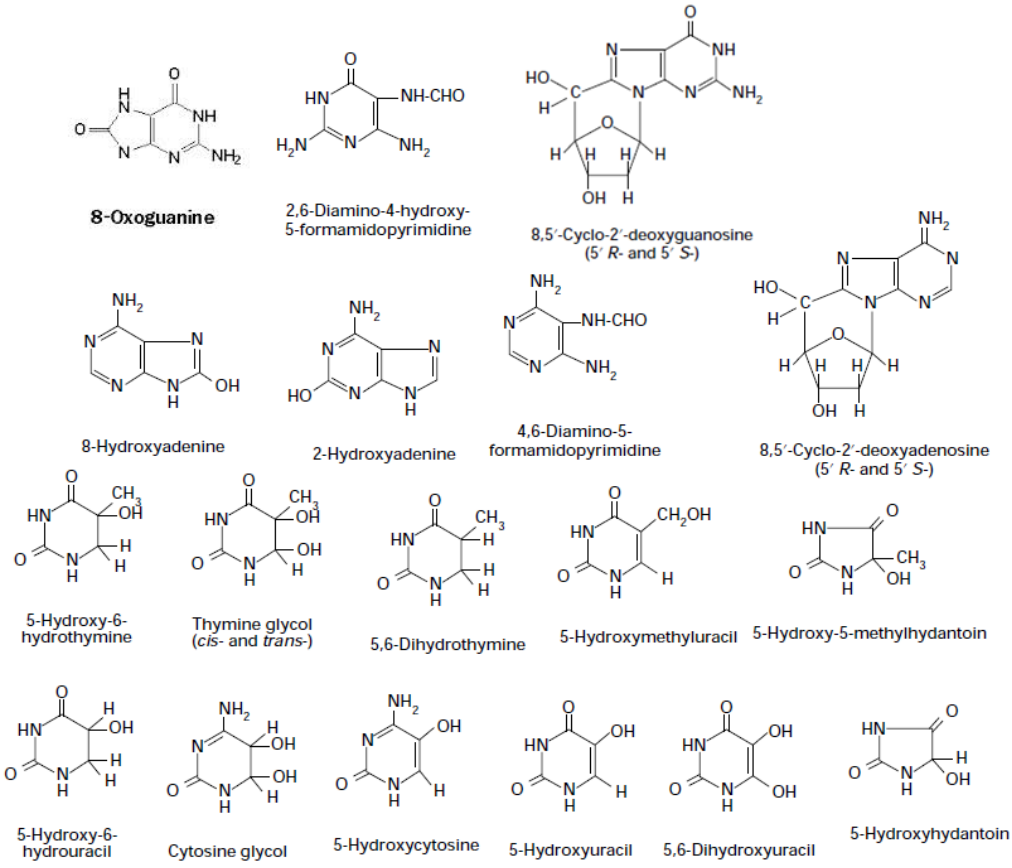

Figure 2 The structures of the products of ROS attack on DNA [modified from (51)]

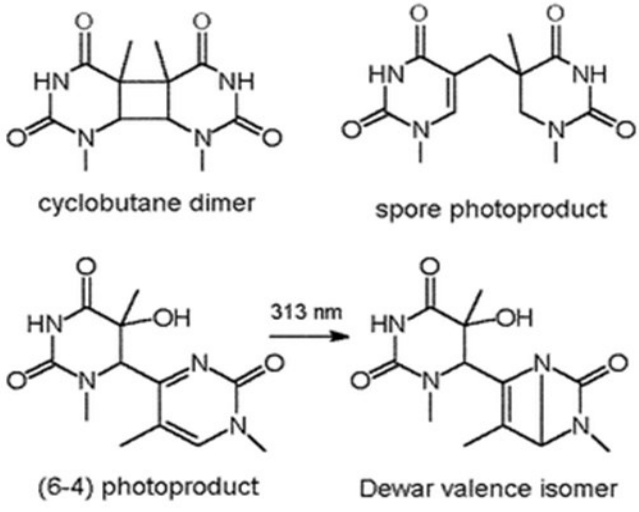

Figure 3 Base damages induced by UV adapted from (48)

1.3.2 AP sites

AP sites (apurinic/apyrimidinic site) also called abasic sites are locations without a purine or a pyrimidine base in DNA/RNA. Normally the bases are attached to the sugar backbone of DNA/RNA by N-glycosylic bonds. Compared to the phosphodiester bonds, N-glycosylic bonds appear to be more labile. AP sites can be created by spontaneous depurination and hydrolysis of the N-glycosylic bond. In addition, AP sites also exist as intermediates during base excision repair processing. Damaged DNA bases such as *N*7-methylguanine (*N*7-meG), 8-oxo-7,8-dihydroguanine(8-oxoG), 5,6-dihydroxy-5,6-dihydrothymine (Tg) and inappropriate bases such as uracil incorporated in DNA after replication or repair can be removed by specific DNA *N*-glycosylases leaving AP sites. It has been estimated that more than 10,000 bases turn over per mammalian cell every day, and if these lesions are not repaired they can generate mutations which over time can accumulate and inactivate the function of any gene (52, 53).

1.3.3 DNA Backbone Damages

Backbone damages here are referred to the "nick" occurring on sugar-phosphate backbone including single- and double-strand DNA breaks. ROS actually not only damage the bases of DNA, but also damage the sugar backbone of DNA, which usually leaves a fragment of the sugar at break sites such as 3`-phosphoglycolate. These lesions are well documented to be produced by ionizing radiation as well as by chemotherapeutic drugs such as bleomycin (54). In addition, ROS can also produce double-strand breaks and these are highly toxic lesions as they can lead to gene deletion, insertion and rearrangement in the genome. However, there are normal double strand breaks that occur in the cells and these are important

intermediates to promote meiosis, mating type switching (in yeast), V(D)J and immunoglobulin class switch recombination (CSR) (55, 56).

1.3.4 Cross-links DNA damage

Crosslinking of DNA includes intrastrand crosslinks, interstrand crosslinks and DNA-protein crosslinks. They occur either exogenously or endogenously. Actually most chemicals bring in several kinds of DNA damages through different mechanisms. For example, these agents including cisplatin, nitrogen mustard, mitomycin D, and psoralen not only damage DNA via ROS production, but also form interstrand/intrastrand cross-links and even DNA-protein cross-links. The reaction of the aldehyde form of abasic sites with proteins may also create DNA-protein cross-links (57). DNA replication is stalled by crosslinks, which can result in replication arrest and cell death if the crosslink is not repaired.

1.4 Consequences of DNA damages and diseases

It is widely speculated that DNA damages can cause cancers, neurodegeneration and even hereditary genetic diseases such as Ataxia-oculomotor apraxia 1 and Spinocerebellar ataxia with axonal neuropathy 1 (SCAN1) (1, 58-60). So DNA damages can affect many aspects of cell which may result in more than one consequences (Figure 4).

Once there are DNA damages and they are not repaired, the DNA replication fork usually stalls in order to give time to sense and repair the damages. If DNA polymerase bypass a modified base or an AP site, this often leads to the misincorporation of bases (61-63), although DNA polymerases have proofreading activity (64). For example, 8-oxoguanine can mismatch with adenine during replication, which finally could result in G: C to T: A transversion mutations. Sometimes abasic lesions can cause frameshifts, which can change the coding sequence of proteins (65, 66). DNA lesions impair transcription too. RNA polymerase

stops at the lesion site once DNA lesions occur in the transcribed strand, which creates a target for proteins that can bind to RNA polymerase in RNA elongation. This can trigger DNA damage response (DDR) (67). DNA damage response is a cascade of signal transduction pathways triggered by DNA damages and replication stress, which is a conserved and multifaceted sensory network aiming mainly at DNA repair and the facilitation of DNA replication. DDR can spare time for DNA repair by controlling cell cycle progression (68). These DDR are controlled by two pathways involving the ataxia telangiectasia and Rad3-related (ATR) and Ataxia telangiectasia mutated (ATM) kinases (69).

In mammalian cells, DNA damage activates p53 through ATM, which then either causes cell cycle arrest by the induction of a major inhibitor of the Cyclin-dependent kinases (CdKs) p21, or promotes apoptosis (70). Moreover, Chk1 and Chk2, the two serine/threonine kinases can relay signalling from ATR/ATM to downstream proteins including Cdc25 by phosphorylation in response to DNA damage. The activation of Chk1 and Chk2 inhibits a dual specificity phosphatase, Cdc25, which ensures the arrest of the cell cycle in response to DNA damage (71). Chk1 is the primary effector of normal S phase and the intra-S phase DNA damage checkpoint as well as G2/M checkpoint in response to ionizing radiation while Chk2 plays a major role in the S phase checkpoint (72). While Claspin is critical for turning on the cellular response to DNA damage and replication stress, Claspin degradation turns off the checkpoint response through the ubiquitin proteasome pathway in ATR-Claspin-Chk1 pathway (73, 74)

Figure 4 DNA damages cause many consequences

1.5 DNA repair mechanisms

As previously mentioned, the maintenance of genomic integrity and fidelity is vital for normal cell life. DNA damages or lesions can cause many consequences, for instances, cell arrest, collapsed DNA replication/transcription, tumorigenesis or apoptosis. So once DNA damages happen, cells use several ways to repair DNA lesions thereby to maintain genomic integrity and fidelity. The following DNA repair mechanisms exist: homologous recombination (HR), non-homologous end joining repair (NHEJ), mismatch repair (MMR), nucleotide excision repair (NER) and base excision repair (BER). Actually each repair mechanism is a multi-step process from DNA lesion recognition to the disassembly of repair machinery involving in many proteins (Table1).

Table 1 The key genes of DNA damage repair pathways

DNA repair mechanism	proteins
Mismatch repair (MMR)	EXO1, HMBG1, LIG1, MLH1, MLH3, MSH2, MSH3, MSH6, PCNA, PMS1, PMS2, POLd, RFC, RPA
Homologous repair (HR)	ATM, ATR, BLM, BRCA1, EME1, EXO1 FANCD/BRCA2, FANCF, FANCM, FANCN, GEN1, MRE11, NBS1, Rad50, Rad51, Rad52, Rad54, RecQ4, RPA, WRN, XRCC2, XRCC3
Nonhomologous end-joining (NHEJ)	ARTEMIS, ATM, ATR, DNA-PKcs, Ku70, Ku80, LIG4, POL4, XRCC4
Nucleotide excision repair (NER)	CEN2, CSA, CSB, CUL4A, DDB1, DDB2/XPE, ERCC1, ERCC4/XPF, HR23B,LIG1, LIG3, POL D/E, RPA, TFIIH, XPA, XPC, XPG, XRCC1
Base excision repair (BER)	APE1, APE2, APTX, DNA2, FEN1, LIG1,LIG3, MBD4, MPG, MUTYH, NEIL1, NEIL2, NEIL3, NTHL1, SMUG1, TDG, TDP1, UNG, XRCC1, NUDT1, OGG1, PARP1, PARP2, PNKP, POLB, POLG

1.5.1 Homologous recombination

As mentioned above, double-strand breaks are produced by reactive oxygen species, ionizing radiation, and chemicals that generate reactive oxygen species. In addition, double-strand breaks are resulted from V (D) J recombination, immunoglobulin class switching processes and meiosis. Double-strand breaks are repaired either by homologous recombination (HR) or nonhomologous end-joining (NHEJ) mechanisms (101–105) (56, 75).

Homologous recombination works in a stepwise manner: strand invasion, branch migration, and Holliday junction formation. Strand invasion and branch migration is initiated by RAD51 in eukaryotes (76). Once DSBs occur, phosphorylated ATM recruits RAD50/MRE11/NBS1 complex to the site, which has 5'–3' exonuclease activity and can process the 5'- termini to create a 3'-single strand tail for the subsequent strand invasion into homologous sequences of a sister chromatid (77). With the help of RPA, RAD51 forms a

nucleoprotein filament onto the single stranded DNA and which may be stimulated by RAD52. RAD51 can exchange the single strand DNA with the same sequence from a double-stranded DNA molecule with the aid of RAD54, a chromatin remodeling protein. Cohesins that facilitate proper positioning of the sister chromatids probably help in identifying a homologous sequence. After identification of the homologous sequence, DNA polymerases use the intact double-stranded DNA as a template to copy the sequence and then the joint molecule forming Holliday junctions which is resolved by the structure-specific endonucleases, resolvases (78, 79). The MUS81/MMS4 heterodimer also can resolve the Holliday junctions or their topologically equivalents (80, 81). Homologous recombination is an exquisitely cooperative process involving large numbers of proteins, including the BRCA1 and BRCA2 proteins. BRCA2 may directly or indirectly affect nuclear translocation of RAD51.

1.5.2 Non-homologous end joining repair (NHEJ)

Although homologous recombination is regarded as an efficient "error-free" repair mechanism for DSB, it may potentially lead to homozygosity for recessive mutations. In addition, it may sometimes be difficult to find homologous sequences in the complex genome, especially in G1 phase cells that only have homologous chromosomes. So non-homologous end joining repair (NHEJ) works as an alternative way to repair DSB too. In eukaryotes, the KU70/80 heterodimer loading to the two ends of a double-strand break is followed by the DNA-PKcs binding. Afterwards the DNA ligase4-XRCC4 heterodimer seals the double strand break, in some cases even if the two ends are from different chromosomes leading to a deleterious event (78, 79, 82, 83). End joining sometimes may gain or lose a few nucleotides when annealing is accompanied with internal microhomology alignment before sealing gaps

and thus leading to mutations. Although end joining does not require homologous sequences as template, homologous recombination (HR) and nonhomologous end-joining (NHEJ) mechanisms share the functions of the RAD50/MRE11/NBS1 complex (84).

1.5.3 Mismatch repair

Mismatch repair (MMR) is a highly conserved biological pathway from human MMR to prototypical *E. coli* MMR based on the similarities of substrate specificity, bidirectionality, and nick-directed strand specificity(85). Mammalian MMR evolved a large set of the *E. coli* MutS and MutL homologs. hMSH2/6 form heterodimers hMutSα that recognize mismatches and single-base loops whereas hMSH2/3 dimers (hMutSβ) distinguish insertion/deletion loops. hMutL-like proteins hMLH1/hPMS2(hMutLα) and hMLH1/hPMS1 (hMutLβ) heterodimeric complexes interact with MSH complexes and replication factors. The proximity of the replication machinery may discriminate the strand to be repaired. Numerous proteins including polδ/ε, RPA, PCNA, RFC, exonuclease 1, and endonuclease FEN1 are required to excise the new strand past the mismatch and resynthesize. MMR components also play roles in NER and recombination. Crystallographic studies have unveiled that a MutS dimer senses the structural instability of a heteroduplex by twisting the DNA at the mismatch site (86). However, similar DNA damage caused by alkylating agents and intercalators, may cause MutS to trigger erroneous or futile MMR. Intact MMR thus confers sensitivity, whereas tumours may become resistant to chemotherapy, therefore this presents a challenge to therapeutic strategies (87)

1.5.4 Nucleotide excision repair

Nucleotide excision repair (NER) is the main repair mechanism to remove bulky DNA lesions caused by UV-radiation or chemicals, or by protein conjugated to DNA. Global

genome NER (GG-NER) and transcription-coupled repair (TCR) consist of two NER subpathways. The two NER subpathways have partly different substrate specificities: the former removes distorting lesions in the whole genome, and the latter glanced through damages that result in RNA elongation stalling (67). A multisubunit enzyme complex known as "excision nuclease" can cleave the damaged strand on both sides of the lesion (88-90). Briefly, nucleotide excision repair is carried out using the following steps: (*a*) damage recognition, (*b*) removal of lesions by dual incisions bracketing the lesion to release a 24–32-nt oligomer containing the lesion in eukaryotes, (*d*) re-filling the resulting gap by DNA repair synthesis, and (*e*) ligation. In TCR, the blockage of RNA polymerase by the lesions seems to be a requirement to trigger TCR. At least two TCR-specific factors, CSB and CSA are needed to displace the stalled polymerase to expose the lesion. GG-NER and TCR may share the subsequent procedures(91). About 30 base pairs of DNA around the damage are unwound by the XPB and XPD helicases of the multi-subunit transcription factor TFIIH. XPA probably checks abnormal backbone structure again to further confirm the presence of injury, and aborts NER if damages are absent. The single-stranded-binding protein RPA (replication protein A) binds to the undamaged strands to stabilize the open intermediate. The endonuclease duo of the NER team, XPG and ERCC1/XPF, respectively cleave the damaged strand from 3' and 5' of the lesion to remove the lesion by generating a 24–32-base oligonucleotide gap containing the injury. DNA polymerase then synthesizes new DNA to fill the gap which is followed by DNA ligase to seal it and mark the completion of NER. At least 25 or more proteins are involved in NER. It seems that the NER machinery assembles in a step-wise fashion in *in vivo* studies. The entire complex disassembles again after finishing a single repair (which maybe takes a few minutes). NER is a predominant and essential DNA

repair mechanism, so NER deficiency can cause many diseases such as Xeroderma Pigmentosum (XP), cockayne syndrome (CS), trichothiodystrophy and photosensitivity (92).

1.5.5 Base excision repair

DNA glycosylase cleaves the damaged base to form an abasic (AP) site in DNA, which initiates base excision repair (Figure 5). Spontaneous AP sites can also be regarded as a direct damage product. There are various DNA glycosylases that recognize different base lesions respectively, for instances, uracil-DNA glycosylase (UDG) recognizes uracil, methyl- purine glycosylase (MPG) can recognize alkylated purines, 8-oxoguanine glycosylase (OGG1) recognizes 8-oxoG and FapyG. Some DNA glycosylases are monofunctional (e.g. UDG, MPG) that only catalyze the hydrolytic removal of the base so as to form an apurinic/ apyrimidinic (AP) site, whereas others (e.g. OGG, NTH, HNEL1-3) are bifunctional enzymes that not only cleave off the base but also catalyze a subsequent AP lyase reaction. The AP lyase reaction generates a 5'-phosphomonoester and a 3'-unsaturated sugar phosphate residue. After the lyase reaction, AP Endonuclease cleaves the 3'-sugar residue to create a 3'-OH end and form a gap that is filled by DNA polymerase, and the resulting nick is ligated. If the glycosylase has no lyase activity, the 5' incision of the AP site is initiated by APE1 in mammalian cells, then DNA polymerase β (DNA Polβ) fills in the 1-nucleotide gap and simultaneously removes the abasic sugar by its dRP lyase activity (93), which is followed by ligation with DNA ligase III in cooperation with XRCC1. This is so-called the short-patch base excision repair. In long-patch base excision repair, APE1 nicks the 5' phosphodiester bond to the AP site leaving a 3'-OH, and then DNA Pol δ/ε, PCNA, and replication factor C (RFC) work together to replace 2-10 nucleotides by DNA synthesis while the old oligomer forms a flap which will be removed by FEN1 endonuclease. The resulting nick is finally

ligated by DNA ligase1 (94, 95). Polβ can also participate in a long-patch base excision repair mechanism (96).

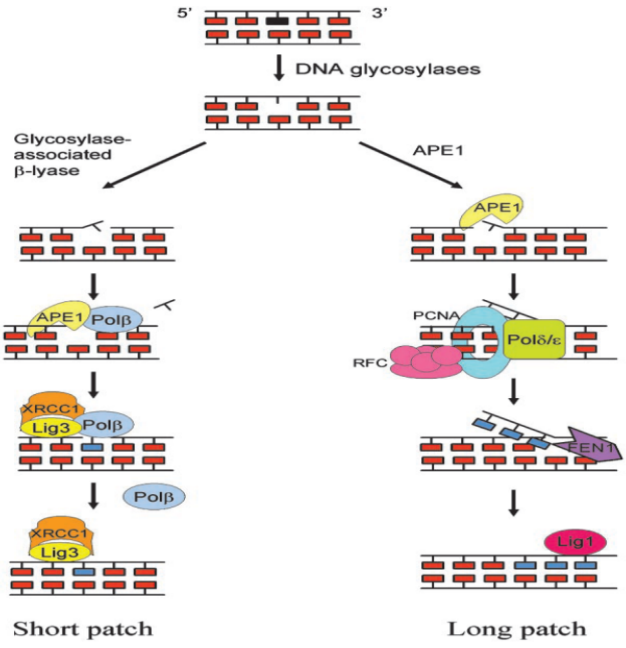

Figure 5 Base excision repair mechanisms in mammalian cells [modified from(97)]

1.6 APE1 and its functions

APE1/Ref-1 (also called APEX1, HAP1or Ref-1 and here referred to as APE1) was first cloned as a DNA repair enzyme in 1991 (98) and characterized as a redox protein in 1992 (99). Human APE1 has 318 amino acids and is consisted of three putative functionally isolated domains (Fig. 6): (1) N-terminus (33–35AA) involved in protein–protein interaction and the modulation of its RNA-binding activity (100) and catalytic activity on abasic DNA (101); the redox domain (35-127AA); and (3) the DNA repair domain (161-318AA). APE1 has been found to be a multifunctional protein that not only possesses both DNA repair and transcriptional regulatory activities, but also plays pleiotropic roles in the cellular response to

oxidative stress(102) (Fig. 6). Recently APE1 also has been proposed to be involved in RNA metabolism (100).

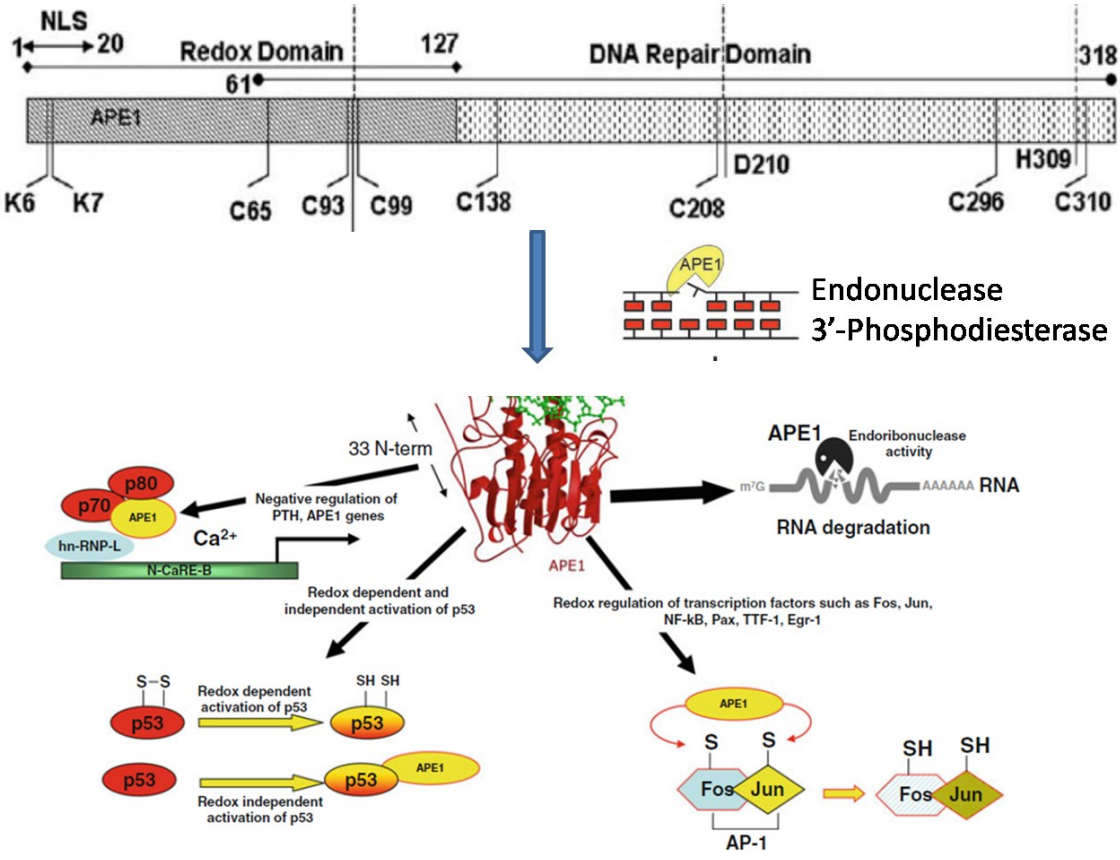

Figure 6 APE1 is a multifunctional protein[modified from (103)]

1.6.1 DNA repair activity of APE1

APE1 is the mammalian ortholog of *Escherichia coli* Xth (Exo III) which is a member of DNA repair enzymes family that consists of three bacterial AP endonucleases (ExoA protein of *Streptococcus pneumonias*, exonuclease III of *Escherichia coli* and Tte AP enzyme of *Thermoanaerobacter tengcongensis*), and Rrpl protein of *Drosophila melanogaster*. In living organisms from bacteria to humans, it has been found up to 100,000 spontaneous lesions/cell/day can occur, 10,000 of which are attributed to depurination and depyrimidination to form AP sites. Base excision repair (BER) is the pivotal DNA repair

pathway that can repair these AP sites (97, 104, 105). In mammalian BER, the AP endonuclease, APE1 can nick the 5'-phosphodiester bond of the AP site to generate a single DNA strand break resulting in 3'-hydroxyl and deoxy-ribose-5'-phosphate (5'-dRp) termini. In addition, APE1 also can generate a 3'-hydroxyl terminus in different situations: APE1 can remove 3'-phospho α, β-unsaturated aldehyde through its 3'-5'exonuclease activity after glycosylases or radiation made DNA strand breaks (106). APE1 can also eliminate a 3'-terminal phosphate through its 3' phosphatase activity that is left by glycosylases such as NEIL1 and NEIL2 (107). Therefore, APE1 is the key enzyme to process 3'-blocking groups into 3'-OH that is used as a primer for DNA synthesis during BER.

1.6.2 Redox-dependent transcriptional activator

As mentioned above, cells produce ROS via various ways either endogenously or exogenously. ROS production can change cellular and extracellular redox states, which have been shown to be involved in cellular signal changes. Proteins with cysteine residues, may act as redox sensitive switches, thereby triggering a variety of ROS mediated cellular signaling given that they possess reversible reactions between oxidation and reduction. Recently, there are more and more experimental evidence that suggests that redox states can regulate gene expression through direct modulation of transcription factor activity. To date, several transcription factors have been demonstrated as targets of redox regulation. APE1 has been found to stimulate the DNA binding activity of several transcription factors such as AP-1 (99), NF-κB (108), Myb (109), Egr-1 (110), p53 (111), hypoxia inducible factor-1 (HIF-1) (112) and Pax proteins (113). It is proposed that APE1 serves as redox dependent transcriptional coactivator through controlling the redox state of the critical cysteine residues that are located either in the DNA-binding domains or within regulatory regions of the transcription factor

itself. Cys65 of APE1 can reduce oxidized cysteines of transcription factors to maintain their reduced states thereby providing a redox-dependent gene regulation mechanism.

Recently it has been found that APE1 has a novel redox chaperone activity, which means APE1 may not only regulate various transcription factors by direct reduction but also by facilitating the third resultants (e.g. GSH and thioredoxin) to reduce transcription factors. The redox-chaperone activity seems to be carried out by direct interactions between APE1 and the target transcription factor, and require lower concentrations of APE1 as does its redox activity (114). In all, the redox and the redox-chaperone activities of APE1 seem very important, and probably protect the cell from the genotoxic insults due to increased ROS concentration. However, the exact mechanisms *in vivo* still remain elusive, particularly in response to a specific stimulus.

1.6.3 Transcriptional repressor activity of APE1

While APE1 can indirectly regulate gene expression by controlling the redox states of many other transcription factors, it can also bind to the negative calcium responsive elements such as nCaRE-A and nCaRE-B in the promoter of various genes including the human parathyroid hormone (PTH) gene, rennin. APE1 is a component of a trans-acting complex (115-117) formed by Ku70/80, heterogeneous ribonucleoprotein-L (hnRNPL) and p300 (118). So this can mitigate gene expression by negative feedback regulation.

1.6.4 APE1 is involved in RNA metabolism

Compared with its DNA repair activity and transcription activity, much less is known about its roles in RNA process. Actually as early as in 1995 Barzilay et al (119) discovered that APE1 has RNase H-activity specific to RNA-DNA hybrid although APE1 produces different products compared with exonuclease III. APE1 binds with relatively low affinity to

intact single- and double-stranded nucleic acid substrates (RNA and DNA) but does not exhibit general nuclease activity against them. In addition, it has been reported that APE1 also can cleave AP sites in single-stranded (ss) DNA at a rate approximately 20-fold less than that against AP sites in ds DNA, suggesting that APE1 plays roles in DNA N-glycosylase initiated BER in ssDNA perhaps during replication and/or transcription (103, 120). Moreover, APE1 was discovered to be able to cleave AP-site-containing single-stranded RNA *in vitro*, which implies APE1 can endonucleolytically destroy detrimental cellular AP-RNA molecules (121). Another evidence is that APE1 is competent to regulate c-myc mRNA turnover by endonucleolytic cleavage of the coding region determinant (CRD) of c-myc mRNA. The endoribonuclease activity may share the same active sites with the AP-DNA endonuclease activity based on the fact that E96A and H309N mutants of APE1 lose their endoribonuclease activity. It is known that RNA is more susceptible to ROS which explains why oxidized RNA molecules are present in huge amounts in brains from Alzheimer patients. Taken together, this supports the speculations that APE1 is presumably involved in RNA metabolism, RNA decay or RNA quality control pathways (122) although more studies are needed to understand this mechanism of action.

1.7 Modulation of APE1 different functions

APE1 has so many functions, which raises a question: How does it manage them? Three different mechanisms may switch on/off and fine-tune different APE1 activities: (1) increase in APE1's protein level after transcriptional activation; (2) translocation of APE1 from the cytoplasm to the nucleus; and (3) modulation of APE1 function by post-translational modification (PTM). To date, at least six different kinds of PTMs have been described for APE1 that occurred *in vivo*: acetylation (118, 123), phosphorylation (124, 125), ubiquitination

(126), S-nitrosation (127), proteolytic cleavage of the N-terminal 33 amino acids (128) and reversible reduction-oxidation. PTM can change APE1 activity distinctly. Lys6 and Lys7 of APE1 are acetylated by the transcriptional co-activator p300 and acetylated Lys6 and Lys7 enhance the binding of APE1 to nCaRE, thereby stabilize the loading of the APE1-HADCs complex on the PTH promoter (118). APE1 indeed can be phosphorylated by the serine/threonine casein kinases (CK) I and II and protein kinase C. Although phosphorylation by CKII completely abolished APE1 DNA repair activity, phosphorylation by CKI and protein kinase C (PKC) did not affect the ability of APE/Ref-1 to act at AP sites in DNA(124).

There is an increasing body of evidence to support that many proteins carry out their biological roles as a component of a complex rather than as a single isolated protein. So an effective way to understand the roles of one protein is unveiling the constituents of the protein complex. Therefore, along with PTMs, the interactome of APE1 could change according to a specific biological function. The whole picture about the interactome of APE1 is not yet clear although around 30 proteins were discovered to interact with APE1 with different approaches (103). The frequently used approaches were proteomics combined with a protein with a small tag such as Flag, HA and V5 although one tag easily brought in nonspecific binding to the antibody used for immunoprecipitation. Moreover, the existing interactions were mainly obtained under normal culture conditions, while it deserves more efforts to decipher APE1 interactome as well after specific challenge, such as oxidative stress. Thus, in this study we employed a more stringent approach to investigate the APE1 interactome after hydrogen peroxide treatment. The N-terminus of APE1 was tagged with Flag and HA, which facilitates tandem sequential immunoprecipitation that was used to ensure the binding specificity. The

subsequent chapters describe our effort to understand the role of one of the partners Prdx1 with APE1.

Hypothesis and rationale: We propose that under the oxidative condition APE1 governs its interacting partners thereby allowing the protein to perform specific functions. Some partners may be involved in DNA repair, energy metabolism, transcriptional regulation and RNA metabolism.

Objectives: To isolate and characterize the specific partners that interact with APE1 when cells are treated with oxidants, hydrogen peroxide is used in this study. We expect to provide a comprehensive understanding of the versatile functions of APE1 by exploring the regulatory roles between APE1 and its interacting proteins.

2 Article #1 manuscript

Peroxiredoxin 1 sequesters the DNA repair and redox factor APE1 from activating interleukin-8 expression

This is unpublished work; manuscript is prepared for the journal, Antioxidants & Redox Signaling

Peroxiredoxin 1 sequesters the DNA repair and redox factor APE1 from activating interleukin-8 expression

Zhiqiang Wang, El Bachir Affar, Janos G. Filep, Dindial Ramotar

Abstract

APE1 is an essential protein that possesses several DNA repair activities and functions in the base-excision repair (BER) pathway. It has the ability to incise abasic sites on the DNA, remove blocked 3′-termini at DNA single strand breaks, as well as possesses a 3' to 5'-exonuclaese activity. More recently, it has been shown to directly incise oxidized base lesions. Mammalian cells knockdown for APE1 are very sensitive to various DNA damaging agents. Besides its role in DNA repair, APE1 also plays a role in transcriptional regulation. It has a unique cysteine C65, which is required to maintain the reduced state of several transcriptional activators such as p53, NFkappa-B, AP-1, c-Jun, and c-Fos. APE1 also undergoes at least four types of post-translational modifications that include acetylation, deacetylation, phosphorylation and ubiquitylation. How APE1 is being recruited to execute the various biological functions remains a challenge, although this could be directly related to its ability to interact with multiple different partners. Under normal growth conditions, APE1 has been shown to interact with a number of proteins that are involved in various functions. We propose that the oxidative state of APE1 governs its interacting partners thereby allowing the protein to perform specific functions. We show that APE1 interacts with a novel partner Prdx1, a member of the peroxiredoxin family that prevents oxidative damage to proteins. In

addition, we show that knockdown of Prdx1 alters APE1 structure and transcriptional activity in HepG2 cells leading to the up-regulation of IL-8, a chemokine involved in cellular stress.

Introduction

Apurinic/apyrimidinic endonuclease1/redox factor-1 (APE1/Ref-1) is a multifunctional protein involved in base excision DNA repair (BER) and transcriptional regulation of gene expression. In mammalian cells, as a key enzyme in BER, APE1 can hydrolyze the 5'-phosphodiester bond of the AP site to generate a single DNA strand break with 3'-hydroxyl, which is required for DNA repair replication. In addition, APE1 can process 3'-phospho α,β-unsaturated aldehydes (106) and 3' terminal phosphates (129) into 3'-hydroxyls through its 3'–5' exonuclease activity and 3'-phosphatase activity respectively to facilitate DNA repair replication (130). Besides its DNA repair activity, APE1 also play transcriptional roles directly or indirectly. APE1 can form a complex with Ku70/80, heterogeneous ribonucleoprotein-L (hnRNPL) and p300 and bind to the negative calcium responsive elements to suppress gene expression, such as that of the human parathyroid hormone (PTH) gene (118). APE1 can influence DNA binding activity of various transcription factors such as AP-1 (99) , NF-κB (108), Myb (109), Egr-1 (110), p53 (111), hypoxia inducible factor-1 (112) and Pax proteins (113) via its redox residue Cysteine 65. Thus, APE1 can reactivate these transcription factors by exerting its redox function. APE1 also was reported to be involved in RNA metabolism (100, 131).

APE1 overexpression was often observed in several human tumors *e.g.* cervical, prostate, and epithelial ovarian cancers, leading to increased tumor resistance towards anti-neoplastic drugs, especially towards alkylating agents (130). Therefore, APE1 is regarded as

a potential target for anti-tumor chemotherapy and prognostic outcome. APE1 is an essential protein and mice deleted for the APE1 gene die early during embryogenesis. In order for APE1 to execute its role in DNA repair and gene regulation, there must be regulatory mechanisms that switch on/off and fine-tune the different APE1 activities and these include (1) increase in APE1's protein level after transcriptional activation, (2) translocation of APE1 from the cytoplasm to the nucleus and (3) modulation of APE1 by post-translational modification (PTMs) that include at least six different kinds of PTMs detected *in vivo* such as acetylation (118, 123), phosphorylation (124, 125), ubiquitylation (126), S-nitrosation (127), proteolytic cleavage of the N-terminal 33 amino acid domain (128) and reversible reduction-oxidation. Besides these mechanisms, APE1 is known to exist in complexes with other proteins and thus modulation of these proteins within the interactome could influence APE1 function.

The whole picture about interactome of APE1 is not yet clear although around 30 proteins were discovered to interact with APE1 using different approaches (103). The frequently used approaches were proteomics combined with a protein with a small tag such as Flag and HA although any single tag easily brought in nonspecific binding to the antibody used for immunoprecipitation. Moreover, the existing interactions were mainly obtained under normal culture conditions, while it deserves more efforts to decipher APE1 interactome after specific challenges as well, such as oxidative stress.

In this study, we employed a more stringent approach to investigate the APE1 interactome after hydrogen peroxide treatment. The N-terminus of APE1 was tagged with Flag and HA, which facilitated tandem sequential immunoprecipitation that was used to ensure the binding specificity. We demonstrated that the APE1 interactome changed in

response to hydrogen peroxide treatment. In addition, we found peroxiredoxin1 (PRDX1) interacted with APE1 under normal conditions either in the nucleus or cytosol, and that hydrogen peroxide treatment disrupted this interaction in the nucleus but not in the cytosol. PRDX1 knockdown amplified the detection of APE1 in the nucleus and this is associated with the upregulation of the proinflammatory interleukin, IL-8. APE1 knockdown abolished the induction of IL-8 in the Prdx1 deficient cells, suggesting that Prdx1 opposes APE1 role in the regulation of IL-8.

Materials and methods

Cells culture:

Human HeLa and HepG2 (hepatocellular cells) cells were kindly provided by Dr.Elliot Drobetsky (University of Montreal). HeLaS were kindly gifted by El Bachir Affar (University of Montreal). 293T, HeLa and HepG2 were cultured in Dulbecco's Modified Eagle Medium(DMEM) (Wisent Inc.) complemented with 10% of fetal bovine serum (FBS) (Wisent Inc.) and 100U/ml penicillin, and 0.1 mg/ml streptomycin. Cells were incubated at 37°C and 5% CO_2. In large scale culture HeLaS were cultured in MEM media complemented with 10% fetal bovine serum (FBS) (Wisent Inc.) and 100U/ml penicillin, and 0.1 mg/ml streptomycin.

Antibodies and reagents

APE1 rabbit mAb(cat# 2851-1, Epitomics), pAb anti-APE1 antibody(NB100-101,Novus Biologicals), mAb anti-peroxiredoxin1 antibody(NBP1-95676, Novus Biologicals), Prdx1 rabbit Ab(#8732S,cell signalling),goat anti-mouse IgG pAb(HRP conjugate)(cat#ADI-SAB-100,Enzo), goat anti-rabbit IgG pAb(HRP conjugate)(Cat#ADI-SAB-300-J,Enzo),mouse-anti-

human Thioredoxin1(Cat#559969,BD pharmingen),goat anti-rabbit IgG-CFL647(sc-362292 Santa Cruz Biotechnology), MitoTracker Red CMXRos(Cat# M-7512,life technology). Amico Ultra(0.5ml,10K,cat#UFC501024,24PK,Millipore)

Plasmid constructs

pOZ-FH-N contains a Kozak sequence, an initiation methionine, and FLAG and HAtags. pOZN-APE1 were constructed by firstly amplifying human APE1 from K562 cell cDNA by PCR with the primers APE1-Xho1-F1(5'-CGTTCGTACTCGAGATGCCGAAGCGTGGGAAAAAG-3') and APE1-Not1-R1(5'-CTTTTCCTTTTGCGGCCGCTCACAGTGCTAGGTATAGGG-3'), and then subcloned into pOZ-FH-N after Xhol and Notl digested them.

To knockdown Prdx1, several constructs were made based on the MSCV-LTRmiR30-PIG (LMP) vector (Thermo Scientific) following the Manufacturer's instructions. They are respectively named as prdx1C1-2, prdx1C2-1, prdx1C3-1 and prdx1C4-1, all of them were sequenced for confirmation. The hairpin shRNA templates are as following, sense and antisense sequences were underscored.

C1(HP_7670)TGCTGTTGACAGTGAGCGACCAGATGGTCAGTTTAAAGATTAGTGAA
GCCACAGATGTAATCTTTAAACTGACCATCTGGCTGCCTACTGCCTCGGA

C2(HP_647595)TGCTGTTGACAGTGAGCGACCAGATGGTCAGTTTAAAGATTAGTG
AAGCCACAGATGTAATCTTTAAACTGACCATCTGGCTGCCTACTGCCTCGGA

C3(HP_142580)TGCTGTTGACAGTGAGCGACCTGTCTGACTACAAAGGAAATAGTG
AAGCCACAGATGTATTTCCTTTGTAGTCAGACAGGCTGCCTACTGCCTCGGA

C4(HP_820446)TGCTGTTGACAGTGAGCGACCTGTCTGACTACAAAGGAAATAGTG

AAGCCACAGATGTATTTCCTTTGTAGTCAGACAGGCTGCCTACTGCCTCGGA

To knockdown APE1, two constructs were made based on vector RNAi-Ready pSIREN-RetroQ-ZsGreen (Clontech Laboratories, Inc.) following the Manufacturer's instructions: pSIREN shAPE1 1-1 and pSIREN shAPE1 2-1. Oligos APE1-shRNA-UP1and APE1-shRNA-DWN1 are used for pSIREN shAPE1 1-1 targeting 5'-TGACAAAGAGGCAGCAGGA-3' in APE1; oligos APE1-shRNA-UP2 and APE1-shRNA-DWN2 are used for pSIREN shAPE1 2-1 targeting 5'-GTCTGGTACGACTGGAGTACC-3'. Oligo sequences are as following:

APE1-shRNA-UP1:

5'-gatccGTGACAAAGAGGCAGCAGGATTCAAGAGATCCTGCTGCCTCTTTGTCATTTTTTg-3'

APE1-shRNA-DWN1:

5'-aattcAAAAAATGACAAAGAGGCAGCAGGATCTCTTGAATCCTGCTGCCTCTTTGTCACg-3'

APE1-shRNA-UP2:

5'-gatccGTCTGGTACGACTGGAGTACCTTCAAGAGAGGTACTCCAGTCGTACCAGACTTTTTTg-3'

APE1-shRNA-DWN2:

5'-aattcAAAAAAGTCTGGTACGACTGGAGTACCTCTCTTGAAGGTACTCCAGTCGTACCAGACg-3'

pOZN-prdx1 were constructed by firstly amplifying human Prdx1from K562 cell cDNA by PCR with the primers pOZN-FH-prdx1F(5'-GCCGGAGGACTCGAGatgtcttcaggaaatgctaaaattggg-3') and POZN-FH-prdx1R(5'-

TCAGTCACGATGCGGCCGCtcacttctgcttggagaaatattcttt-3') and then subcloned into pOZ-FH-N after XhoI and NotI digestion.

Retrovirus preparation and infection

293T cells were plated in 10cm tissue cell culture plates day prior to transfection at 70 % confluence. After 1 day retroviral vectors were cotransfected with pVSV-G and pCL-Eco retrovirus packaging vector using Calcium phosphate transfection method. Supernatants were collected 36-48 h after transfection, filtered through a 0.45 μm filter and used directly to infect target cell lines.

To infect HeLaS, HeLa or HepG2 cells, cells were plated into 10cm tissue cell culture plates 1day prior to infection at the 35% confluence. After 1 day the old media were removed and replaced with viral supernatants/fresh media mixture (1:1) supplemented with 0.4μg/ml Polybrene® (Sigma-Aldrich). 24h after infection, the viral media was removed and cells were washed at least twice with 1xPBS and fresh media was added. Cells were subjected to selection 48h after infection.

Cell proliferation assay

To determine the average rate of population doublings, HepG2 LMP (empty vector) and HepG2 C1-2(prdx1 knockdown) were plated into 10cm-diameter petri dishes in duplicate at $1.6X10^6$ cells/dish. After indicated intervals, cells were trypsized and counted by cell counter (Invitrogen). The numbers were converted into population doublings according to the following formula: [log (No. of cells counted)-log (No. of cell plated)]/log(2)(132).

HepG2 LMP and HepG2 C1-2(prdx1 knockdown) were plated in 6cm diameter plates at $8X10^5$cells/plate one day before treatment. Cells were treated by at the H_2O_2 of indicated concentration into complete DMEM media. Cells were cultured for another 10 days and then

were trypsinized and countered by a Countess® Automated Cell Counter (Life Technologies). The data was normalized to the untreated group and finally was represented as percentage. Each group was set up as replicates.

Purification of APE1 complex from HeLaS cells

A stable HeLa S cell line that expresses a cDNA encoding wild-type human APE1 with N-terminal FLAG and HA tags was generated by retroviral transduction by using the procedure described by Nakatani and Ogryzko (2003). Nuclear extracts were prepared from 10 L of these cells as follows. The cells were washed twice with cold 1 x PBS, resuspended in hypotonic buffer [20mM Hepes (K+), pH7.6, 10mM KCl, 1.5mM $MgCl_2$, 0.2mM PMSF, 0.5mM benzamidine, and 1 μg/mL each of leupeptin, aprotinin, and pepstatin], and incubated on ice for 10 min. The cells were then disrupted with approximately 10 strokes of a Wheaton Dounce homogenizer (B pestle) on ice. The nuclei were pelleted for 5 min at 4˚C in a clinical centrifuge and washed once with the same volume of hypotonic buffer as pellets, then resuspended in extraction buffer [20mM Hepes (K+), pH7.6, 0.42M KCl, 1.5mM $MgCl_2$, 0.2mM EDTA, 25% (v/v) glycerol, 0.2mM PMSF, 0.5mM benzamidine, and 1μg/mL each of leupeptin, aprotinin, and pepstatin], and sonicated for 2 min on ice. Insoluble material was pelleted for 15 min at 13,000 rpm in a Sorvall SS-34 rotor at 4˚C, and the soluble extract was dialyzed overnight against dialysis buffer [20 mM Hepes (K+), pH 7.6, 100mM KCl, 1.5mM $MgCl_2$, 0.2mM EDTA, 0.2mM PMSF, 0.5mM benzamidine, and 1 μg/mL each of leupeptin, aprotinin, and pepstatin]. The extract was subjected to centrifugation for 15 min at 13,000 rpm in a Sorvall SS-34 rotor at 4˚C to remove insoluble material, and then used for immunoaffinity purification of the APE1 complex. To prepare the cytoskeleton fraction, KCl concentration were adjusted to 100 mM KCl and insoluble material was pelleted for 15 min at

13,000 rpm in a Sorvall SS-34 rotor at 4˚C. The supernatants were used for immunoaffinity purification of the APE1 complex.

The immunoaffinity purification of APE1 was performed by sequential anti-FLAG and anti-HA immunoaffinity purification steps by using methods similar to those previously described (Nakatani and Ogryzko 2003). Nuclear extracts were combined with 200 µL of FLAG (M2) resin (Sigma) and incubated overnight at 4˚C. The beads were pelleted and washed twice in batch with wash buffer [20mM Hepes (K+), pH 7.6, 100mM KCl, 5mM $MgCl_2$, 0.2mM EDTA, 0.05% (v/v)NP-40, 10% (v/v) glycerol, 0.2mM PMSF, 0.5mM benzamidine, and 1 µg/mL each of leupeptin, aprotinin, and pepstatin]. The beads were then transferred to a 1.5 mL column (Bio-Rad) and washed with 10 mL of wash buffer. Bound proteins were eluted by three successive 1 h incubations of the beads with 200 µL (for each incubation) of FLAG Elution buffer [Wash buffer plus 0.36 mg/mL FLAG peptide (Bio-basic)]. The FLAG eluates were pooled, combined with 100 µL of HA resin, and incubated overnight at 4˚C. The resin was then washed washed in 1.5 mL column (Bio-Rad) with 10 mL of Wash buffer. Bound proteins were eluted by three successive 1 h incubations of the beads with 200 µL (for each incubation) of HA elution buffer [Wash buffer plus 0.2 mg/mL HA peptide (Bio-basic)]. The HA elutes were pooled and concentrated into 100µl by 20% (w/v) trichloroacetic acid precipitation, and an aliquot (10 µL) was analyzed by SDS-polyacrylamide gel electrophoresis and silver staining. Some bands and the remaining eluents were identified by the Taplin Biological Mass Spectrometry Facility of Harvard Medicial School.

Co-immunoprecipitation of APE1 and Prdx1 from HeLaS cell extracts

pOZN and pOZN-APE1 expressing HeLaS cells from a 10 cm plate were washed twice in 1 x PBS, resuspended in 500 µL Lysis buffer [20 mM Hepes (K+), pH 7.6, 0.3 M KCl, 1.5 mM $MgCl_2$, 0.2 mM EDTA, 0.3% (v/v) NP-40, 0.2 mM PMSF, 0.5mM benzamidine, and 1 µg/mL each of leupeptin, aprotinin, and pepstatin], and sonicated for 2 seconds. Insoluble material was pelleted 15 min at 13,000 rpm in a microcentrifuge, and the soluble extract was diluted with 1ml of Lysis buffer with 10% (v/v) glycerol but lacking KCl and NP-40. Insoluble material was pelleted, and the soluble lysate was added 30µl of FLAG (M2) resin (Sigma) after 50 µL aliquots were taken for input, following incubation for 4 h at 4°C, The beads were pelleted and washed with 3 x 1 mL of Wash buffer [20 mM Hepes (K+), pH 7.6, 0.1M KCl, 1.5 mM $MgCl_2$, 0.2 mM EDTA, 0.01% (v/v) NP-40,10%(v/v) glycerol, 0.2mM PMSF, 0.5mM benzamidine, and 1µg/mL each of leupeptin, aprotinin, and pepstatin]. Bound proteins were eluted by Elution buffer[10mM Tris pH 7.9, 10mM EDTA, 1%SDS], and the beads were pelleted at 2000RPM for 1mins. The supernatants were added sample buffer for SDS-polyacrylamide gel electrophoresis and western blot analysis.

Gel filtration

If two proteins interact, they are assumed to co-elute in the size-excluding columns. Fast protein liquid chromatography(FPLC) ÄKTA purifier 10/100 system were used. 0.5ml of samples were loaded onto superose^{TM} 6 column , buffer A [20 mM Hepes (K+), pH 7.6, 100 mM KCl, 1.5 mM $MgCl_2$, 0.2 mM EDTA, 0.2 mM PMSF, 0.5 mM benzamidine, and 1 µg/mL each of leupeptin, aprotinin, and pepstatin] were degased and pumped at flow rate of 0.25 ml/min. All eluents were collected at 0.5 ml/fractions. Each fraction was concentrated by Amicon Ultra before western blot.

AP endonuclease activity assay

The synthetic oligonucleotides used in this study are shown as following:

U^{21} G

5'-GCTGCATGCCTGCAGGTCGA*U*TCTAGAGGATCCCGGGTACCT-3'

3'-CGACGTACGGACGTCCAGCT*G*AGATCTCCTAGGGCCCATGGA-5'

They were purchased from Integrated DNA Technologies (IDT). The upper-strand oligonucleotides (100 ng) were radiolabelled as previously described (133) at the 5' ends with 50 μCi of [γ-^{32}P]ATP (6000 Ci/mmol; Perkin Elmer) using T4 polynucleotide kinase (Promega). The labelled oligonucleotides were ethanol-precipitated to remove enzyme and unincorporated ATP, and gel-purified, prior to annealing with an equimolar concentration of a complementary strand of DNA. The upper strand of 42-bp oligonucleotides bear a uracil (U) residue at position 21 opposite a guanine residue to form two different double-strand DNA substrates U^{21} G after annealing with bottom strand. They were used to measure AP endonuclease activity of APE1 in Buffer A (10 mM Hepes pH 7.5, 10 mM KCl, 2 mM MgCl2, 0.2 mM DTT, 0.2 ug/ml BSA, 0.01% Triton-100). Before that U^{21} G needs UDG to create AP site. UDG treatment was carried out at 37 ^{o}C for10 mins followed by heating 90^{o}C for 2 mins to inactivate UDG. 50 ng proteins of each sample were mixed with 100 pmol substrates U^{21} G in buffer A respectively. Then they were incubated at 37 ^{o}C for 10 mins, which was followed the incubation of 90^{o}C for 2 mins to stop the reaction. The reaction products were separated on 10% (w/v) polyacrylamide/7 M urea gels and visualized by autoradiography.

Immunofluorescence assay

Normally the sterile cover slips were placed in 24 well plates and the cells were plated on the cover slips 1 day prior to treatment, After the required treatment on day2, cells were washed with 1X PBS rapidly, and fixed for 30 min with 4% PFA containing 0.1% TritonX 100. Then samples were washed three times with PBS, each for 5 min, and incubated with the 1st antibody in PBS containing 5% FBS (fetal bovine serum) room temperature for 1h or overnight at 4°C. Next samples were washed with PBS three times for 5 min with gentle shaking and incubated with 2nd antibody in PBS containing 5% FBS for 0.5h at 37°C in dark, which is followed by three times washes 5 min/each with PBS. 20-30µl of mount media is dropped on clean glass slides. The cover slips with the cells were mounted facing down on the glass slides. Excess liquid is removed with filter paper. Finally the cover slips were sealed with polish nail. The pictures were taken by Carl Zeiss Microscopy.

IL-8 quantification by ELISA

Human IL-8 ELISA set (Cat.No.555244, BD Biosciences) were used to quantify IL-8 in culture supernatants following the instructions. Briefly 100 µl diluted Capture Ab is added to each well of 96-well plates and incubated overnight at 4 °C followed by 3X 300 µl washes; block plates: 200 µl Assay Diluent is added to each well and incubated 1 h at room temperature (RT) followed by 3X 300 µl washes; next 100 µl standard or samples are added to each well and incubated 2 h at RT followed by 5X 300 µl washes; 100 µl Working Detector(Detection Ab+SAv-HRP) is added to each well and incubated 1 h RT followed by 7X 300 µl washes; 100 µl Substrate Solution is added to each well and incubated 30 mins at RT in dark; add 50 µl Stop Solution is added to each well and the plate is read at 450 nm within 30 mins with correction at 570 nm. All samples were set as duplicates.

Results

Expression and purification of APE1 complex from HeLaS cells.

Previous study used a single tag to explore APE1 interacting partners from total cell extracts. In this work we examined for the partners under more stringent purification conditions by employing two affinity purification tags. In addition, we used this approach to determine whether the APE1 interactome would be influenced upon exposing cells to oxidative stress. We created stable HeLaS cell lines expressing a N-terminal FLAG-HA tagged APE1 from the pOZ vector (Fig.1A) (referred herein as FH-APE1) (134). The ectopic expression of FH-APE1 in HeLaS was validated by Western blot probed with three different antibodies, anti-APE1, anti-HA and anti-FLAG (Fig.1B). The pOZ vector expressed FH-APE1 with the expected molecular weight of 39 kDa and to nearly the same level as the endogenous APE1 (37 kDa).

We used this expression system to examine the proteins associated with FH-APE1 derived from nuclear and cytosolic extracts of the HeLaS cells. The FH-APE1 complex from nuclear extracts was purified by tandem immunoprecipitation using anti-FLAG and -HA resins. The final HA elutions were concentrated by trichloroacetic acid (TCA) and an aliquot analyzed by SDS-PAGE that was stained with silver (Fig.2A). Instead of isolating individual bands from the SDS-PAGE, the entire HA eluate was subjected to mass spectrometry in order to identify all the proteins. HA eluate from nuclear extract carrying the pOZ empty vector was used as a control. This approach identified only five proteins (APE1, LMNA, NPM1, PRDX1 and RPS19) from the nuclear fraction and each protein was considered a hit after setting a limit for three unique peptides (Fig.2B and supple Table S1). Amongst these

proteins only NPM1 was previously reported to interact with APE1 using a single affinity purification (100). LMNA, PRDX1 and RPS19 were found for the first time to be part of the APE1 complex.

The same approach was used to identify FH-APE1 complex in the cytosol. FH-APE1 was found to interact with 14 proteins (Fig.2E and supple Table S1) and of these proteins, four (Prdx1, PDIA6, Prdx2, Prdx3) played a direct role in mitigating oxidative stress (135-138) (Supple Table S1). In fact, the STRING database of known and predicted protein interactions suggested a connection between HSP90AB1 and APE1 on the basis that HSP90AB1 interacts with some of the same proteins found to interact with FH-APE1 (Fig. 2E) (139). These findings suggest that APE1 forms distinct complexes in the nucleus and the cytoplasm and it appears that in the cytosol APE1 forms complexes with proteins that are involved in oxidative stress responses.

APE1 interactome changes upon treatment with H_2O_2

From the above data, we suggest that APE1 interaction with its partners could be influenced by oxidative stress. Since previous studies did not examine whether APE1 interactome could be altered by oxidative stress, we treated cells with the chemical oxidant hydrogen peroxide (H_2O_2) and analyzed for the proteins associated with APE1. Upon treatment with H_2O_2 (1 mM for 1 h) at a concentration that has minimal effects on cell viability, the nuclear APE1 interacting partners disappeared for the exception of LMNA. We performed the same analysis for the APE1 interacting partners in the cytosol and found that APE1 existed in complex with at least 25 proteins (Fig 2D). The treatment did not interfere with the interaction of some of the proteins with APE1 as compared to the interactome that co-existed under normal

conditions, but other interactions were lost and new ones appeared (Supple Table S1). Importantly, H_2O_2 treatment preserved the interaction of APE1 with proteins involved in oxidative stress responses such as Prdx1, PDIA6, as well as gained an interaction with Prdx6. These data suggest that APE1 interaction with its partners can be regulated by oxidative stress.

Validation of interaction between APE1 and Prdx1

Under normal conditions, Prdx1 was the only common partner that existed with APE1 in either the nucleus or the cytosol. Prdx1 has been documented to function as an antioxidant that scavenges H_2O_2. Recent studies demonstrated that mice deficient in Prdx1 caused tissue specific loss of heterozygosity implying that this enzyme may be involved in maintaining genomic stability(140). APE1 is a key enzyme for base excision repair pathway. The interaction between APE1 and Prdx1 has been found by mass spectrometry as mentioned above. So we went further to look into whether Prdx1 affect the function of APE1. To test whether APE1 and Prdx1 indeed belong to a complex, we carried out co-immunoprecipitation experiments with anti-FLAG resin and using total protein extracts derived from HeLaS cells carrying either the empty pOZ vector as control or pOZN-APE1 under conditions where the cells were untreated or treated with 1 mM H_2O_2 for 1h. The anti-FLAG antibodies pull down Prdx1 from total extracts expressing FH-APE1 but not from extracts carrying the empty vector. The co-immunoprecipitation of Prdx1 with FH-APE1 was not affected when the cells were treated with H_2O_2 (Fig.3A), consistent with the mass spectrometry data.

We conducted the reciprocal experiment by using FH-tagged Prdx1 expressed from the pOZ vector in the HeLa cells. The anti-FLAG resin was capable of pulling down APE1 from total cell extracts expressing the FH-Prdx1, but not from extract derived from cells carrying

only the empty pOZ vector (Fig.3B). To further validate the interaction between APE1 and Prdx1, we used gel filtration and analyzed the elution profile of both proteins. The analysis revealed that Prdx1 co-eluted with APE1 using either nuclear (Fig.3C and E) or cytosolic (Fig.3G and I) extracts prepared from HeLa cells that were grown under normal condition. However, if the cells were first treated with H_2O_2 and the cytosolic and nuclear extracts examined for the co-elution of Prdx1 and APE1, only the cytosolic extract showed the co-elution of Prdx1 and APE1 (Fig.3H and J .). In the case of the nuclear extract, the Prdx1 protein could not be recovered in any of fractions (Fig.3D and F). Taken together, these data suggest that Prdx1 interacts with APE1 in both the cytosol and the nucleus under normal condition, and that oxidative stress caused by H_2O_2 treatment may disrupt the nuclear interaction.

Prdx1 knockdown did not affect APE1 protein abundance

To explore the role of Prdx1 on APE1 function, we knocked down Prdx1 in two different cell lines HeLa cell and HepG2 by using via a retroviral system to express shRNA against Prdx1. The shRNA-Prdx1 or shRNA LMP control vector transfected cells were selected for one week in the presence of puromycin (0.5 ug/ml), harvested and examined for Prdx1 levels by Western blot analysis using anti-Prdx1 monoclonal antibody (Fig. 4A). All four shRNA that targeted different regions of Prdx1 decreased the level of the protein in HeLa cells, as compared to the control LMP vector. One of these, shRNA-Prdx1 C1-2 was chosen for the rest of the studies and as shown in Fig. 4B it also diminished the protein level in HepG2 cells. Although Prdx1 level was decreased by the shRNAs, the level of APE1 remained unchanged as determined by Western blot probed with anti-APE1 monoclonal antibody, indicating that

Prdx1 is not involved in regulating the expression level of APE1. It is noteworthy that the Prdx1 knockdown cells displayed higher oxidative stress environment as judged by MitoTracker analysis. MitoTracker Red CMXRos is a red-fluorescent dye that stains mitochondria in live cells and its accumulation is dependent upon membrane potential. We stained HeLa LMP and HeLa C1-2 with MitoTracker Red CMXRos and found that Prdx1 knockdown HeLa C1-2 had stronger fluorescence compared to HeLa LMP control, which suggested that Prdx1 knockdown caused more mitochondrial oxidation (Fig.5C).

Prdx1 knockdown enhances APE1 detection in the nucleus

Because Prdx1 was found associated with APE1 in both the cytosol and the nucleus, we checked whether Prdx1 knockdown would alter APE1 cellular distribution. We performed indirect immunofluorescence using two different antibodies against APE1 and found that APE1 detection by monoclonal antibody was much more intense in the shRNA-Prdx1 HeLa cells, as opposed to the control cells carrying the empty LMP vector (Fig. 5A). APE1 detection was even more intense using the anti-APE1 polyclonal antibody and independent of whether the experiment was conducted in HeLa (Fig. 5B). Under H_2O_2 treatment conditions whereby Prdx1 was no longer co-eluting with APE1, APE1 was again more intensely stained by anti-APE1 antibody. To test the possibility of translocation of APE1 in response to H_2O_2, we fractionized Prdx1 knockdown HepG2 and control cell after exposure to H_2O_2. Western analysis revealed APE1 indeed translocate into nucleus from cytosol in Prdx1 knockdown cells and H_2O_2 treatment even exacerbates the translocation (Fig.6A). Since the total amount of APE1 in cells did not change (Fig. 4A) and the translocation of APE1 between the cytosolic or the nuclear extracts cannot suffice to account for the different

immunofluorescence signals, we raised the possibility that Prdx1 may prevent both the monoclonal and polyclonal antibodies from properly recognizing APE1. While this interpretation is consistent with Prdx1 forming a complex with APE1, it also suggests that Prdx1 could perform a regulatory role in controlling APE1 function.

Prdx1 knockdown did not significantly affect APE1 AP endonuclease activity

Prdx1 exists in the nucleus, but the majority of the protein is localized to the cytosol of cells(136). Prdx1 binds to chromatin in a genome-wide manner with a slight enrichment in coding regions in *Plasmodium falciparum*(27, 141). Prdx1 deficiency causes more oxidative DNA damages (24). APE1 is the key enzyme for base excision repair that can repair oxidative DNA damages. So we postulate that Prdx1 deficiency would impair the AP endonuclease activity of APE1. To test this hypothesis, we used a 42-mer double stranded oligonucleotide substrate containing a single uracil at position 21 that generates a 20-mer product when cleaved. Cytosolic or nuclear extracts prepared from HepG2 cells did not show any significant differences in the AP endonuclease activity between the control or when Prdx1 level was diminished by the shRNA-PRDX1 (Fig.6B-C). Moreover, the shRNA-Prdx1 knockdown cells were no more sensitive nor showed a proliferation defect when treated with H_2O_2 as compared to the cells carrying the LMP vector (Fig.7A-B). Thus, Prdx1 does not seem to govern the role of APE1 in DNA repair.

Prdx1 downregulation stimulates IL-8 expression and depends on APE1

A recent study documented that specific inhibition of the redox activity of APE1 by the inhibitor E3330 blocks TNF-α induced activation of the proinflammatory chemokine

Interleukin-8 (IL-8) in HepG2 cells (142). In fact, IL-8 can be regulated at the transcriptional level by several factors including NF-kB when cells encounter different stimuli such as chemical and environmental stresses (143). Since APE1 can influence NF-kB function, we checked whether disrupting Prdx1 interaction with APE1 would alter IL-8 production in the HepG2 cells.

When Prdx1 level was diminished, IL-8 secretion was stimulated by nearly 4-fold after 24 h of seeding the cells and analyzing the media, as compared to the control cells carrying the empty vector. Treatment of the cells with increasing H_2O_2 for 24h further elevated the secretion of IL-8 in the Prdx1 knockdown cells by another fold, but only slightly in the control cells. These observations indicate that Prdx1 suppresses IL-8 production in the HepG2 cells and that its inactivation by H_2O_2 could also stimulate IL-8 level.

We next tested if the stimulation of IL-8 production in the PRDX1 knockdown cells would depend on APE1 functional level. As such, we first designed a system using the pSIREN-Zs-Green vector to knockdown APE1 in the HepG2 cells and then used the resulting clone shAPE1-1 (Fig. 8B) to downregulate PRDX1 using a different vector LMP (Fig. 8C, lane 2 and 4). In the HepG2 cells, the shRNA against APE1 downregulated APE1 level by 60 % and the shRNA against PRDX1 downregulated PRDX1 by 80%, as compared to the vector controls (Fig. 8B-C). APE1 knockdown did not interfere with the basal level of IL-8 production, but prevented the stimulated amount caused by PRDX1 downregulation (Fig.8D). We interpret these data to indicate that Prdx1 may perform a function to sequester APE1 from turning on the transcription of stress response genes (Fig.8E).

Discussion

In this study, we compared APE1 the interactome under physiological condition and hydrogen peroxide treatment with more stringent tandem immunoprecipitation combined with mass spectrometry in nucleus and cytosol, respectively. In the nucleus, under physiological condition we found NPM1, RPS19, LMNA and PRDX1 interacted with APE1, given their functions on chromatin and RNA processing (see Table S1), these suggested APE1 may regulate genomic stability and gene expression, particularly ribosomal RNA maturation through these proteins although only the role of NPM1-APE1 interaction on rRNA quality control was characterized (100). Hydrogen peroxide treatment disrupted the interaction between NPM1, RPS19, PRDX1 and APE1. Given the fact that oxidative stress induced specific changes in gene expression in hydrogen peroxide-treated lens cells (144), it can be inferred that disrupting the interaction of these proteins may play roles in gene expression. These data imply APE1 could change its interactome to govern gene expression. APE1 mainly distributes in nucleus, but it also exists in cytosol and mitochondria. The mechanism by which APE1 regulates oxidative status and confers resistance to stress is not clearly understood. The interactome analysis of cytosolic APE1 revealed that APE1 gained interaction with a set of proteins including CPS1, P4HB, EEF1A2, HSP90AA1, TRAP1, PKM2, HSPB1, HSPA8 and PRDX6, in response to H_2O_2 treatment. These genes are involved in important life events from metabolism, antioxidation, translation to energy regeneration. Of note, TRAP1, a mitochondrial chaperone with antioxidant and antiapoptotic functions, promotes neoplastic growth by inhibiting succinate dehydrogenase (145). PKM2 is critical for aerobic glycolysis and tumor growth in response to rapamycin (146, 147).

Carbamoyl phosphate synthetase 1 (CPS1), is an enzyme catalyzing the initial step of the urea cycle for ammonia detoxification and disposal (148). Prolyl 4-hydroxylase is essential for viability and morphogenesis in *Caenorhabditis elegans* (149, 150). PHGDH alters glucose metabolism and catalyses the first step in the serine biosynthesis pathway to promote tumorigenesis(151, 152). Thus it is plausible that cytosolic APE1 harnesses those proteins to mobilize cells to adapt to stress for survival, although the influences on those proteins by APE1 remain to be validated.

We found APE1 interacted with Prdx1 in the nucleus as well as in the cytosol under physiological condition, whereas H_2O_2 treatment disrupted the interaction in the nucleus, but not in the cytosol. Prdx1 is an important antioxidant to scavenge H_2O_2. During catalysis, the peroxidatic cysteine (C_P-SH) is oxidized to a sulfenic acid (C_P-SOH), which then reacts with the resolving cysteine (C_R-SH from the other subunit of the dimer) to form a disulfide, which can be reduced by thioredoxin or another enzyme (153). Oxidation of cysteine impairs the DNA binding ability of transcription factors (99, 114). We tested if Prdx1 knockdown affected APE1 DNA repair activity by measuring APE1 endonuclease activity. Unexpectedly Prdx1 knockdown did not significantly decrease its AP endonuclease activity compared to normal cells, but slightly increase AP endonuclease. H_2O_2 treatment indeed diminished AP endonuclease in Prdx1 knockdown and normal cell similarly. This may be attributed to S-glutathionylation of APE1(154). As to the fact that Prdx1 knockout cells have more oxidative DNA damages than wild type, this could be attributed to more ROS production by virtue of Prdx1 knockout, instead of compromised APE1 DNA repair activity.

In our study, we showed there was more APE1 immunofluorescence staining signals in the nucleus of Prdx1 knockdown cell than in normal cells. Although we also found the

translocation of APE1 from cytosol to nucleus in Prdx1 knockdown HepG2 cells and normal HepG2 cells under H_2O_2 stimulation, it seemed that translocation cannot account for the difference in immunofluorescence staining, suggesting a new mechanism to increase accessibility of APE1. One possibility is that Prdx1 may unblock anti-APE1 epitopes making APE1 accessible for detection.

Interleukin-8 (IL-8) is a proinflammatory CXC chemokine. In healthy tissues, IL-8 is hardly detectable, but it is rapidly induced by 10- to 100-fold in response to proinflammatory cytokines such as tumor necrosis factor or IL-1, bacterial or viral products, and cellular stress (143). We found that Prdx1 knockdown in HepG2 cells produced four times IL-8 as much as normal HepG2 within 24h. Prdx1 knockdown HepG2 increased IL-8 secretion by a much bigger margin than in normal HepG2 cell in response to H_2O_2. Increased expression of IL-8 and/or its receptors has been found in endothelial cells, cancer cells, infiltrating neutrophils, and tumor-associated macrophages, which implied that IL-8 may implicate the tumor microenvironment, angiogenesis, metastasis and tumorigenicity as a significant regulatory factor(155). In addition, secreted IL-8 can activate multiple transcription factors including NF-κB, HIF-1, AP-1, signal transducers and activators of transcription 3 (STAT3) and β-catenin (155). It remains elusive whether APE1 is recruited to the IL-8 promoter turn it on which then goes out and activate more transcription factor for oxidative stress such as NF-kB. PRDX1 promoter hypermethylation and reduced expression were frequently detected in oligodendroglial tumours and secondary glioblastomas (156). In addition the importance of Prdx1 was also highlighted by the fact that Prdx1 deficient mice are viable and fertile but prematurely die and age owing to the development beginning at about 9 months of severe haemolytic anaemia and several malignant cancers (28). Taken together, it seems Prdx1

inactivation, IL-8 induction and activation of transcription factors form a positive feedback cycle that drive tumorigenesis. Prdx1 could be one target for oxidative carcinogens such as hydrogen peroxide. We demonstrate that IL-8 induction is dependent on APE1 in response to hydrogen peroxide in this study, which is consistent with a previous report that Ref-1 suppression inhibited TNF-alpha-stimulated IL-8 expression (157). This suggests Prdx1 regulates gene expression through the transcription co-activator APE1.

In summary, our study provides new insights into how Prdx1 regulates APE1 mediated gene expression and Prdx1 deficiency promotes tumorigenesis and inflammation. It is useful to understand the relationship between oxidation and tumorigenesis in order to optimize anti-cancer therapeutics strategies.

Legends

Figure 1. FH-APE1 is stably expressed in HeLaS cells. A, schematics of FH-APE1 construct in which LTR is used as promoter and IL2Rα is used for selection. **B,** Western blot validated ectopic FH-APE1 expression. HeLaS cell were infected with retroviruses containing empty vector pOZ or pOZN-FH-APE1 respectively, then were subjected to three rounds of selection by anti-IL2Rα magnetic beads and positive cells were expanded. Afterwards total cell extracts were analyzed by western blot probed with monoclonal anti-APE1, anti-FLAG and anti-HA respectively.

Figure 2. APE1 complex purification and interactome in response to H_2O_2. APE1 complex purification from nuclear(**A**) and cytosol(**C**). HeLaS cells expressing FH-APE1 were treated with or without 1mM H_2O_2 for 1h, HeLaS cells containing empty vector pOZ were treated with 1mM as negative control for subsequent immunoprecipitation. After treatment, cells were harvested and fractionized into nuclear and cytosol. Each fraction was subjected to tandem immunoprecipitation with anti-FLAG resins followed by anti-HA resins. APE1 complex were finally eluted by HA peptides and separated in 4%-12% gradient SDS-PAGE which followed by silver staining. Pooled eluents were subjected to mass spectrometry to identify all the proteins composed of the APE1 complex. The proteins interactome were visualized by searching STRING software, a database of known and predicted protein interactions. **B,** APE1 nuclear interactome under normal condition. **D,** APE1 cytosolic interactome from H_2O_2 treated HeLaS cytosol. **E,** APE1 cytosolic interactome from untreated

HeLaS cytosol. **F,** differences between panel D and E, which indicated changes of APE1 cytosolic interactome in response to H_2O_2.

Figure 3. Validation of APE1-Prdx1 interaction. A, FH-APE1 pulled down Prdx1 during immunoprecipitation. HeLaS cells expressing FH-APE1 were treated with or without 1mM H_2O_2 for 1h, HeLaS cells containing empty vector pOZ were treated with 1mM as negative control for immunoprecipitation. After treatment, cells were harvested and total cell extracts were subjected to immunoprecipitation with anti-FLAG resins. Eluents were separated by 10% SDS-PAGE and probed with monoclonal anti-Prdx1. **B,** FH-Prdx1pulled down APE1 during immunoprecipitation. HeLa cells expressing FH-Prdx1 were subjected to immunoprecipitation with anti-FLAG resins. Eluents were separated by 10% SDS-PAGE and probed with monoclonal anti-APE1. pOZN empty was used as negative control. **C-J,** Co-elution assay by fast protein liquid chromatography (FPLC). HeLa cells were treated with and without 1mM H_2O_2, then harvested and fractionized into nuclear and cytosol. Each fraction was loaded on superose^{TM} 6 column eluted with buffer A at flow rate of 0.25ml/min. All eluents were collected at 0.5ml/fractions. Each eluent fraction was concentrated by Amicon Ultra and analyzed by western blot probed with monoclonal anti-APE1 and monoclonal anti-Prdx1.

Figure 4. Prdx1 knockdown in HeLa and HepG2 cells. Several different Prdx1 shRNA (C1-2, C2-1, C3-1, and C4-1) and empty vector LMP (negative control) were packaged into reroviruses and HeLa cells (**A**) and HepG2 cells (**B**) were infected by viruses. After 1 week

selection by 0.5 μg/ml puromycin, cells were analyzed by western blot to confirm knockdown effects.

Figure 5. Prdx1 knockdown facilitates APE1 detection in nucleus and increases mitochondria membrane potential. HeLa LMP and Prdx1 knockdown C1-2 cells were stained by monoclonal (**A**) and polyclonal anti-APE1 (**B**), respectively. (C) MitoTracker Red CMXRos staining.

Figure 6. Prdx1 knockdown causes APE1 translocation from cytosol into nucleus but did not impair endonuclease activity. (A) Prdx1 knockdown HepG2 and control cells were treated with or without 2mM H_2O_2 for 1.5h; cytosol and nuclear extracts were fractionated and subjected to western blot analysis, in which the same blot was probed with anti-APE1,anti-Prdx1 and anti-β-actin sequentially. HeLa LMP and HeLa C1-2 were treated with or without 1mM H_2O_2 for 1h. HepG2 LMP and HepG2 C1-2 were treated with or without 2mM H2O2 for 1h. After treatment, cells were harvested and fractionized into nuclear and cytosol. Then APE1 endonuclease activity was measured in all samples with $U^{21}G$ substrates described in Materials and Methods **(B).** This is representative of three independent experiments. **(C)** The graph showed the relative APE1 endonuclease activity of each samples after quantification by the Multigauge image quantification software.

Figure 7. Prdx1 knockdown did not significantly affect cell survival and proliferation (A) doubling time curve of HepG2 LMP and HepG2 C1-2. To determine the average rate of population doublings, HepG2 LMP (empty vector) and HepG2 C1-2(Prdx1 knockdown) were plated into 10cm diameter petri dishes in duplicate at $1.6X10^6$cells/dish. After indicated

intervals (0, 3, 6, 9 day), cells were trypsinized and counted by Countess® Automated Cell Counter (Life Technologies)**.** The numbers were converted into population doublings according to the following formula: [log (No. of cells counted)-log (No. of cell plated)]/log (2). The plot was doublings time versus time. **(B)** Proliferation assay of HepG2 LMP and C1-2 under different doses of H_2O_2 treatment. HepG2 LMP and HepG2 C1-2(Prdx1 knockdown) were plated in 3cm diameter plates at $8X10^5$cells/plate one day before treatment. Cells were treated by putting H_2O_2 of indicated concentration into complete DMEM media. Cells were cultured for 9 days and then were trysinized and counted by Countess® Automated Cell Counter (Life Technologies)**.** The data was normalized to untreated group and finally was represented as percentages. Each group was set up replicates.

Figure 8. (A) IL-8 induction in Prdx1 knockdown HepG2 cells at 24h after different doses of H_2O_2 treatment. HepG2 LMP (control) and C1-2(Prdx1 KD) were plated in 96-well plate at 15000 cells/ well in duplicates. Cells/well were treated with 200ul complete DMEM with 10% FBS containing H_2O_2 at indicated doses. 24 h after treatment, the supernatants were collected for ELISA. **(B-C)** Prdx1/APE1 double knockdown in HepG2. HepG2 were infected with indicated virus, pSIREN shAPE1 1-1 and control shLuc. 72h after infection, cells were sorted and expanded. 2 weeks after, HepG2 were collected for western blot, which confirmed APE1 knockdown in HepG2 cell.APE1 knockdown HepG2 cell and its control shLuc HepG2 were infected with viruses containing shPrdx1C1-2 or its control LMP. After selection by 1ug/ml puromycin for 1 week, cells were analyzed by western blot to confirm APE1 knockdown and Prdx1 knockdown**. (D)** IL-8 induction ablated in Prdx1/APE1 knockdown HepG2 cells at 24h after normal condition and 100μM H_2O_2 treatment. HepG2 LMP (control)

and C1-2(Prdx1 KD) were plated in 96-well plate at 30000 cells/well in duplicates. Cells/well were treated with 200ul complete DMEM containing 100μM H_2O_2. 24 h after treatment, supernatants were collected for ELISA. (E) Working model. Prdx1 in the nuclear can prevent APE1 from activating IL-8. Prdx1 deficiency can free APE1 to activate IL-8.

Figures:

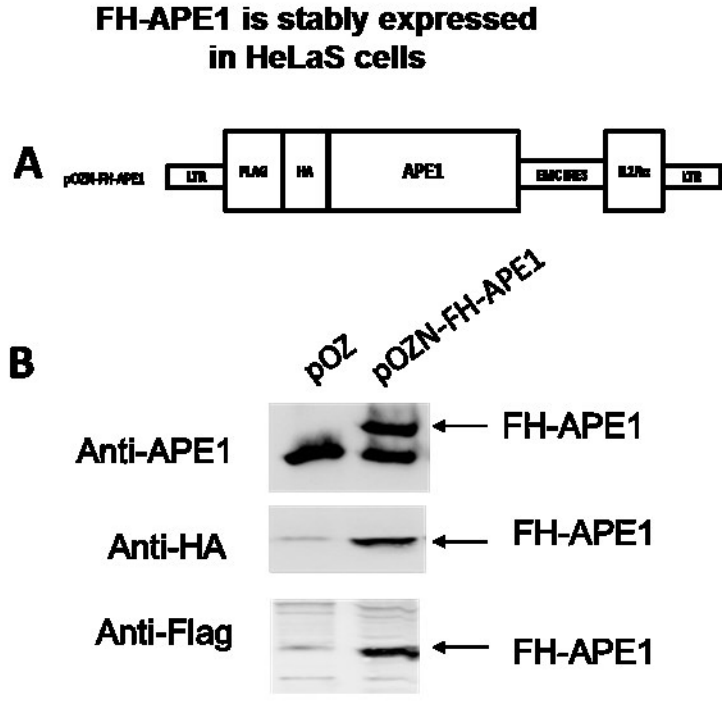

Figure 1

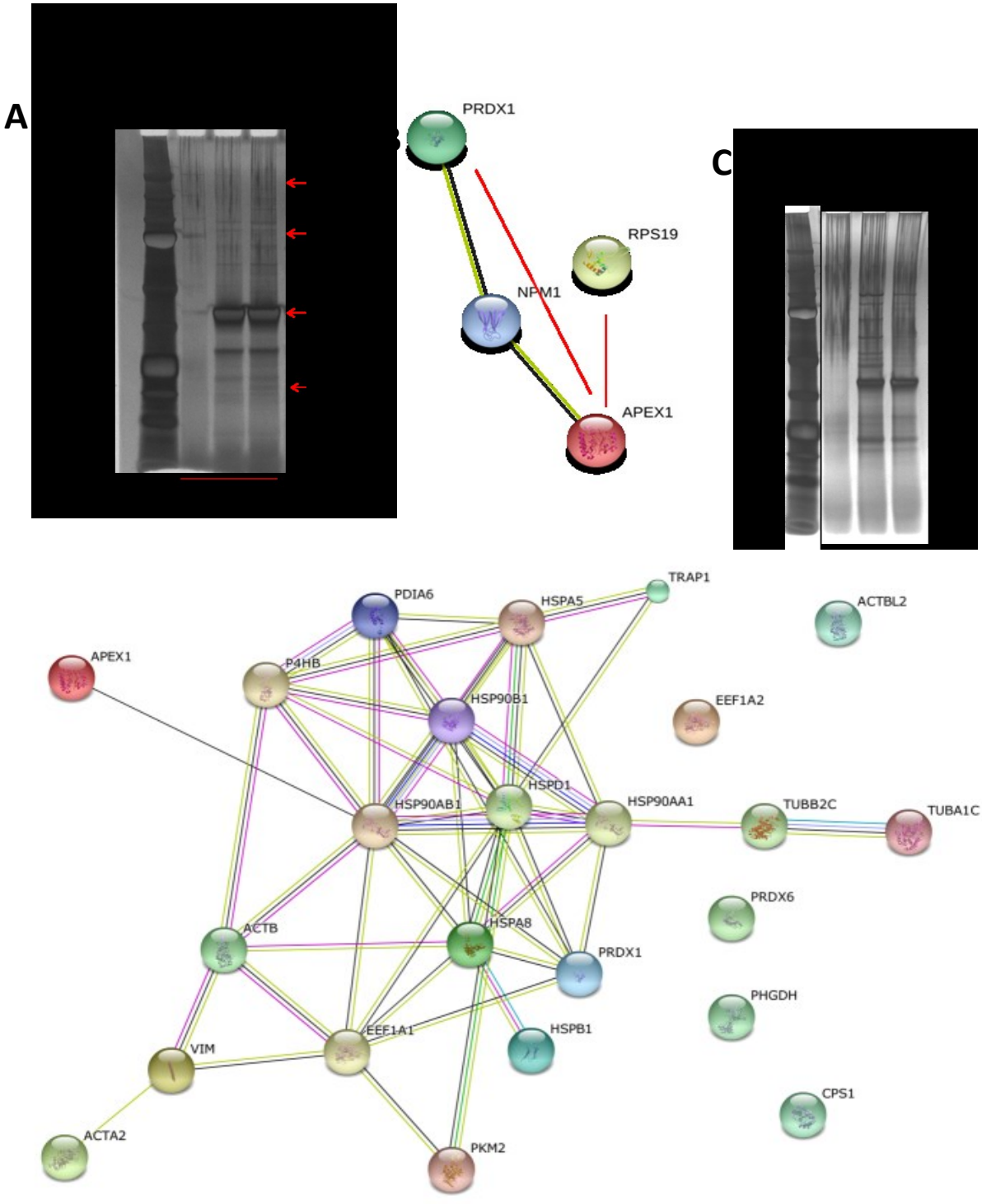

D APE1 interactome from H_2O_2 treated HeLaS cytosol

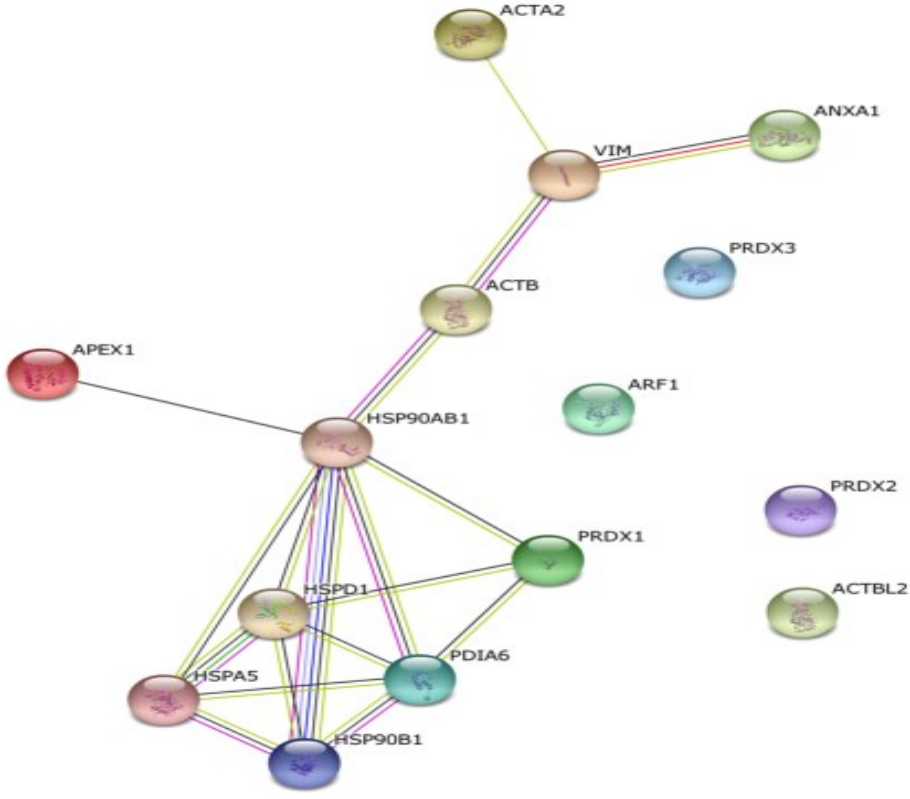

E APE1 interactome from untreated HeLaS cytosol

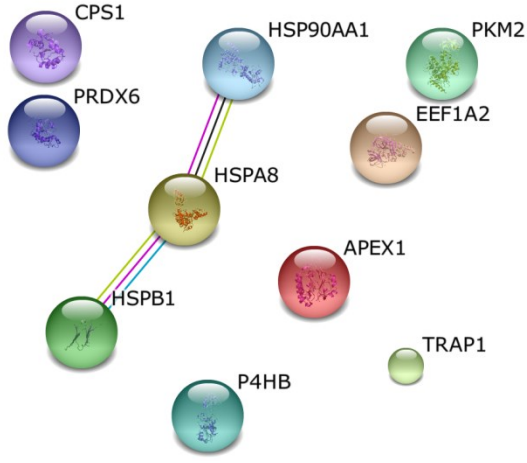

F Changes of cytosolic APE1 interactome in response to H_2O_2

Figure 2

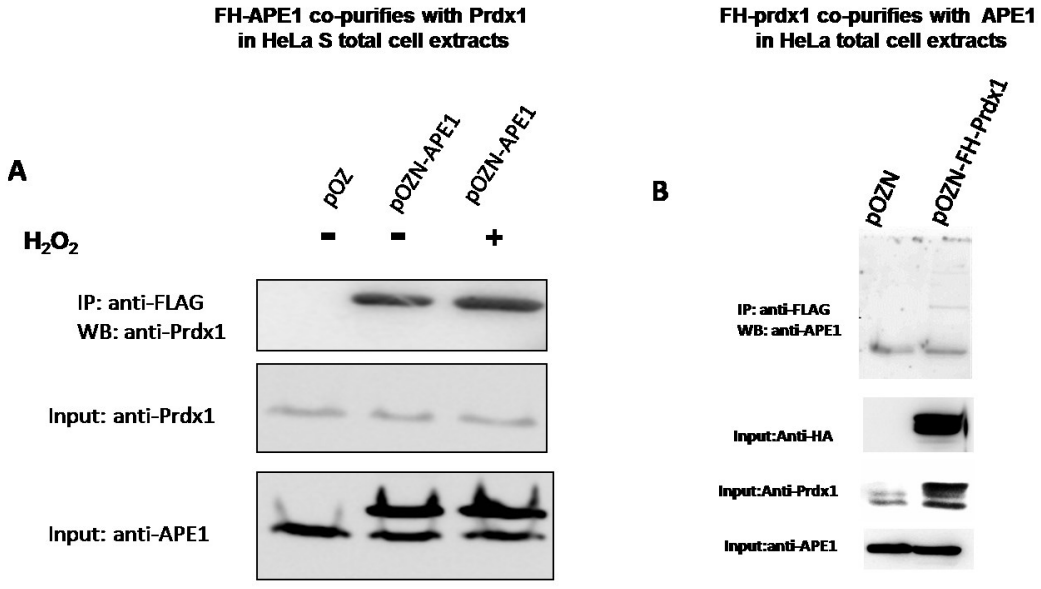
FH-APE1 co-purifies with Prdx1
in HeLa S total cell extracts
A
pOZ
pOZN-APE1
pOZN-APE1
H2O2
-
-
+
IP: anti-FLAG
WB: anti-Prdx1
Input: anti-Prdx1
Input: anti-APE1
FH-prdx1 co-purifies with APE1
in HeLa total cell extracts
B
pOZN
pOZN-FH-Prdx1
IP: anti-FLAG
WB: anti-APE1
Input:Anti-HA
Input:Anti-Prdx1
Input:anti-APE1

Figure3

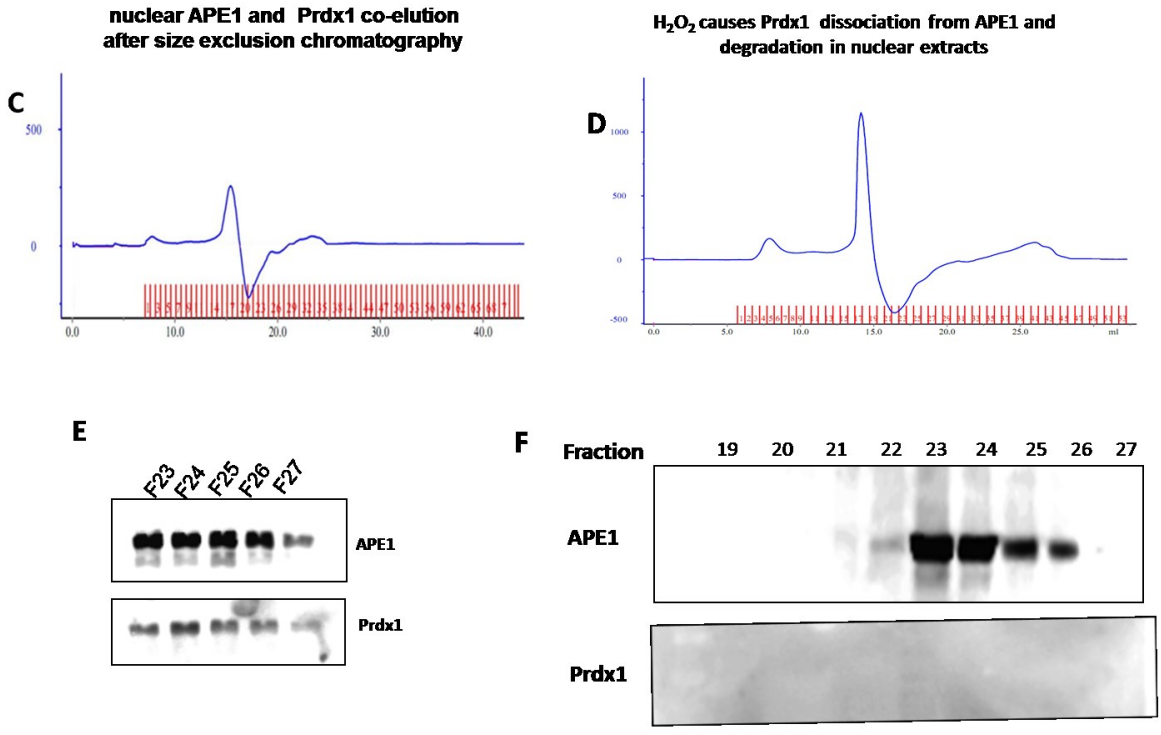
nuclear APE1 and Prdx1 co-elution
after size exclusion chromatography
C
500
0
0.0
10.0
20.0
30.0
40.0
H2O2 causes Prdx1 dissociation from APE1 and
degradation in nuclear extracts
D
1000
500
0
-500
0.0
5.0
10.0
15.0
20.0
25.0
ml
E
F23
F24
F25
F26
F27
APE1
Prdx1
F
Fraction
19
20
21
22
23
24
25
26
27
APE1
Prdx1

Figure3

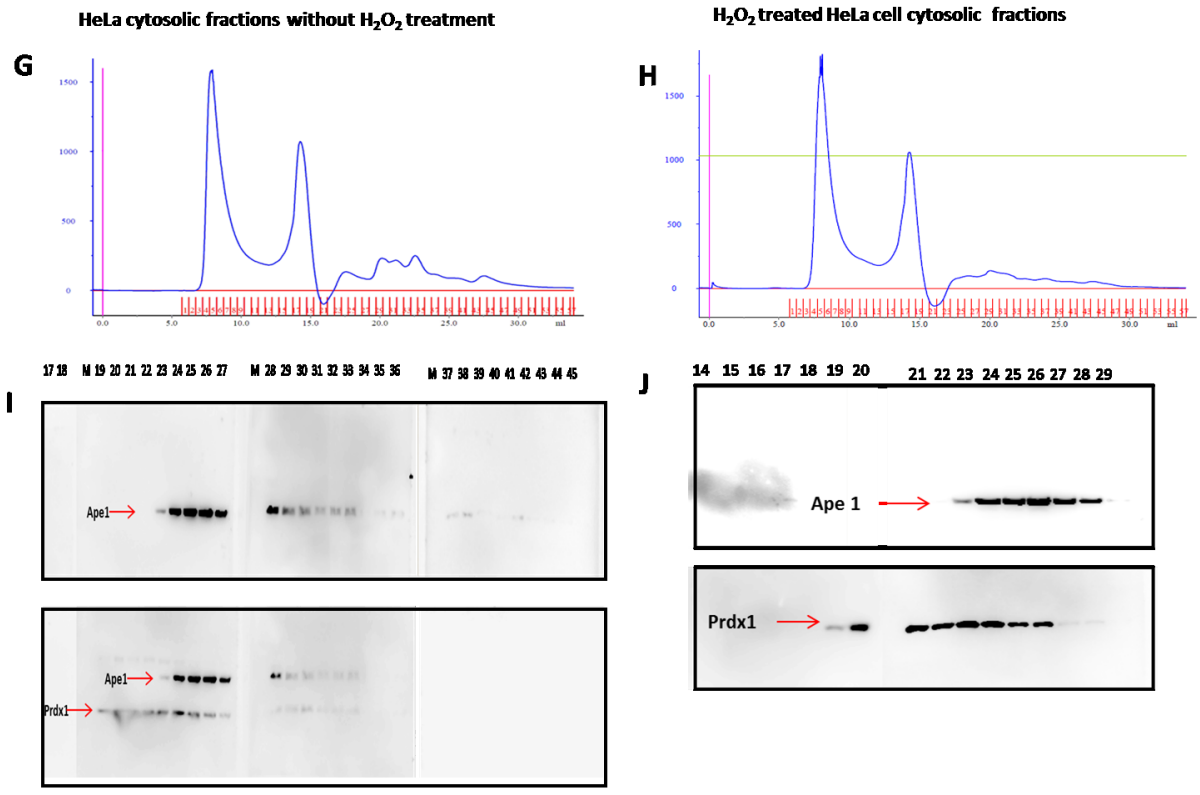
HeLa cytosolic fractions without H_2O_2 treatment
H_2O_2 treated HeLa cell cytosolic fractions
G
H
I
J
17 18 M 19 20 21 22 23 24 25 26 27 M 28 29 30 31 32 33 34 35 36 M 37 38 39 40 41 42 43 44 45
Ape1
Prdx1
14 15 16 17 18 19 20 21 22 23 24 25 26 27 28 29
Ape 1
Prdx1

Figure 3

Prdx1 knockdown did not affect the abundance of APE1 in HeLa cells

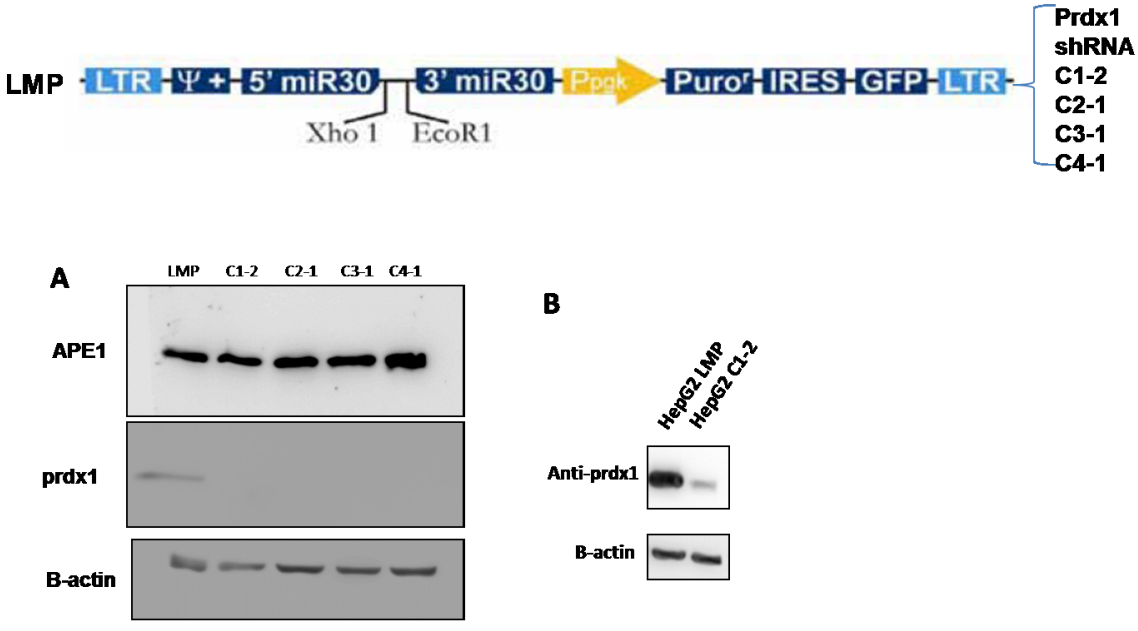

Figure 4

Monoclonal anti-APE1 staining

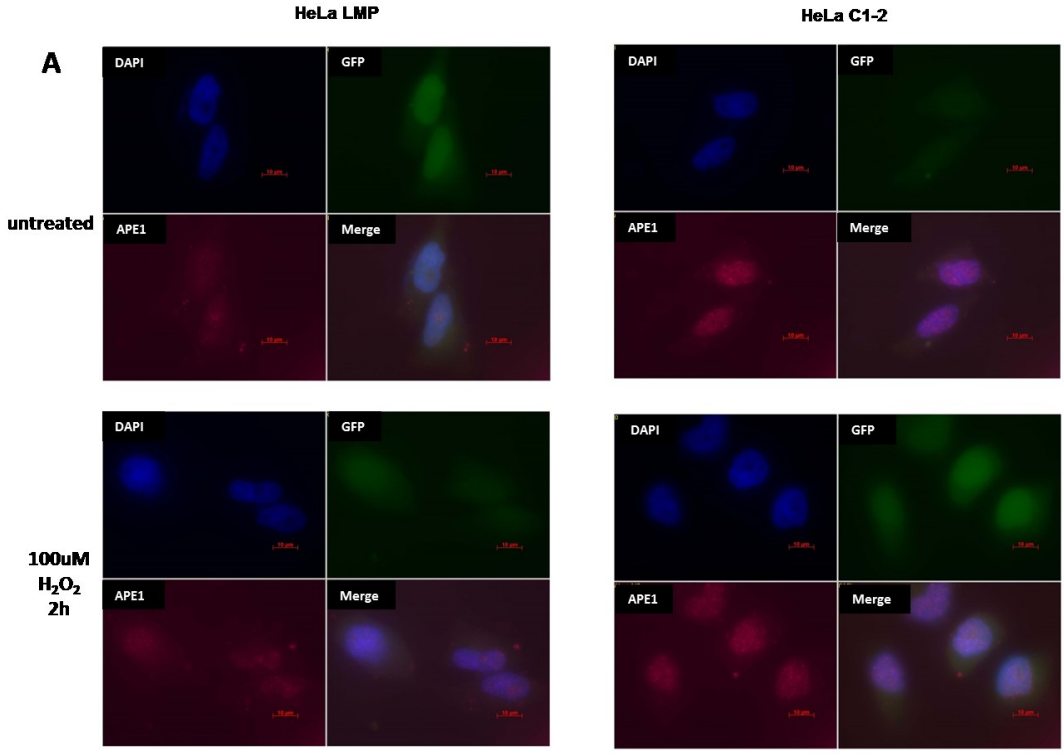

Figure 5

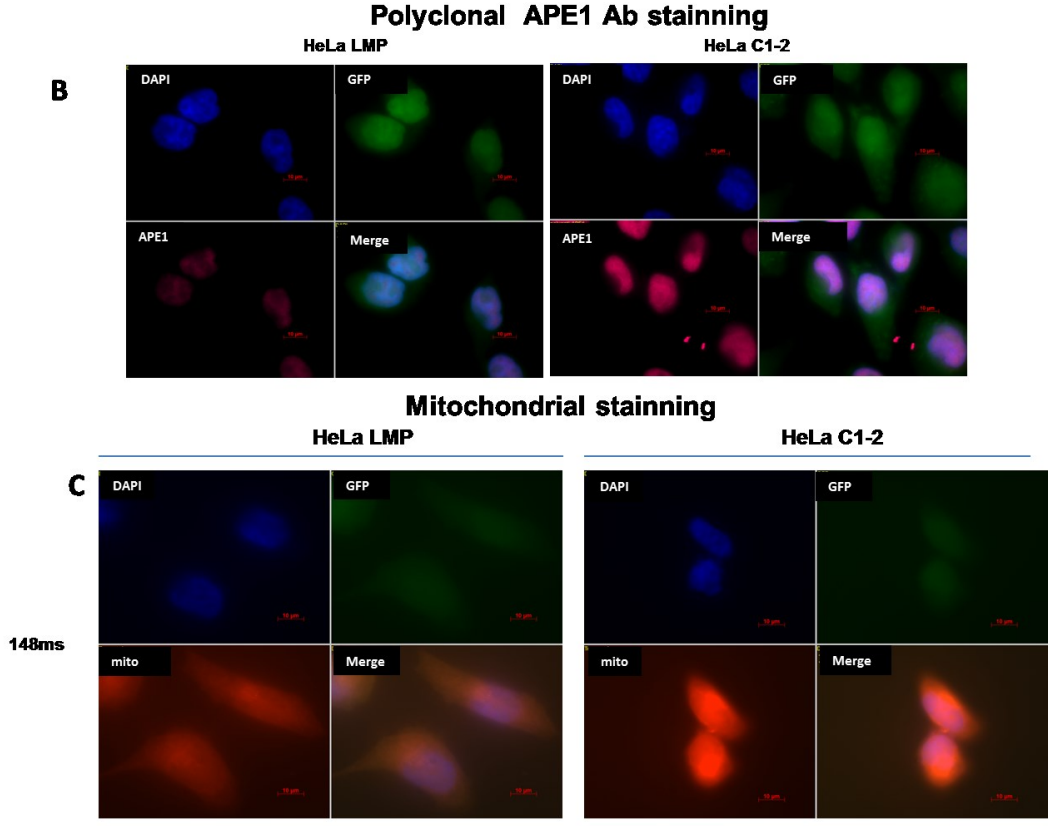
Polyclonal APE1 Ab stainning
HeLa LMP
HeLa C1-2
B
DAPI
GFP
APE1
Merge
DAPI
GFP
APE1
Merge
Mitochondrial stainning
HeLa LMP
HeLa C1-2
C
148ms
DAPI
GFP
mito
Merge
DAPI
GFP
mito
Merge

Figure 5

H_2O_2 alters the cellular distribution of APE1 and Prdx1

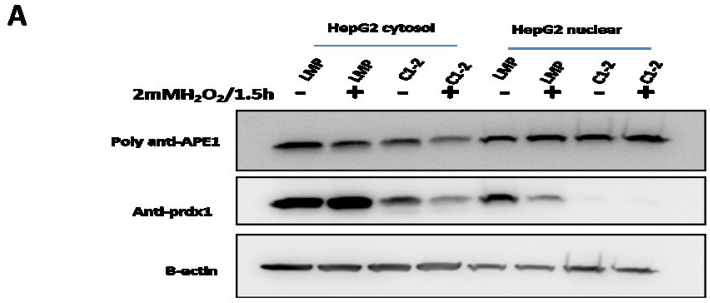

Prdx1 knockdown did not influence APE1 DNA repair activity

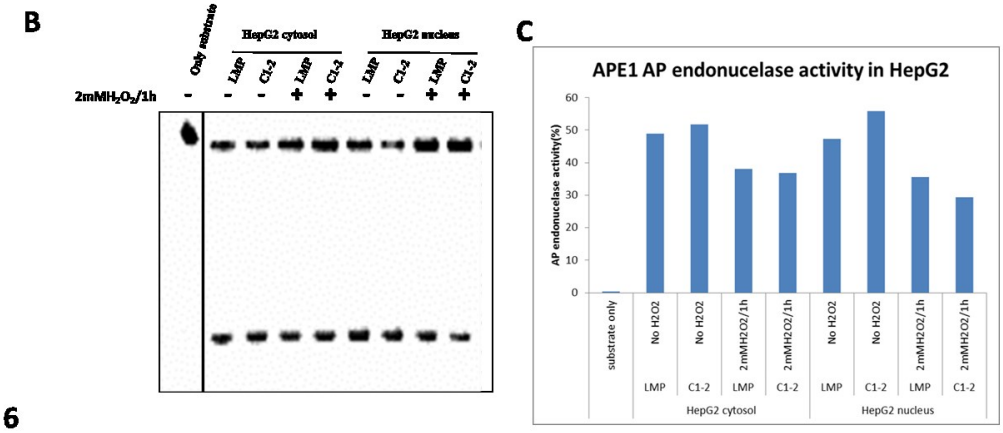

Figure 6

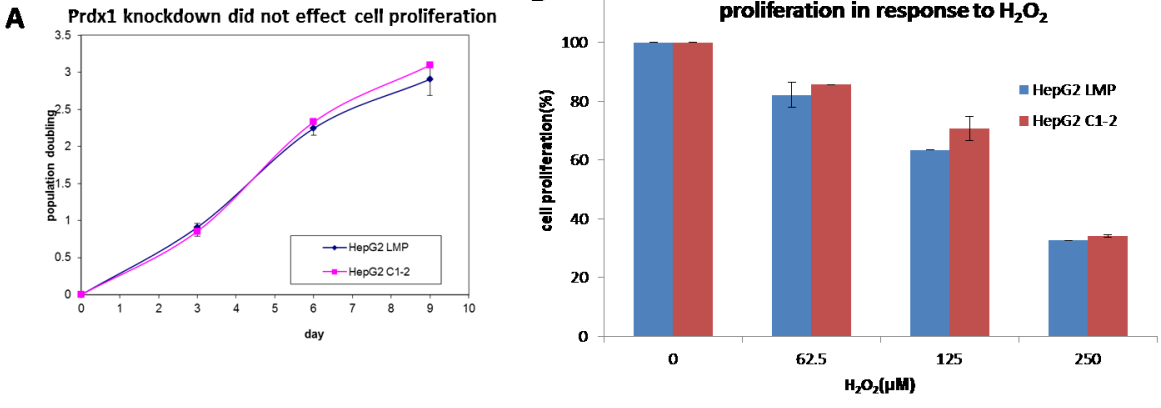

Figure 7

Prdx1 knockdown increases IL-8 secretion in APE1-dependent manner

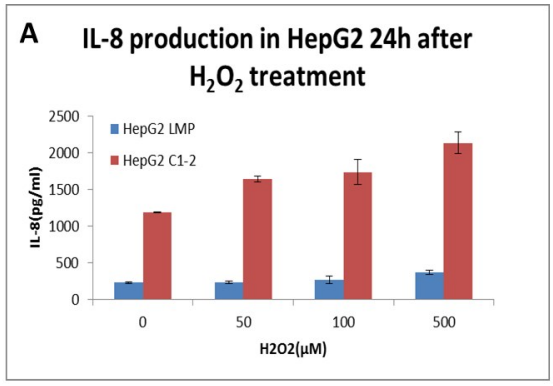

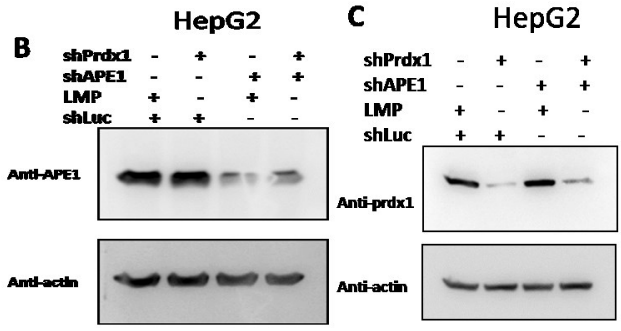

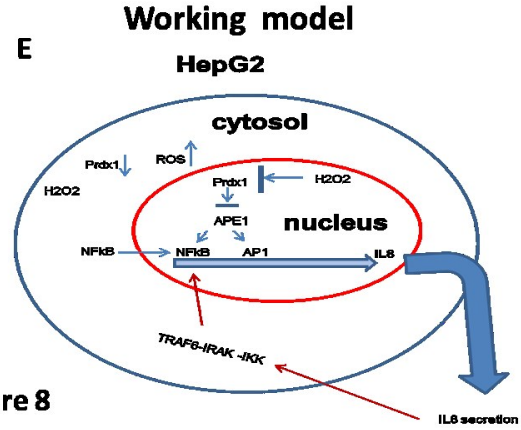

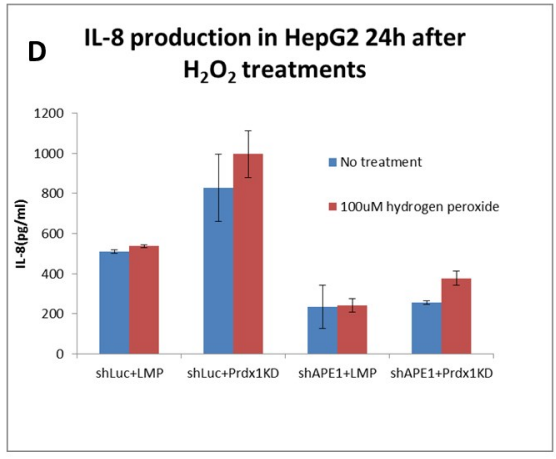

Figure 8

Table S 1

	Proteins interacting with APE1 in cytosol under normal condition
Protein name	functions
APEX nuclease 1	Repairs oxidative DNA damages *in vitro*. May have a role in protection against cell lethality and suppression of mutations. Removes the blocking groups from the 3'-termini of the DNA strand breaks generated by ionizing radiations and bleomycin (318 aa)
VIM vimentin	Vimentins are class-III intermediate filaments found in various non-epithelial cells, especially mesenchymal cells (466 aa)
ACTA2 actin, alpha 2	smooth muscle, aorta; Actins are highly conserved proteins that are involved in various types of cell motility and are ubiquitously expressed in all eukaryotic cells (By similarity) (377 aa)
ANXA1 annexin A1	Calcium/phospholipid-binding protein which promotes membrane fusion and is involved in exocytosis. This protein regulates phospholipase A2 activity. It seems to bind from two to four calcium ions with high affinity (346 aa)
PRDX1 peroxiredoxin 1	Involved in redox regulation of the cell. Reduces peroxides with reducing equivalents provided through the thioredoxin system but not from glutaredoxin. May play an important role in eliminating peroxides generated during metabolism. Might participate in the signaling cascades of growth factors and tumor necrosis factor-alpha by regulating the intracellular concentrations of H_2O_2. Reduces an intramolecular disulfide bond in GDPD5 that gates the ability to GDPD5 to drive postmitotic motor neuron differentiation (By similarity) (199 aa)
ARF1 ADP-ribosylation factor 1	GTP-binding protein that functions as an allosteric activator of the cholera toxin catalytic subunit, an ADP- ribosyltransferase. Involved in protein trafficking among different compartments. Modulates vesicle budding and uncoating within the Golgi complex. Deactivation induces the redistribution of the entire Golgi complex to the endoplasmic reticulum, suggesting a crucial role in protein trafficking. In its GTP-bound form, its triggers the association with coat proteins with the Golgi membrane. The hydrolysis of ARF1-bound GTP, which is mediated by ARFGAPs(181 aa)
PDIA6 protein disulfide isomerase family A, member 6	May function as a chaperone that inhibits aggregation of misfolded proteins. Plays a role in platelet aggregation and activation by agonists such as convulxin, collagen and thrombin
PRDX3 peroxiredoxin 3	Involved in redox regulation of the cell. Protects radical-sensitive enzymes from oxidative damage by a radical- generating system. Acts synergistically with MAP3K13 to regulate the activation of NF-kappa-B in the cytosol (256 aa)

HSP90B1 heat shock protein 90kDa beta (Grp94), member 1	heat shock protein 90kDa beta (Grp94), member 1; Molecular chaperone that functions in the processing and transport of secreted proteins. Functions in endoplasmic reticulum associated degradation (ERAD). Has ATPase activity (803 aa)
PRDX2 peroxiredoxin 2	Involved in redox regulation of the cell. Reduces peroxides with reducing equivalents provided through the thioredoxin system. It is not able to receive electrons from glutaredoxin. May play an important role in eliminating peroxides generated during metabolism. Might participate in the signaling cascades of growth factors and tumor necrosis factor-alpha by regulating the intracellular concentrations of H_2O_2 (198 aa)
HSPA5 heat shock 70kDa protein 5	Probably plays a role in facilitating the assembly of multimeric protein complexes inside the ER (654 aa)
HSP90AB1 heat shock protein 90kDa alpha (cytosolic)	class B member 1; Molecular chaperone. Has ATPase activity (724 aa)
HSPD1 heat shock 60kDa protein 1 (chaperonin)	Implicated in mitochondrial protein import and macromolecular assembly. May facilitate the correct folding of imported proteins. May also prevent misfolding and promote the refolding and proper assembly of unfolded polypeptides generated under stress conditions in the mitochondrial matrix (573 aa)
ACTB actin, beta	Actins are highly conserved proteins that are involved in various types of cell motility and are ubiquitously expressed in all eukaryotic cells (By similarity) (375 aa)
ACTBL2 actin, beta-like 2	Actins are highly conserved proteins that are involved in various types of cell motility and are ubiquitously expressed in all eukaryotic cells (By similarity) (376 aa)
	Proteins interacting with APE1 in cytosol under hydrogen peroxide treatment
EEF1A2 eukaryotic translation elongation factor 1 alpha 2	This protein promotes the GTP-dependent binding of aminoacyl-tRNA to the A-site of ribosomes during protein biosynthesis (463 aa)
VIM vimentin	class-III intermediate filaments found in various non-epithelial cells, especially mesenchymal cells (466 aa)
ACTA2 actin, alpha 2	smooth muscle, aorta; Actins are highly conserved proteins that are involved in various types of cell motility and are ubiquitously expressed in all eukaryotic cells (By similarity) (377 aa)
HSPA8	Chaperone. Isoform 2 may function as an endogenous inhibitory regulator

heat shock 70kDa protein 8	of HSC70 by competing the co-chaperones (646 aa)
TRAP1 TNF receptor-associated protein 1	Chaperone that expresses an ATPase activity (704 aa)
HSPB1 heat shock 27kDa protein 1	Involved in stress resistance and actin organization (205 aa)
PRDX1 peroxiredoxin 1	Involved in redox regulation of the cell. Reduces peroxides with reducing equivalents provided through the thioredoxin system but not from glutaredoxin. May play an important role in eliminating peroxides generated during metabolism. Might participate in the signaling cascades of growth factors and tumor necrosis factor-alpha by regulating the intracellular concentrations of H_2O_2. Reduces an intramolecular disulfide bond in GDPD5 that gates the ability to GDPD5 to drive postmitotic motor neuron differentiation (By similarity) (199 aa)
PDIA6 protein disulfide isomerase family A member 6	May function as a chaperone that inhibits aggregation of misfolded proteins. Plays a role in platelet aggregation and activation by agonists such as convulxin, collagen and thrombin
HSP90B1 heat shock protein 90kDa beta (Grp94), member 1	Molecular chaperone that functions in the processing and transport of secreted proteins. Functions in endoplasmic reticulum associated degradation (ERAD). Has ATPase activity (803 aa)
TUBA1C tubulin, alpha 1c	Tubulin is the major constituent of microtubules. It binds two moles of GTP, one at an exchangeable site on the beta chain and one at a non-exchangeable site on the alpha-chain (By similarity) (449 aa)
PKM2 pyruvate kinase	Glycolytic enzyme that catalyzes the transfer of a phosphoryl group from phosphoenolpyruvate (PEP) to ADP, generating ATP. Stimulates POU5F1-mediated transcriptional activation. Plays a general role in caspase independent cell death of tumor cells. The ratio betwween the highly active tetrameric form and nearly inactive dimeric form determines whether glucose carbons are channeled to biosynthetic processes or used for glycolytic ATP production. The transition between the 2 forms contributes to the control of glycolysis and is important for tumor cell proliferat (531 aa)
HSPA5 heat shock 70kDa protein	Probably plays a role in facilitating the assembly of multimeric protein complexes inside the ER (654 aa)

5	
HSP90AB1 heat shock protein 90kDa alpha (cytosolic)	Molecular chaperone. Has ATPase activity (724 aa)
P4HB prolyl 4-hydroxylase, beta polypeptide	This multifunctional protein catalyzes the formation, breakage and rearrangement of disulfide bonds. At the cell surface, seems to act as a reductase that cleaves disulfide bonds of proteins attached to the cell. May therefore cause structural modifications of exofacial proteins. Inside the cell, seems to form/rearrange disulfide bonds of nascent proteins. At high concentrations, functions as a chaperone that inhibits aggregation of misfolded proteins. At low concentrations, facilitates aggregation (anti-chaperone activity). (508 aa)
EEF1A1 eukaryotic translation elongation factor 1 alpha-like 7	This protein promotes the GTP-dependent binding of aminoacyl-tRNA to the A-site of ribosomes during protein biosynthesis (By similarity) (462 aa
HSP90AA1 heat shock protein 90kDa alpha (cytosolic)	class A member 1; Molecular chaperone. Has ATPase activity (By similarity) (854 aa)
HSPD1 heat shock 60kDa protein 1 (chaperonin)	Implicated in mitochondrial protein import and macromolecular assembly. May facilitate the correct folding of imported proteins. May also prevent misfolding and promote the refolding and proper assembly of unfolded polypeptides generated under stress conditions in the mitochondrial matrix (573 aa)
TUBB2C tubulin, beta 2C	Tubulin is the major constituent of microtubules. It binds two moles of GTP, one at an exchangeable site on the beta chain and one at a non-exchangeable site on the alpha-chain (By similarity) (445 aa)
PRDX6 peroxiredoxin 6	Involved in redox regulation of the cell. Can reduce H_2O_2 and short chain organic, fatty acid, and phospholipid hydroperoxides. May play a role in the regulation of phospholipid turnover as well as in protection against oxidative injury (224 aa)
ACTB actin, beta	Actins are highly conserved proteins that are involved in various types of cell motility and are ubiquitously expressed in all eukaryotic cells (By similarity) (375 aa)
PHGDH	phosphoglycerate dehydrogenase (533 aa)
CPS1 carbamoyl-phosphate synthetase 1	mitochondrial; Involved in the urea cycle of ureotelic animals where the enzyme plays an important role in removing excess ammonia from the cell (1506 aa)

ACTBL2 actin, beta-like 2	Actins are highly conserved proteins that are involved in various types of cell motility and are ubiquitously expressed in all eukaryotic cells (By similarity) (376 aa)
	Proteins interacting with APE1 in nucleus under normal condition
RPS19 ribosomal protein S19	Required for pre-rRNA processing and maturation of 40S ribosomal subunits (145 aa)
ACTA2 actin, alpha 2	smooth muscle, aorta; Actins are highly conserved proteins that are involved in various types of cell motility and are ubiquitously expressed in all eukaryotic cells (By similarity) (377 aa)
PRDX1 peroxiredoxin 1	Involved in redox regulation of the cell. Reduces peroxides with reducing equivalents provided through the thioredoxin system but not from glutaredoxin. May play an important role in eliminating peroxides generated during metabolism. Might participate in the signaling cascades of growth factors and tumor necrosis factor-alpha by regulating the intracellular concentrations of H_2O_2. Reduces an intramolecular disulfide bond in GDPD5 that gates the ability to GDPD5 to drive postmitotic motor neuron differentiation (By similarity) (199 aa)
NPM1 nucleophosmin	Involved in diverse cellular processes such as ribosome biogenesis, centrosome duplication, protein chaperoning, histone assembly, cell proliferation, and regulation of tumor suppressors TP53/p53 and ARF. Binds ribosome presumably to drive ribosome nuclear export. Associated with nucleolar ribonucleoprotein structures and bind single-stranded nucleic acids. Acts as a chaperonin for the core histones H3, H2B and H4 (294 aa)
LMNA lamin A/C	Lamins are components of the nuclear lamina, a fibrous layer on the nucleoplasmic side of the inner nuclear membrane, which is thought to provide a framework for the nuclear envelope and may also interact with chromatin. Lamin A and C are present in equal amounts in the lamina of mammals (664 aa)
	Proteins interacting with APE1 in nucleus under H_2O_2 treatment
LMNA lamin A/C	Lamins are components of the nuclear lamina, a fibrous layer on the nucleoplasmic side of the inner nuclear membrane, which is thought to provide a framework for the nuclear envelope and may also interact with chromatin. Lamin A and C are present in equal amounts in the lamina of mammals (664 aa)

3. Article #2 manuscript

This is unpublished work; manuscript is prepared for the journal, Antioxidants & Redox Signaling.

APE1 promotes H_2O_2 mediated signal transduction by stimulating Prdx1 hyperoxidation

Zhiqiang Wang, Dindial Ramotar

Abstract

Reactive oxygen species (ROS) such as H_2O_2 are regarded as the inevitable but unwanted by-product of oxidative metabolism or respiration in cells. H_2O_2 is discovered to act as a second messenger in regulation of fundamental processes. Peroxiredoxin 1 (Prdx1) has been shown to play a role in detoxifying H_2O_2 and more recently we have found that it can interact with the redox and DNA repair protein APE1. However, the functional interplay between Prdx1 and APE1 interaction has not been resolved. Herein, we show that Prdx1 is required to reduce cytosolic APE1 while APE1 facilitates the conversion of dimeric Prdx1 to the monomeric form in response to H_2O_2. In the absence of APE1, H_2O_2-induced conversion of Prdx1 is blocked, suggesting APE1 initiates the conversion and consequently becomes reduced. We provide a model to explain these events in response to H_2O_2

Introduction

Reactive oxygen species (ROS) such as H_2O_2 are regarded as the inevitable but unwanted by-product of oxidative metabolism or respiration in cells. ROS are also produced when cells are exposed to ionizing radiation, ultraviolet light and toxic chemicals. Cells can use H_2O_2 as a second messenger molecule to initiate transcriptional responses to mitigate damages or maintain the redox homeostasis in the cells (158, 159), as exemplified by the observation in fungi, following exposure to H_2O_2, whereby an AP-1-like transcription factor promotes expression of ROS defense and DNA repair enzymes. In pathogenic fungi, this is a vital response to ROS triggered by the host immune cells (160, 161). In mammalian cells, ROS can regulate transcription factor activity by changing redox status of specific cysteine that usually locates in DNA-binding domain of the transcription factor. For instances, NF-κB and AP-1 require reducing status for DNA binding *in vitro*, in contrary *in vivo* they are activated by ROS-inducing reagents such as H_2O_2, bleomycin and ionization (162). Hence, H_2O_2 signals are implicated in regulation of fundamental processes, including cell division, differentiation, migration, and death.

Peroxiredoxin 1 (Prdx1) is a member of 2-Cysteine peroxiredoxins (Prxs) consisting of four isoforms (Prdx1-4) in mammalian cells, which are highly abundant peroxidase enzymes that play important roles in responses to H_2O_2. Prdxs execute their protective role as antioxidants in cells through their peroxidase activity, whereby H_2O_2 is broken down and scavenged. Prdx1 can also play essential roles in maintaining genome stability, protecting against cancer and promoting longevity (28). In addition, Prdx1 has chaperone and signaling activities (163). In the cytosol of mammalian cells, the Prdx1 appears to be involved in the

redox regulation of cell signaling and differentiation by regulating the levels of H_2O_2 (164-166). However, in many cases, the H_2O_2-sensing/-signaling mechanisms are poorly defined, particularly in mammalian cells with an abundance of antioxidants. Therefore, understanding how H_2O_2 targets signaling proteins in cells rich in Prdxs draws a considerable interest (167).

APE1 was identified as an essential base excision repair (BER) enzyme that repairs oxidative DNA damages resulting from oxidative stress such as ionizing radiation. In addition to its role in repairing DNA lesions, APE1 can perform another function by enhancing the DNA binding activities of the AP-1 family of transcription factors via a redox-dependent mechanism (109, 168), which is mediated by reducing a conserved cysteine residue located at the DNA-binding domains of c-Fos and c-Jun (169). It can also modulate the activities of other classes of transcription factors that regulate cell growth, differentiation, survival, and death including NF-kB, p53, Egr-1, c-Myb, HLF, and Pax-8 (103, 170). Therefore APE1 is speculated to influence multiple cancer survival mechanisms, including growth, proliferation, metastasis, angiogenesis, and stress responses by its reduction-oxidation activity (171). In our previous study, we found APE1 to interact with Prdx1. Although the DNA repair and transcription factor reducing properties of APE1 are well known, other fundamental mechanisms via which it may regulate redox cell signaling, and influence cell fate are yet to be elucidated.

Herein, we report that Prdx1 exists in a dimeric form which is converted to the monomeric form in response to H_2O_2. We further show that APE1 is required to facilitate this conversion and that during this process APE1 becomes reduced.

Materials and Methods

Cell culture

Human HeLa and HepG2 (liver hepatocellular cells) cell line were kindly provided by Dr.Elliot Drobetsky (University of Montreal).293T, HeLa and HepG2 were cultured in Dulbecco's Modified Eagle Medium(DMEM) (Wisent Inc.) complemented with 10% of fetal bovine serum (FBS) (Wisent Inc.) and 100U/ml penicillin, and 0.1 mg/ml streptomycin. Cells were incubated at 37°C and 5% CO_2.

Antibodies and reagents

APE1 rabbit mAb(cat# 2851-1, Epitomics), pAb anti-APE1 antibody(NB100-101,Novus Biologicals), mAb anti-peroxiredoxin1 antibody(NBP1-95676, Novus Biologicals), Prdx1 rabbit Ab(#8732S,cell signalling),goat anti-mouse IgG pAb(HRP conjugate)(cat#ADI-SAB-100,Enzo), goat anti-rabbit IgG pAb(HRP conjugate)(Cat#ADI-SAB-300-J,Enzo),mouse-anti-human Thioredoxin1(Cat#559969,BD pharmingen), Iodoacetic acid(IAA,sigma) hydrogen peroxide (sigma)

Plasmid constructs

pOZ-FH-N contains a Kozak sequence, an initiation methionine, and FLAG and HA tags. pOZN-Prdx1 were constructed by firstly amplifying human Prdx1from K562 cell cDNA by PCR with the primers pOZN-FH-Prdx1F(5'-GCCGGAGGACTCGAGatgtcttcag gaaatgctaa aattggg-3') and POZN-FH-Prdx1R(5'-TCAGTCACGATGCGGCCGCtcacttctgcttggagaaatattcttt-3'), and then subcloned into pOZ-FH-N after Xhol and Notl digestion.

To knockdown Prdx1, shRNA Prdx1 C1-2 was constructed based on MSCV-LTRmiR30-PIG (LMP) vector (Thermo Scientific) following the Manufacturer's instructions.

It was sequenced for confirmation before usage. The hairpin shRNA template is as following, sense and antisense sequences were underscored.

C1(HP_7670)TGCTGTTGACAGTGAGCGACCAGATGGTCAGTTTAAAGATTAGTGAA
GCCACAGATGTAATCTTTAAACTGACCATCTGGCTGCCTACTGCCTCGGA

To knockdown APE1, pSIREN shAPE1 1-1 was constructed using vector RNAi-Ready pSIREN-RetroQ-ZsGreen (Clontech Laboratories, Inc.) following the Manufacturer's instructions: pSIREN shAPE1 1-1 Oligos APE1-shRNA-UP1and APE1-shRNA-DWN1 are used for pSIREN shAPE1 1-1 targeting 5'-TGACAAAGAGGCAGCAGGA-3' in APE1; Oligos sequences are as following:

APE1-shRNA-UP1:

5'-GATCCGTGACAAAGAGGCAGCAGGATTCAAGAGATCCTGCTGCCTCTTTGTCATTTTTTG-3'

APE1-shRNA-DWN1:

5'-AATTCAAAAAATGACAAAGAGGCAGCAGGATCTCTTGAATCCTGCTGCCTCTTTGTCACG-3'

Thioredoxin1 knockdown was achieved by transient transfection of shTRX11-259 gifted by Dr. Priyamvada Rai from University of Miami.

Retrovirus preparation and infection

293T cells were plated in 10cm tissue cell culture plates day prior to transfection at 70 % confluence. Next day retroviral vectors were cotransfected with pVSV-G and pCL-Eco retrovirus packaging vector using Calcium phosphate transfection method. Supernatants were collected 36-48 h after transfection, filtered through a 0.45 μm filter and used directly to infect target cell lines.

To infect HeLa, HeLaS or HepG2 cells, cells were plated into 10cm tissue cell culture plates day prior to infection at 35% confluence. Next day the old media was removed and

replaced with viral supernatants/fresh media mixture (1:1) supplemented with 0.4μg/ml Polybrene® (Sigma-Aldrich). 24h after infection, the viral media were removed and cells were washed at least twice with 1xPBS and added fresh media. Cells were subjected to selection 48h after infection.

Redox western blot

For 6-well plates, cells were washed once with 2ml 1XPBS rapidly and lysed into 350μl RIPA buffer (150 mM sodium chloride, 1.0% NP-40, 0.5% sodium deoxycholate, 0.5% SDS, 50mM Tris, pH 8.0) including 10-20mM IAA(iodoacetic acid) and protease inhibitor cocktails. Each sample was subject to 10s sonication at 30% magnitude and spun down for 5mins at maximum speeds to remove debris. Proteins were quantified and mixed with non-reducing Laemlli Buffer (5X) [Bromophenol blue (0.25%), Glycerol (50%), SDS (10%), Tris-Cl (0.3 M, pH 6.8)] before loading onto SDS-PAGE gel. The following procedures are the same as regular western blot.

Purification of thiol-trapped Prdx1 from HeLa cell extracts

pOZN and pOZN-Prdx1 expressing HeLa cells from a 15 cm plate were treated with or without 1mM H_2O_2 for 0.5h. Afterwards cells were harvested by trypsin-EDTA and washed twice in 1 x PBS, resuspended in 1ml Lysis buffer [20 mM Hepes (K+), pH 7.6, 0.3 M KCl, 1.5 mM $MgCl_2$, 0.2 mM EDTA, 0.3% (v/v) NP-40, 50mM iodocetic acids, 0.2 mM PMSF, 0.5mM benzamidine, and 1 μg/mL each of leupeptin, aprotinin, and pepstatin], and sonicated for 10sec. Samples were incubated at 50 Celsius degree for 0.5h. Insoluble material was pelleted 15 min at 13,000 rpm in a microcentrifuge, and the soluble extract was dialyzed overnight against 4L of Dialysis buffer [20 mM Hepes (K+), pH 7.6, 100mM KCl, 1.5mM $MgCl_2$, 0.2mM EDTA, 0.2mM PMSF, 0.5mM benzamidine, and 1 μg/mL each of leupeptin,

aprotinin, and pepstatin]. Insoluble material was pelleted, and the soluble lysate was added 30µl of FLAG (M2) resin (Sigma) after 50 µL aliquots were taken for input, following incubation for 4 h at 4°C, The beads were pelleted and washed with 3 x 1 mL of Wash buffer [20 mM Hepes (K+), pH 7.6, 0.1M KCl, 1.5 mM $MgCl_2$, 0.2 mM EDTA, 0.01% (v/v) NP-40,10%(v/v) glycerol, 0.2mM PMSF, 0.5mM benzamidine, and 1µg/mL each of leupeptin, aprotinin, and pepstatin]. Bound proteins were eluted by Elution buffer [10mM Tris pH 7.9, 10mM EDTA, 1%SDS], and the beads were pelleted at 2000RPM for 1mins. The supernatants were mixed with non-reducing loading buffer for SDS-polyacrylamide gel electrophoresis, silver staining and western blot analysis. Prdx1 dimer and monomer were cut for mass spectrometry (IRIC, University of Montreal). Before mass spectrometry, samples were reduced by DTT that was followed by chloroacetamide to alkylate the free cysteines.

Results

Sublethal H_2O_2 converts Prdx1 from dimer to monomer in dose/time-dependent manner

To test the effect of H_2O_2 on Prdx1 *in vivo*, we used 2 mM H_2O_2 containing complete DMEM media to treat HepG2 cells for different times (0 to 120 mins). Non-reducing western blots showed that Prdx1 existed as a dimer under normal condition while H_2O_2 treatment converts dimeric Prdx1 into the monomeric form in a time-dependent manner (Fig.1A). Cleavage of Caspase-3 and PARP-1 by caspases is considered to be a hallmark of apoptosis (172, 173). To monitor for this event in our cells, so we probed the same samples with anti-PARP-1 and caspase-3 in western blot, in which we found neither protein was cleaved (Fig.1A). This suggests that the treatment conditions were not lethal. Next we used different doses of H_2O_2 to treat HeLa and HepG2 cells for 1.5h. After treatment cells were fractionated into cytosol

and nuclear extracts. Non-reducing western blot analysis showed the conversion of Prdx1 driven by H_2O_2 occurred in both cytosol and nuclear extracts of HeLa and HepG2 cells in dose-dependent manner (Fig.1B-C). In addition, it also showed cytosolic Prdx1 was converted into monomers at a more rapid rate than that found in nuclear extracts. The rate of conversion differed between HeLa and HepG2 cells, which may be attributed to different tolerance of various cell lines to stress.

Given that Prdx1 is a member of peroxiredoxin family consisting of six mammalian isoforms and these proteins show striking amino acid sequence similarities (174), to exclude other isoforms, we cloned Prdx1 cDNA into pOZ-FH-N to make pOZN-FH-Prdx1 construct. We expressed pOZN-FH-Prdx1 in HeLa by retroviral system (Fig.2A). pOZN-FH-Prdx1 expressing HeLa and its empty vector control pOZN were treated with or without 1 mM H_2O_2 for 1.5h. After treatment we immunoprecipitated FH-Prdx1 from cytosolic extracts with anti-FLAG resin, the eluents of which was subject to non-reducing western blot probed with anti-HA (Fig.2B). The result showed ectopic FH-Prdx1 converted from dimer to monomer after 1mM H_2O_2 treatment for 1.5h although a few of Prdx1 monomer appeared in untreated HeLa cells expressing pOZN-FH-Prdx1, which could be resulted from stress during the cell fractionation process. Thus, the ectopic Prdx1 behaved the same as endogenous Prdx1 in response to H_2O_2 treatment. Taken together, the results suggest that sublethal doses of H_2O_2 can convert Prdx1 from dimer to monomer in a time-dependent manner.

Conversion of Prdx1 from dimer to monomer is ascribed to C52/173 hyperoxidation by H_2O_2

To accurately determine which cysteine is responsible to form Prdx1 dimer, we mutated 4 cysteine of Prdx1 into alanines individually and in combination (C52A, C71A, C83A, C173A,

C52/173A) and expressed them in HeLa cells using retroviral system. Except for C71A, all other Prdx1 mutants and wild type (wt Prdx1) expressed very well. Redox western blot analysis showed that C52/173A completely abolished dimer formation while C52A and C173A still formed dimers but less than wild type, which suggested that the Prdx1 dimer is formed by C52/173 disulfide bond and C52A or C173A single mutation impaired their ability to form dimers with endogenous Prdx1 (Fig.3). 1mM H_2O_2/1h treatment caused wild-type Prdx1 conversion from dimer to monomer that resembles C52/173A (Fig.3), which implied H_2O_2 oxidized C52/173 residues into hyperoxidation status such as sulfenic acid (Cys–SOH) or sulfinic acid (Cys–SO_2H).

For further confirmation, we purified Prdx1 dimer and momoner via immunoprecipitation with anti-FLAG resins followed by non-reducing SDS-PAGE after iodoacetic acids (IAA) was used to trap free thiols in samples (Fig.4A-B). After treatment, the IAA-treated samples were reacted with DTT to prevent the reduced sulfenic/sulfenic groups from reconverting into thiols, and were subsequently treated with chloracetamide to alkylate the free cysteines prior to mass spectrometry analysis. Therefore, in mass spectrum iodoacetic acid can produce carboxymethyl (+58) modification while chloroacetamide produces carbamidomethyl (+57) modification. The results showed Prdx1 dimer were carboxymethylated on cysteine 83 whereas all cysteines underwent carbamidomethyl (+57) modification in Prdx1 monomers. This indicates Prdx1 monomer is hyperoxidized. Given the fact that human peroxiredoxin I inactivates during catalysis as the result of the oxidation of the catalytic site cysteine to cysteine-sulfinic acid(175), our observation that Prdx1 converts from dimer to monomer after H_2O_2 treatment is consistent with Prdx1 undergoing a redox catalytic function.

Cytosolic APE1 reduction requires Prdx1 and is coupled with Prdx1 hyperoxidation

Prdx1 is an important antioxidant for H_2O_2 scavenger. We found Prdx1 interacted with APE1 in our previous study. To determine if Prdx1 prevents APE1 from being oxidized by H_2O_2, we created Prdx1 knockdown HepG2 cells, namely HepG2 C1-2 (Fig.5A). Prdx1 knockdown HepG2 C1-2 cells and its empty vector control HepG2 LMP were treated with and without 2m MH_2O_2 for 1.5h. After treatment, cells were collected and fractionized into cytosol and nuclear extract, which were then subjected to non-reducing SDS-PAGE. Redox western analysis showed cytosolic APE1 of HepG2 LMP to have a slower mobility corresponding to the reduced form of APE1 following H_2O_2 treatment, but which did not occur in the Prdx1 knockdown HepG2 C1-2 cells. In addition, it seems that APE1 in the nucleus did not change significantly in response to the same treatment and remained in the reduced state (Fig.5B). Under these conditions, Prdx1 was converted from the dimer to the monomer and became hyperoxidized (Fig.5C). We speculate that Prdx1 reduces cytosolic APE1 and Prdx1 becomes hyperoxidized.

Thioredoxin 1 is required for Prdx1 hyperoxidation in response to H_2O_2

Prdx1 is a typical 2-Cys and an obligate dimer. During catalysis, the peroxidatic cysteine (C_P-SH) is oxidized to a sulfenic acid (C_P-SOH), which then reacts with the resolving cysteine (C_R-SH from the other subunit of the dimer) to form a disulfide, which is in turn can be reduced by thioredoxin or other enzymes (153). We down-regulated thioredoxin 1 by transiently transfecting 293T cells with plasmid shTRX1 1-259 and found that the conversion of Prdx1 dimer into monomer was diminished in response to H_2O_2 in thioredoxin 1 knockdown cells compared to empty vector control (Fig.6C). This observation indicates that thioredoxin 1 is required to efficiently reduced the disulfide bridge of Prdx1 dimer, which is

consistent with *in vitro* study (175). This finding further implies our observation that Prdx1 converts from dimer to monomer after H_2O_2 treatment is a consequence of Prdx1 catalysis

APE1 mediated Prdx1 hyperoxidation independent of APE1 Cys65 residue in response to H_2O_2

Except for its AP endonuclease activity, APE1 also possesses redox function with its cysteine 65 residue(102). To explore the possibility that APE1 is involved in the Prdx1 catalysis process, we knockdowned APE1 in HepG2 and 293T cells. APE1 knockdown significantly diminished Prdx1 hyperoxidation in both cell lines compared to control cells (Fig.6B-C). This finding suggests APE1 mediates Prdx1 hyperoxidation. To investigate whether cysteine 65 of APE1 plays roles in Prdx1 conversion, we used 100 μM of E3330, APE1 redox specific inhibitor (176, 177) to pre-treat HepG2 for 24h. After pre-treatment, HepG2 were treated with 2mM H_2O_2 for 30 mins. We found that although E3330 treatment caused APE1 alteration compared to non-treatment (Fig.7A). E3330 did not alter the conversion of Prdx1 (Fig.7B), which indicated cysteine 65 of APE1 may not contribute to the conversion of Prdx1 in response to H_2O_2. Overexpression of APE1C65A mutant did not alter Prdx1 conversion as well after H_2O_2 treatment (Fig.7C), which is consistent with the finding from E3330 inhibition experiment. Both experiments indicate that APE1 plays roles in Prdx1 hyperoxidation independent of APE1 Cys65 residue in response to H_2O_2. So it is inferred that APE1 mediated Prdx1 hyperoxidation independent of APE1 Cys65 residue in response to H_2O_2. It is possible that the redox chaperon function of APE1 may be important in the conversion of Prdx1 dimer to monomer in response to H_2O_2.

Discussion

Mammalian cells produce H_2O_2 to mediate diverse physiological responses such as cell proliferation, differentiation, and migration. This has implicated cellular "redox" signaling in regulating normal processes as well as disease progression, including angiogenesis, oxidative stress and aging, and cancer (159). Many mammalian cell types can produce H_2O_2 in response to stimulation for example by growth factors (PDGF, EGF), chemical oxidants and ionizing irradiation (166, 178). H_2O_2 is a distinct messenger molecule because it acts not by binding to ligands/effectors directly, but instead acts by oxidizing critical cysteine residues of its target proteins, for instances, the inhibition of protein-tyrosine phosphatases (PTPs), the tumor suppressor PTEN (phosphatase and tensin homolog) and peroxiredoxin I (175, 179). Peroxiredoxin 1 is one of peroxiredoxin family comprised of six isoform that catalyze peroxide reduction of H_2O_2, organic hydroperoxides and peroxynitrite as antioxidants. How H_2O_2 modulates cell signaling through oxidizing Prdx1 is not clear. However, in our previous study, we found that APE1 interacts with Prdx1. So the question how APE1 regulate Prdx1 mediated cell response to H_2O_2 is of great interest.

Besides its DNA repair function, APE1 serves as a redox coactivator of many transcription factors, including the early growth response protein-1 (Egr-1), nuclear factor-kB (NF-kB), p53, hypoxia-inducible factor (HIF-1a), CREB, AP-1 to regulate gene expression (130). So APE1 is regarded as a multifunctional protein. In this study, we found in the cytoplasm of normal cell that almost all APE1 is reduced in response to H_2O_2 but not if Prdx1 is knockdown in the cells. This indicates APE1 reduction requires Prdx1 that is accompanied with Prdx1 hyperoxidation and APE1 may be one substrate of Prdx1 in vivo. Although this is found mainly in cytosol, given the translocation from cytosol to nucleus of APE1 when cells

are exposed to oxidative stresses, it seems logical that H_2O_2 transduces signalling to APE1 via Prdx1 to propagate its effects. This is also consistent with the finding that inducible AP-1 DNA binding activity in response to IR is triggered by cytoplasmic factor. Immunodepletion of Ref-1 from nuclear extracts showed inhibition of inducible AP-1 DNA binding activity in response to IR (180). Moreover, our finding also recapitulate what happens to yeast *Schizosaccharomyces pombe*, the thioredoxin peroxidase activity of the 2-Cys Prx, Tpx1, is required for the H_2O_2-induced activation of the AP-1-like transcription factor Pap1. Accordingly, hyperoxidation of Tpx1 actually prevents Pap1 activation (181).

It is noteworthy that we also find APE1 regulate H_2O_2-Prdx1 signalling transduction, which is demonstrated by the experiment that APE1 knockdown prevent Prdx1 conversion from dimer to monomer and consequently hyperoxidized in response to H_2O_2. This further implies that APE1 may be a substrate of Prdx1 and central target of H_2O_2 mediated signalling transduction. However, we cannot exclude the possibility that APE1 acts as redox chaperon (114), because overexpression of APE1 C65A mutant, assumed redox inactivation, does not impair the process after exposure to H_2O_2. We find TRX1 knockdown also prevent Prdx1 conversion from dimer to monomer and consequent hyperoxidation in response to H_2O_2, which implicates the involvement of TRX1 in this process. In *S. pombe* Prxs can promote H_2O_2 signaling by stimulating the oxidation of thioredoxin. Thioredoxin provides the electrons that reduce Prxs as part of their catalytic cycle. Tpx1 disulfides are the major substrate for the single cytoplasmic thioredoxin, Trx1. Coupling of the peroxidase activity of 2-Cys Prx to thioredoxin provides a mechanism for the H_2O_2-dependent regulation of multiple thioredoxin substrates (181). Therefore we think this mechanism is conserved in mammalian cells based on our observation. For decades, it has been demonstrated that exposure to IR and

other oxidants immediately results in an elevated NADPH pools caused by stimulating glucose metabolism through the pentose cycle (182). NADPH act as a cofactor for reductive biosynthetic pathways and is essential for oxidative defense, since it replenishes the glutaredoxin and thioredoxin systems (183). APE1 promotes H_2O_2 mediated signalling by accelerating Prdx1 hyperoxidation, which is coupled with accelerating NADPH usage. So it seems plausible to infer that APE1 indirectly mobilize and harness the anti-oxidant defence and coordinate oxidation homeostasis, H_2O_2 mediated signalling and transcription regulation.

Legends:

Figure 1 Prdx1 converted from dimer to monomer after exposure to H_2O_2. (A) HepG2 cells were treated with 2mM H_2O_2 for indicated time. After treatment cells were lysed into 10mM IAA containing RIPA buffer. Samples were quantified and subjected to western blot analysis probed with anti-Prdx1 (upper), anti-PARP1 (middle) and anti-caspase3 (bottom), respectively. HeLa cells **(B)** and HepG2 cells**(C)** were treated with indicated dose of H_2O_2 for 1.5h. Afterwards cells were typsinized and washed once with 0.1mM IAA-containing PBS. Cytosol and nuclear fractionation was done with IAA (0.1mM) containing hypotonic buffer. All samples were quantified by Bradford and adjusted to same concentration, then separated in non-reducing SDS-PAGE and blotted with anti-Prdx1.

Figure 2 Ectopic Prdx1 converted from dimer to monomer after exposure to H_2O_2. (A) The expression of pOZN-prdx1 in HeLa cells. **(B)** HeLa cells that express pOZN or pOZN-prdx1 were treated with or without H_2O_2 (1mM) for 1.5h, cells were harvested and suspend in IAA containing hypotonic buffer. HeLa cytosolic extract were prepared in 50mM IAA containing hypotonic buffer, then dialysed and spun down at 13000RPM for 10mins. Then IP were done with anti-Flag, Elute of IP were separated on non-reducing SDS-PAGE, probed with anti-HA.

Figure 3 cysteine 52/173 residue is responsible for Prdx1 dimer. HeLa cells were infected with Prdx1 wild type (wt) and its mutants, after two rounds of anti-IL2Rα selection, cell were treated with and without 1mM H_2O_2 for 1h. After treatment, cells were lysed into 10mM IAA-

containing RIPA buffer. Samples were quantified and separated on non-reducing 10%SDS-PAGE gel. The blot were probed with anti-HA and beta-actin antibodies.

Figure 4 Purification of thiol-trapped Prdx1 from HeLa cell extracts. pOZN-Prdx1 expressing HeLa cell were treated with or without 1mM H_2O_2 for 0.5h.The procedure is detailed as **Materials and Method.** Eluents were separated in the same non-reducing 12% gradient SDS-PAGE gel in duplicate. One part was for western blot probed with anti-Prdx1 **(A);** another part was for silver staining **(B).**

Figure 5 Cytosolic APE1 reduction required Prdx1 and coupled with Prdx1 hyperoxidation. (A) Prdx1 knockdown in HepG2, which was validated by western blot probed with anti-Prdx1 and beta-actin antibodies. **(B-C)** Prdx1 knockdown HepG2 C1-2 and empty vector control HepG2 LMP were treated with 2mM H_2O_2 for 1.5h. After treatment cells were fractionized into cytosol and nuclear extracts. Samples were quantified and separated on non-reducing 10%SDS-PAGE gel. The blots were probed with anti-APE1 **(B)** and anti-Prdx1**(C)** antibodies.

Figure 6 APE1 and TRX1 knockdown prevent Prdx1 conversion from dimer to monomer. (A) APE1 was knockdowned by shAPE11-1 and shAPE12-1 in HepG2, which were validated by western blot probed with anti-APE1 and anti-β-actin. **(B)** APE1 knockdown HepG2 and HepG2 shLuc (control) were treated with and without 2mM H_2O_2 for 0.5h, then lysed into 10mM IAA containing RIPA and separated on 10% non-reducing SDS-PAGE, the same blot was probed with mono-anti Prdx1 Ab and β-actin, respectively. **(C)** 293T cells were plated in 6-well plate 1 day prior to transfection. One day after cells were transfected with 1ug of each indicated DNA using lipofactamine^{2000}. 4 days after transfection, cells were treated

with or without 1mM H_2O_2 for 0.5h in complete media, and removed the media after treatment. Cells were lysed into 10mM IAA containing RIPA buffer. Protein was quantified and then separated on 10% non-reducing SDS-PAGE. The same blot was probed with anti-Prdx1 and anti-actin sequentially.

Figure 7 E3330 and APE1 C65A mutant overexpression cannot affect Prdx1 conversion from dimer to monomer after exposure to H_2O_2. HepG2 was treated with or without 100μM E3330 or DMSO (control) for 24h. After pre-treatment, cells were treated with or without 2mM H2O2 for 30min. Then cells were scraped into 1mM EDTA-PBS, and then lysed into 10mM IAA containing RIPA buffer. Sample were quantified and adjusted to same concentration before separating on non-reducing 10%SDS-PAGE. The blots were probed with anti-APE1 **(A)** and anti-Prdx1 **(B)**; β-actin was as loading control. **(C)** 293T was plated in 6-well plate 1 day prior to transfection. Next day cells were transfected with 1ug of each indicated DNA using lipofactamine. 3 days after transfection, cells were treated 3ml complete media with or without 1mM H_2O_2 for 0.5h in complete media, and removed the media after treatment. Cells were lysed into 10mM IAA containing RIPA buffer. Protein was quantified and then separated on 10% non-reducing SDS-PAGE. The same blot was probed with anti-Prdx1 and anti-actin sequentially.

Figure 8 Proposed work model. Prdx1 is inactivated in response to H_2O_2 by hyperoxidizing C52/173 residue, which could be reversed by thioredoxin1/ sulfiredoxin1. APE1 become via Prdx1. APE1 may be one substrate of Prdx1. Therefore H_2O_2 signals are transduced into APE1. APE1 as a central target of H_2O_2 signals reversely harness the rate of transduction.

Figures:

Prdx1 converted from dimer to monomer after exposure to H_2O_2

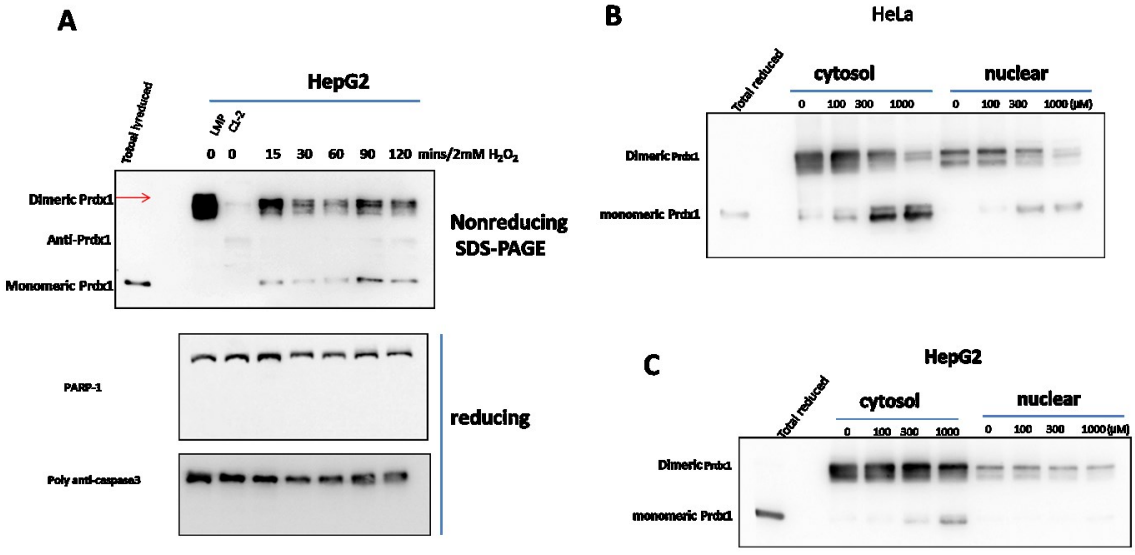

Figure 1

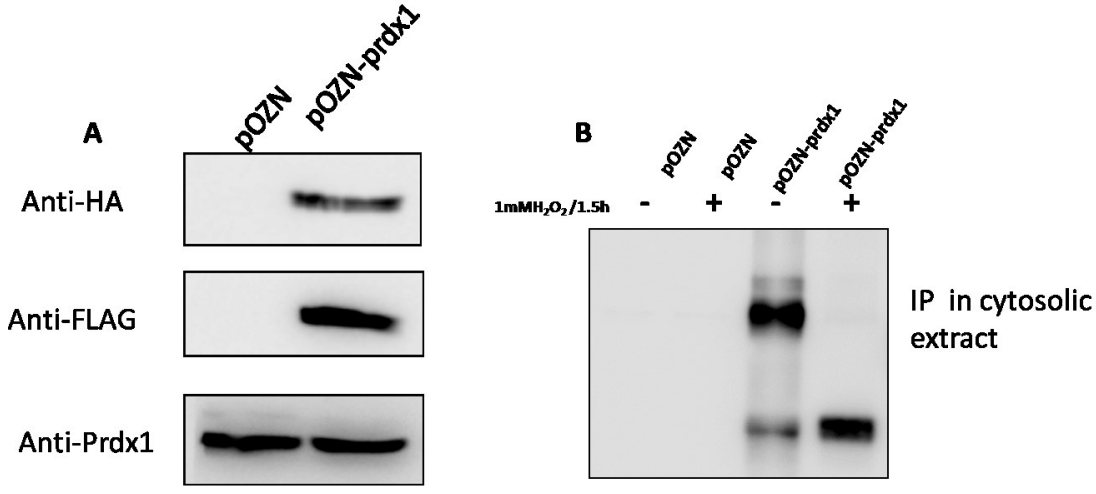

Figure 2

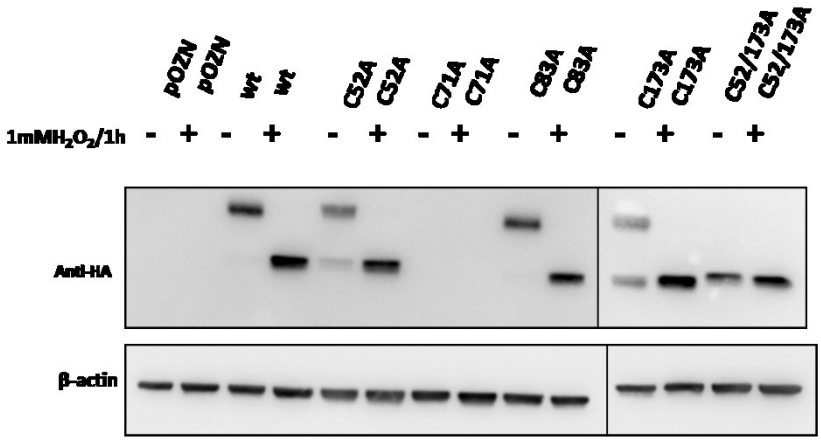

Figure 3

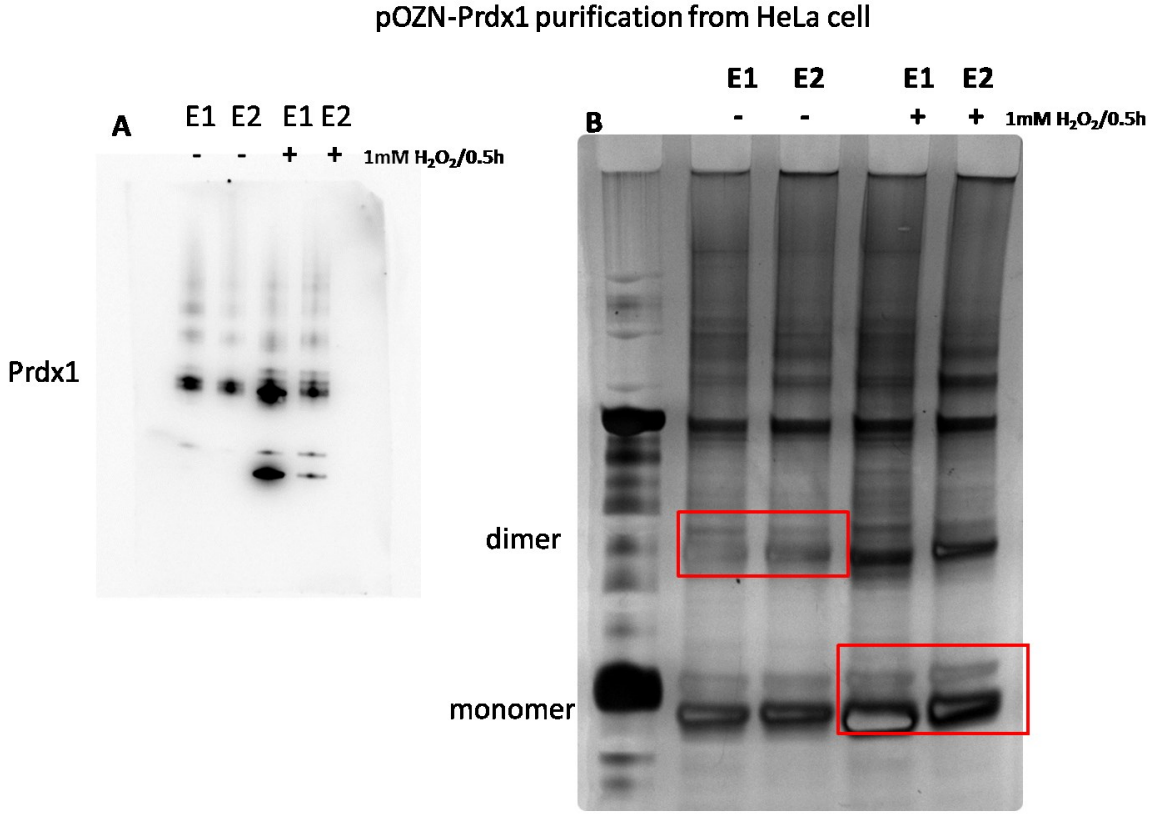

Figure 4

Cytosolic APE1 reduction required prdx1 and coupled with Prdx1 hyperoxidation

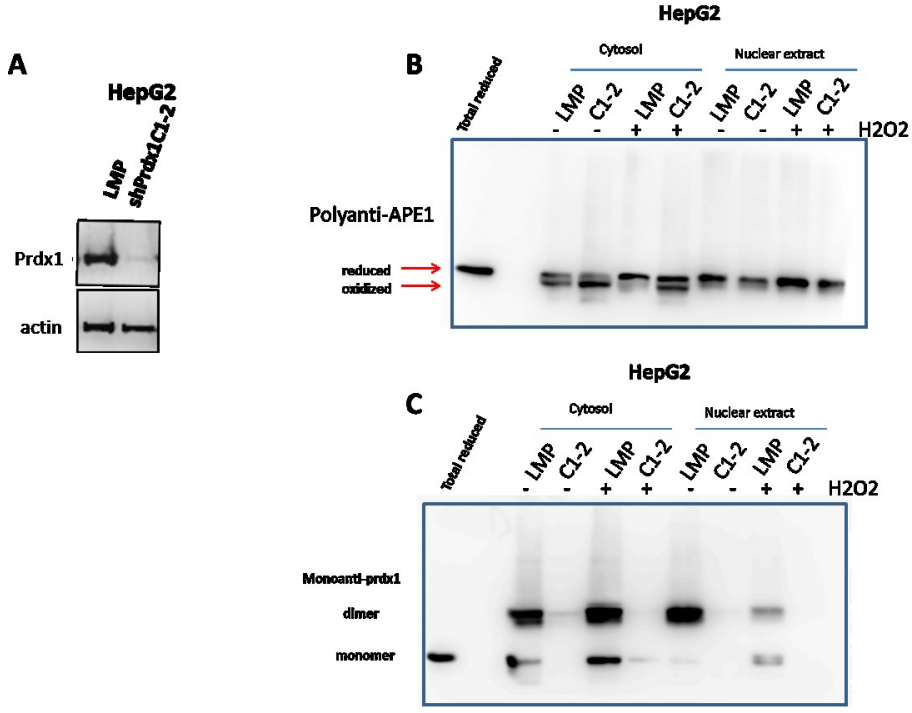

Figure 5

APE1 and TRX1 knockdown prevent Prdx1 conversion from dimer to monomer

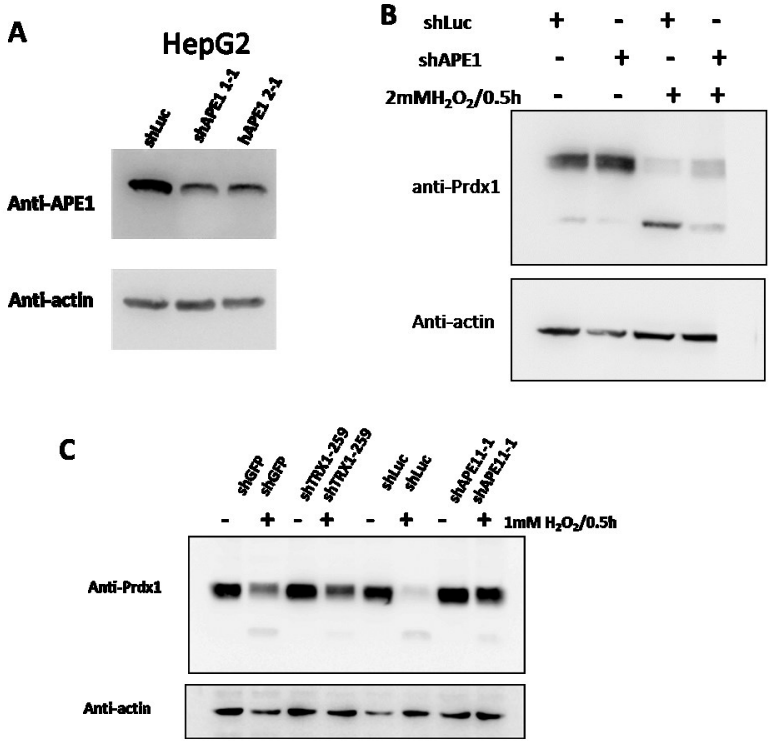

Figure 6

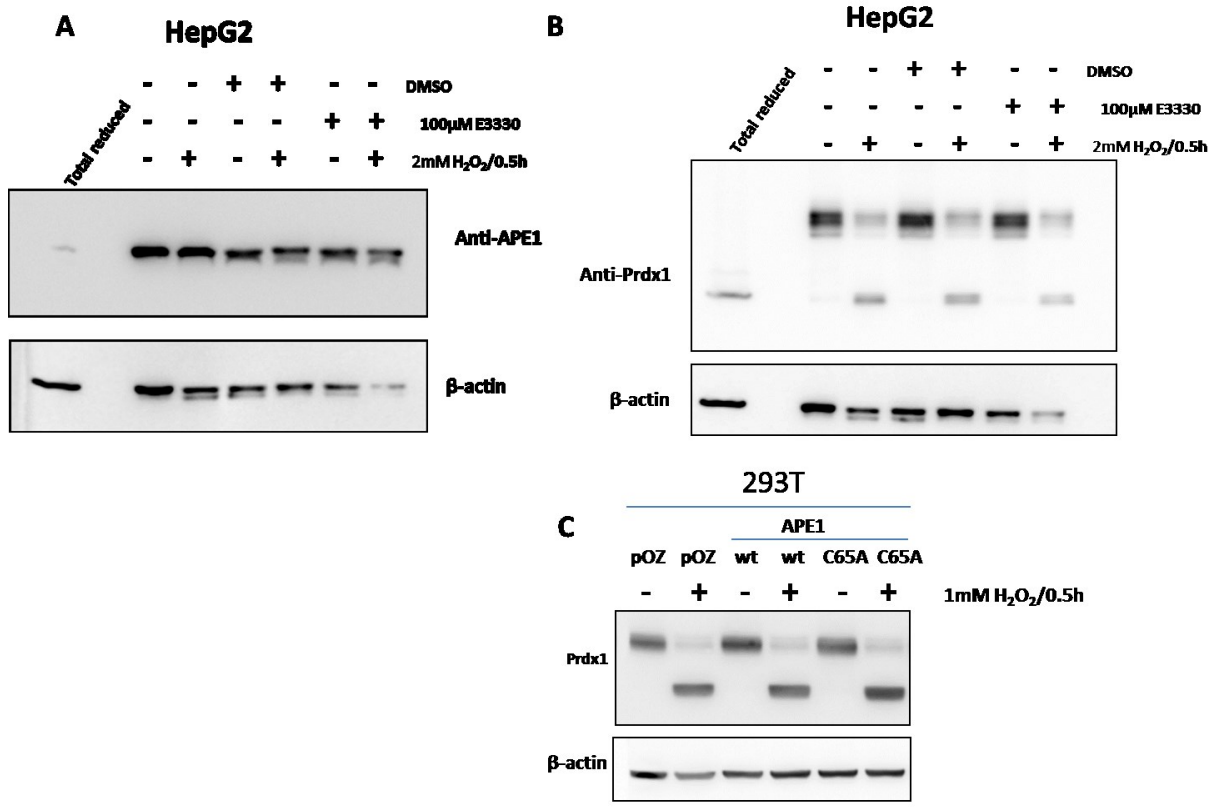

Figure 7

Working Model

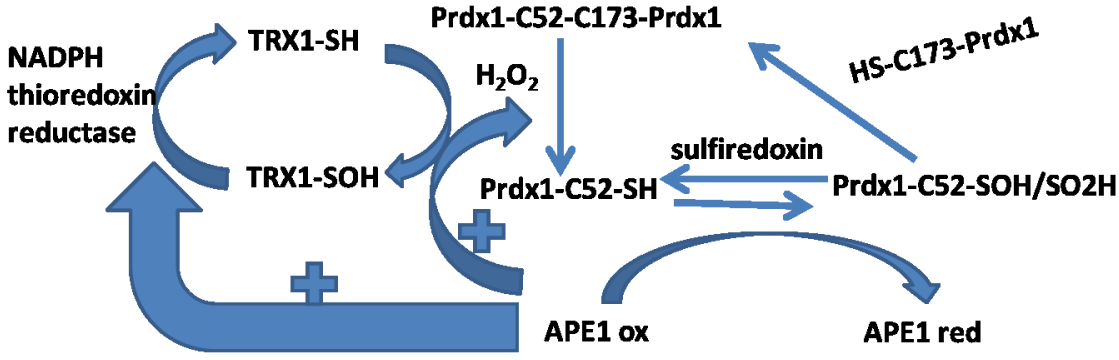

Figure 8

4. Conclusion

To conclude, in this study we find that oxidative stress alters APE1 interactome using immunoprecipitation combined with mass spectrometry analyses. For instances, it seems that H_2O_2 disrupt the interaction between APE1 and other proteins including NPM1, PRDX1 and RPS19 in the nucleus, while in cytosol APE1 loss some interacting partners and gain new ones in response to H_2O_2. As discussed in manuscript 1, these genes are involved in important life events from metabolism, antioxidation, translation to energy regeneration. These findings support our hypotheses that APE1 could play specific role by changing its interacting partners, and thus participates in multiple biological functions besides DNA repair and gene regulation. The APE1 knockout is lethal to mice (184), although the axact nature of this lethality is not known. However, this could be explained by its interaction with multiple partners and thus the loss of APE1 would lead to a combination of various phenotypes. Current studies in other laboratories are developing inhibitors to block APE1 DNA repair functions in order to specifically sensitize tumor cells that are already defective in at least one other DNA repair pathway besides BER. The goal of this approach is to spare normal tissues and cells from the lethality of genotoxic chemotherapeutic drugs, while targeting the tumors. We believed that it is also relevant to target sites of APE1 that specifically interact with proteins that could alter biological functions in tumor cells.

We validate APE1-Prdx1 interaction by IP and FPLC in cytosol and nuclear fractions under physiological condition and these two proteins maintain interaction in the cytosol despite treatment with H_2O_2, unlike the situation in the nucleus. Prdx1 knockdown neither affect APE1 abundance nor its AP endonuclease activity, but Prdx1 knockdown facilitates APE1 detection in the nucleus by immunofluorescence assay. Although Prdx1 knockdown

indeed causes translocation of a fraction of APE1 from the cytosol into the nucleus, this amount of translocated protein cannot entirely explain the enhanced immunofluorescence detection of APE1 in the nucleus. We think that APE1, in the absence of Prdx1, is more accessible to the anti-APE1 antibodies and thus facilitate APE1 detection. Given that Prdx1 can bind to DNA and RNA (27, 141), it is possible that Prdx1 knockdown could simple cause remodeling of the chromatin and facilitate APE1 exposure to the antibody, although we have no evidence to support this possibility. In addition, we find that Prdx1 knockdown up-regulate IL-8 secretion under physiological condition and further enhanced by the oxidative stress caused by H_2O_2. Since the APE1 knockdown abrogates IL-8 induction, we propose that Prdx1-APE1 interaction in nucleus may suppress IL-8 expression. IL-8 is a pro-inflammatory CXC chemokine. It is well documented that overexpression of IL-8 by tumor cells, often elicited in response to chemotherapeutic interventions or environmental stresses such as hypoxia. Our finding that Prdx1 knockdown induces IL-8, may suggest that the cells use a backup mechanism to maintain a defense against oxidative stress as IL-8 induction leading to the stimulation of NF-kB involved in protecting cells against oxidative stress. This might therefore explain why Prdx1 knockdown cells in our studies are not sensitive to H_2O_2. The increased synthesis and secretion of IL-8 from tumor cells has wider significance to the tumor microenvironment and metastasis given the characterized expression of CXCR1 and CXCR2 receptors on cancer cells, endothelial cells, and neutrophils/tumor associated macrophages, which underpin the significance of this chemokine in promoting the malignant progression of cancer (155). Although IL-8 can promote cell invasion, migration, proliferation and survival of cancer cells through autocrine signaling pathway, tumor-associated macrophages secreted additional growth factors elicited by IL-8 will be a further impetus for cell proliferation and

cancer cell invasion at the tumor site. This could partly account for the cancer predisposition of Prdx1 knockout mice and why APE1 would be a potential anticancer target as it would block the expression of IL-8.

In addition, we observed that sublethal dose of H_2O_2 acts as a signal to trigger the conversion of the dimeric form of Prdx1 into the monomeric form and this exists in the reduced state. The monomeric reduced form of Prdx1 then serves to reduce the oxidized APE1 into its reduced state and during this process the monomeric Prdx1 finally becomes oxidized. In the cells, knockdown of APE1 prevents the conversion of the dimeric form of Prdx1 into the monomer. We postulate that APE1 could regulate the conversion of dimeric Prdx1 into the monomeric form by one of the following mechanisms. First, APE1 could upregulate Trx1 to convert Prdx1 dimer to the monomer. Second, APE1 is the actual substrate and thus in its absence this will block the forward reaction. A third possibility is that APE1 could serve as a redox chaperone in order to promote the conversion of the dimeric Prdx1 to the monomer. Future studies will be required to investigate the role of APE1 in triggering the molecular changes induced by Prdx1 in response to H_2O_2. Our finding indicates APE1 may contribute to redox homeostasis by promoting inactivation of Prdx1 by hyperoxidation. It has been demonstrated that in *Schizosaccharomyces pombe* treated with H_2O_2, the peroxredoxin Tpx1, an orthologue of mammalian Prdx1, is a major substrate for thioredoxin in the fission yeast and thus competitively inhibits thioredoxin-mediated reduction of other oxidized proteins. Hyperoxidation of Tpx1 is critical to allow thioredoxin to act on other substrates ensuring repair of oxidized proteins and cell survival following exposure to toxic levels of H_2O_2 (185). Therefore, inactivation of the thioredoxin peroxidase activity of Prdx1 is important to maintain thioredoxin activity and cell viability under

oxidative stress conditions. Given the fact that H_2O_2 is implicated in cellular "redox" signaling in regulating normal processes and disease progression, including angiogenesis, oxidative stress and aging, and cancer (159) and the inactivation of peroxiredoxin 1 allows localized H_2O_2 accumulation for cell signaling (186), it seems APE1 promoting Prdx1 inactivation is beneficial to cells under oxidative stress. At the same time, during Prdx1 catalysis, APE1 becomes reduced, which may be used for maintaining the active state of important transcription factors, and thereby contributing to anti-oxidation and survival.

5. References:

1. Wiseman H & Halliwell B (1996) Damage to DNA by reactive oxygen and nitrogen species: role in inflammatory disease and progression to cancer. *Biochem J* 313 (Pt 1):17-29.
2. Fridovich I (1986) Biological effects of the superoxide radical. *Arch Biochem Biophys* 247(1):1-11.
3. Schafer FQ, Qian SY, & Buettner GR (2000) Iron and free radical oxidations in cell membranes. *Cellular and molecular biology* 46(3):657-662.
4. Vignais PV (2002) The superoxide-generating NADPH oxidase: structural aspects and activation mechanism. *Cell Mol Life Sci* 59(9):1428-1459.
5. Van Heerebeek L*, et al.* (2002) NADPH oxidase(s): new source(s) of reactive oxygen species in the vascular system? *J Clin Pathol* 55(8):561-568.
6. Hawkins CL & Davies MJ (2001) Generation and propagation of radical reactions on proteins. *Biochim Biophys Acta* 1504(2-3):196-219.
7. Knight JA (2000) Review: Free radicals, antioxidants, and the immune system. *Annals of clinical and laboratory science* 30(2):145-158.
8. Blokhina O, Virolainen E, & Fagerstedt KV (2003) Antioxidants, oxidative damage and oxygen deprivation stress: a review. *Ann Bot* 91 Spec No:179-194.
9. Pryor WA (2000) Vitamin E and heart disease: basic science to clinical intervention trials. *Free Radic Biol Med* 28(1):141-164.
10. Valko M, Izakovic M, Mazur M, Rhodes CJ, & Telser J (2004) Role of oxygen radicals in DNA damage and cancer incidence. *Mol Cell Biochem* 266(1-2):37-56.

11. Chae HZ, Chung SJ, & Rhee SG (1994) Thioredoxin-dependent peroxide reductase from yeast. *J Biol Chem* 269(44):27670-27678.

12. Baud O*, et al.* (2004) Glutathione peroxidase-catalase cooperativity is required for resistance to hydrogen peroxide by mature rat oligodendrocytes. *J Neurosci* 24(7):1531-1540.

13. Jang HH*, et al.* (2004) Two enzymes in one; two yeast peroxiredoxins display oxidative stress-dependent switching from a peroxidase to a molecular chaperone function. *Cell* 117(5):625-635.

14. Shea TB & Ortiz D (2003) 17 beta-estradiol alleviates synergistic oxidative stress resulting from folate deprivation and amyloid-beta treatment. *Journal of Alzheimer's disease : JAD* 5(4):323-327.

15. Li J*, et al.* (2003) Novel role of vitamin k in preventing oxidative injury to developing oligodendrocytes and neurons. *J Neurosci* 23(13):5816-5826.

16. Woo HA*, et al.* (2005) Reduction of cysteine sulfinic acid by sulfiredoxin is specific to 2-cys peroxiredoxins. *J Biol Chem* 280(5):3125-3128.

17. Chang TS*, et al.* (2004) Characterization of mammalian sulfiredoxin and its reactivation of hyperoxidized peroxiredoxin through reduction of cysteine sulfinic acid in the active site to cysteine. *J Biol Chem* 279(49):50994-51001.

18. Jonsson TJ, Murray MS, Johnson LC, Poole LB, & Lowther WT (2005) Structural basis for the retroreduction of inactivated peroxiredoxins by human sulfiredoxin. *Biochemistry* 44(24):8634-8642.

19. Yoshizumi M, Tsuchiya K, & Tamaki T (2001) Signal transduction of reactive oxygen species and mitogen-activated protein kinases in cardiovascular disease. *The journal of medical investigation : JMI* 48(1-2):11-24.

20. Mieyal JJ & Chock PB (2012) Posttranslational modification of cysteine in redox signaling and oxidative stress: focus on s-glutathionylation. *Antioxidants & redox signaling* 16(6):471-475.

21. Woo HA*, et al.* (2003) Reversing the inactivation of peroxiredoxins caused by cysteine sulfinic acid formation. *Science* 300(5619):653-656.

22. Neumann CA, Cao J, & Manevich Y (2009) Peroxiredoxin 1 and its role in cell signaling. *Cell Cycle* 8(24):4072-4078.

23. Mu ZM, Yin XY, & Prochownik EV (2002) Pag, a putative tumor suppressor, interacts with the Myc Box II domain of c-Myc and selectively alters its biological function and target gene expression. *J Biol Chem* 277(45):43175-43184.

24. Egler RA*, et al.* (2005) Regulation of reactive oxygen species, DNA damage, and c-Myc function by peroxiredoxin 1. *Oncogene* 24(54):8038-8050.

25. Park SY*, et al.* (2007) Peroxiredoxin 1 interacts with androgen receptor and enhances its transactivation. *Cancer Res* 67(19):9294-9303.

26. Wang X, He S, Sun JM, Delcuve GP, & Davie JR (2010) Selective association of peroxiredoxin 1 with genomic DNA and COX-2 upstream promoter elements in estrogen receptor negative breast cancer cells. *Molecular biology of the cell* 21(17):2987-2995.

27. Kim JH*, et al.* (2012) RNA-binding properties and RNA chaperone activity of human peroxiredoxin 1. *Biochemical and biophysical research communications*.

28. Neumann CA*, et al.* (2003) Essential role for the peroxiredoxin Prdx1 in erythrocyte antioxidant defence and tumour suppression. *Nature* 424(6948):561-565.

29. Iraqui I*, et al.* (2008) Human peroxiredoxin PrxI is an orthologue of yeast Tsa1, capable of suppressing genome instability in Saccharomyces cerevisiae. *Cancer Res* 68(4):1055-1063.

30. Routledge MN, Wink DA, Keefer LK, & Dipple A (1994) DNA sequence changes induced by two nitric oxide donor drugs in the supF assay. *Chem Res Toxicol* 7(5):628-632.

31. Kahramanoglou C*, et al.* (2012) Genomics of DNA cytosine methylation in Escherichia coli reveals its role in stationary phase transcription. *Nat Commun* 3:886.

32. Walsh CP & Xu GL (2006) Cytosine methylation and DNA repair. *Current topics in microbiology and immunology* 301:283-315.

33. Weitzman SA, Turk PW, Milkowski DH, & Kozlowski K (1994) Free radical adducts induce alterations in DNA cytosine methylation. *Proc Natl Acad Sci U S A* 91(4):1261-1264.

34. Box HC, Freund HG, Budzinski EE, Wallace JC, & Maccubbin AE (1995) Free radical-induced double base lesions. *Radiat Res* 141(1):91-94.

35. Mao H, Deng Z, Wang F, Harris TM, & Stone MP (1998) An intercalated and thermally stable FAPY adduct of aflatoxin B1 in a DNA duplex: structural refinement from 1H NMR. *Biochemistry* 37(13):4374-4387.

36. Boiteux S & Radicella JP (2000) The human OGG1 gene: structure, functions, and its implication in the process of carcinogenesis. *Arch Biochem Biophys* 377(1):1-8.

37. Weimann A, Belling D, & Poulsen HE (2001) Measurement of 8-oxo-2'-deoxyguanosine and 8-oxo-2'-deoxyadenosine in DNA and human urine by high performance liquid chromatography-electrospray tandem mass spectrometry. *Free Radic Biol Med* 30(7):757-764.

38. Dizdaroglu M, Olinski R, Doroshow JH, & Akman SA (1993) Modification of DNA bases in chromatin of intact target human cells by activated human polymorphonuclear leukocytes. *Cancer Res* 53(6):1269-1272.

39. Murata M, Imada M, Inoue S, & Kawanishi S (1998) Metal-mediated DNA damage induced by diabetogenic alloxan in the presence of NADH. *Free Radic Biol Med* 25(4-5):586-595.

40. Halliwell B & Aruoma OI (1991) DNA damage by oxygen-derived species. Its mechanism and measurement in mammalian systems. *FEBS Lett* 281(1-2):9-19.

41. Park S & Imlay JA (2003) High levels of intracellular cysteine promote oxidative DNA damage by driving the fenton reaction. *Journal of bacteriology* 185(6):1942-1950.

42. Ames BN (1989) Endogenous oxidative DNA damage, aging, and cancer. *Free radical research communications* 7(3-6):121-128.

43. Floyd RA, Watson JJ, Wong PK, Altmiller DH, & Rickard RC (1986) Hydroxyl free radical adduct of deoxyguanosine: sensitive detection and mechanisms of formation. *Free radical research communications* 1(3):163-172.

44. Jaruga P, Rodriguez H, & Dizdaroglu M (2001) Measurement of 8-hydroxy-2'-deoxyadenosine in DNA by liquid chromatography/mass spectrometry. *Free Radic Biol Med* 31(3):336-344.

45. Kolodner RD & Marsischky GT (1999) Eukaryotic DNA mismatch repair. *Current opinion in genetics & development* 9(1):89-96.

46. Cox MM*, et al.* (2000) The importance of repairing stalled replication forks. *Nature* 404(6773):37-41.

47. Cox MM (2002) The nonmutagenic repair of broken replication forks via recombination. *Mutat Res* 510(1-2):107-120.

48. Sinha RP & Hader DP (2002) UV-induced DNA damage and repair: a review. *Photochemical & photobiological sciences : Official journal of the European Photochemistry Association and the European Society for Photobiology* 1(4):225-236.

49. Rastogi RP, Richa, Kumar A, Tyagi MB, & Sinha RP (2010) Molecular mechanisms of ultraviolet radiation-induced DNA damage and repair. *J Nucleic Acids* 2010:592980.

50. Douki T (2013) The variety of UV-induced pyrimidine dimeric photoproducts in DNA as shown by chromatographic quantification methods. *Photochemical & photobiological sciences : Official journal of the European Photochemistry Association and the European Society for Photobiology* 12(8):1286-1302.

51. Halliwell B (1999) Oxygen and nitrogen are pro-carcinogens. Damage to DNA by reactive oxygen, chlorine and nitrogen species: measurement, mechanism and the effects of nutrition. *Mutat Res* 443(1-2):37-52.

52. Boiteux S & Guillet M (2004) Abasic sites in DNA: repair and biological consequences in Saccharomyces cerevisiae. *DNA Repair (Amst)* 3(1):1-12.

53. Lindahl T (1993) Instability and decay of the primary structure of DNA. *Nature* 362(6422):709-715.

54. Chen J & Stubbe J (2005) Bleomycins: towards better therapeutics. *Nat Rev Cancer* 5(2):102-112.

55. Dudley DD, Chaudhuri J, Bassing CH, & Alt FW (2005) Mechanism and control of V(D)J recombination versus class switch recombination: similarities and differences. *Advances in immunology* 86:43-112.

56. Shrivastav M, De Haro LP, & Nickoloff JA (2008) Regulation of DNA double-strand break repair pathway choice. *Cell Res* 18(1):134-147.

57. Minko IG, Zou Y, & Lloyd RS (2002) Incision of DNA-protein crosslinks by UvrABC nuclease suggests a potential repair pathway involving nucleotide excision repair. *Proc Natl Acad Sci U S A* 99(4):1905-1909.

58. Kastan MB & Bartek J (2004) Cell-cycle checkpoints and cancer. *Nature* 432(7015):316-323.

59. Shimada M & Nakanishi M (2006) DNA damage checkpoints and cancer. *Journal of molecular histology* 37(5-7):253-260.

60. Caldecott KW (2008) Single-strand break repair and genetic disease. *Nature reviews. Genetics* 9(8):619-631.

61. Green CM & Lehmann AR (2005) Translesion synthesis and error-prone polymerases. *Adv Exp Med Biol* 570:199-223.

62. Chiapperino D*, et al.* (2005) Error-prone translesion synthesis by human DNA polymerase eta on DNA-containing deoxyadenosine adducts of 7,8-dihydroxy-9,10-epoxy-7,8,9,10-tetrahydrobenzo[a]pyrene. *J Biol Chem* 280(48):39684-39692.

63. Gan GN, Wittschieben JP, Wittschieben BO, & Wood RD (2008) DNA polymerase zeta (pol zeta) in higher eukaryotes. *Cell Res* 18(1):174-183.

64. Reha-Krantz LJ (2010) DNA polymerase proofreading: Multiple roles maintain genome stability. *Biochim Biophys Acta* 1804(5):1049-1063.

65. Bebenek K, Garcia-Diaz M, Blanco L, & Kunkel TA (2003) The frameshift infidelity of human DNA polymerase lambda. Implications for function. *J Biol Chem* 278(36):34685-34690.

66. Ling H, Boudsocq F, Woodgate R, & Yang W (2004) Snapshots of replication through an abasic lesion; structural basis for base substitutions and frameshifts. *Mol Cell* 13(5):751-762.

67. Tornaletti S & Hanawalt PC (1999) Effect of DNA lesions on transcription elongation. *Biochimie* 81(1-2):139-146.

68. Harper JW & Elledge SJ (2007) The DNA damage response: ten years after. *Mol Cell* 28(5):739-745.

69. McKinnon PJ (2004) ATM and ataxia telangiectasia. *EMBO Rep* 5(8):772-776.

70. Weinert T (1998) DNA damage checkpoints update: getting molecular. *Current opinion in genetics & development* 8(2):185-193.

71. Bartek J & Lukas J (2003) Chk1 and Chk2 kinases in checkpoint control and cancer. *Cancer Cell* 3(5):421-429.

72. Nurse P (1997) Checkpoint pathways come of age. *Cell* 91(7):865-867.

73. Peschiaroli A*, et al.* (2006) SCFbetaTrCP-mediated degradation of Claspin regulates recovery from the DNA replication checkpoint response. *Mol Cell* 23(3):319-329.

74. Gewurz BE & Harper JW (2006) DNA-damage control: Claspin destruction turns off the checkpoint. *Curr Biol* 16(21):R932-934.

75. D'Amours D & Jackson SP (2002) The Mre11 complex: at the crossroads of dna repair and checkpoint signalling. *Nat Rev Mol Cell Biol* 3(5):317-327.

76. Sung P (1994) Catalysis of ATP-dependent homologous DNA pairing and strand exchange by yeast RAD51 protein. *Science* 265(5176):1241-1243.

77. Petrini JH (2000) The Mre11 complex and ATM: collaborating to navigate S phase. *Curr Opin Cell Biol* 12(3):293-296.

78. Khanna KK & Jackson SP (2001) DNA double-strand breaks: signaling, repair and the cancer connection. *Nat Genet* 27(3):247-254.

79. van Gent DC, Hoeijmakers JH, & Kanaar R (2001) Chromosomal stability and the DNA double-stranded break connection. *Nature reviews. Genetics* 2(3):196-206.

80. Chen XB*, et al.* (2001) Human Mus81-associated endonuclease cleaves Holliday junctions in vitro. *Mol Cell* 8(5):1117-1127.

81. Boddy MN & Russell P (2001) DNA replication checkpoint. *Curr Biol* 11(23):R953-956.

82. Ramsden DA & Gellert M (1998) Ku protein stimulates DNA end joining by mammalian DNA ligases: a direct role for Ku in repair of DNA double-strand breaks. *EMBO J* 17(2):609-614.

83. Nick McElhinny SA, Snowden CM, McCarville J, & Ramsden DA (2000) Ku recruits the XRCC4-ligase IV complex to DNA ends. *Mol Cell Biol* 20(9):2996-3003.

84. Hsu HL*, et al.* (2000) Ku acts in a unique way at the mammalian telomere to prevent end joining. *Genes Dev* 14(22):2807-2812.

85. Li GM (2008) Mechanisms and functions of DNA mismatch repair. *Cell Res* 18(1):85-98.

86. Obmolova G, Ban C, Hsieh P, & Yang W (2000) Crystal structures of mismatch repair protein MutS and its complex with a substrate DNA. *Nature* 407(6805):703-710.

87. Karran P & Bignami M (1994) DNA damage tolerance, mismatch repair and genome instability. *BioEssays : news and reviews in molecular, cellular and developmental biology* 16(11):833-839.

88. Yamaguchi Y*, et al.* (1999) NELF, a multisubunit complex containing RD, cooperates with DSIF to repress RNA polymerase II elongation. *Cell* 97(1):41-51.

89. Petit C & Sancar A (1999) Nucleotide excision repair: from E. coli to man. *Biochimie* 81(1-2):15-25.

90. Sancar A, Lindsey-Boltz LA, Unsal-Kacmaz K, & Linn S (2004) Molecular mechanisms of mammalian DNA repair and the DNA damage checkpoints. *Annual review of biochemistry* 73:39-85.

91. Gerlitz G (2010) HMGNs, DNA repair and cancer. *Biochim Biophys Acta* 1799(1-2):80-85.

92. de Boer J & Hoeijmakers JH (2000) Nucleotide excision repair and human syndromes. *Carcinogenesis* 21(3):453-460.

93. Liu Y*, et al.* (2007) Coordination of steps in single-nucleotide base excision repair mediated by apurinic/apyrimidinic endonuclease 1 and DNA polymerase beta. *J Biol Chem* 282(18):13532-13541.

94. Frosina G*, et al.* (1996) Two pathways for base excision repair in mammalian cells. *J Biol Chem* 271(16):9573-9578.

95. Klungland A & Lindahl T (1997) Second pathway for completion of human DNA base excision-repair: reconstitution with purified proteins and requirement for DNase IV (FEN1). *EMBO J* 16(11):3341-3348.

96. Prasad R, Dianov GL, Bohr VA, & Wilson SH (2000) FEN1 stimulation of DNA polymerase beta mediates an excision step in mammalian long patch base excision repair. *J Biol Chem* 275(6):4460-4466.

97. Zharkov DO (2008) Base excision DNA repair. *Cell Mol Life Sci* 65(10):1544-1565.

98. Demple B, Herman T, & Chen DS (1991) Cloning and expression of APE, the cDNA encoding the major human apurinic endonuclease: definition of a family of DNA repair enzymes. *Proc Natl Acad Sci U S A* 88(24):11450-11454.

99. Xanthoudakis S & Curran T (1992) Identification and characterization of Ref-1, a nuclear protein that facilitates AP-1 DNA-binding activity. *The EMBO journal* 11(2):653-665.

100. Vascotto C*, et al.* (2009) APE1/Ref-1 interacts with NPM1 within nucleoli and plays a role in the rRNA quality control process. *Mol Cell Biol* 29(7):1834-1854.

101. Yu E, Gaucher SP, & Hadi MZ (2010) Probing conformational changes in Ape1 during the progression of base excision repair. *Biochemistry* 49(18):3786-3796.

102. Tell G, Quadrifoglio F, Tiribelli C, & Kelley MR (2009) The many functions of APE1/Ref-1: not only a DNA repair enzyme. *Antioxid Redox Signal* 11(3):601-620.

103. Tell G, Fantini D, & Quadrifoglio F (2010) Understanding different functions of mammalian AP endonuclease (APE1) as a promising tool for cancer treatment. *Cell Mol Life Sci* 67(21):3589-3608.

104. Baute J & Depicker A (2008) Base excision repair and its role in maintaining genome stability. *Critical reviews in biochemistry and molecular biology* 43(4):239-276.

105. Nilsen H & Krokan HE (2001) Base excision repair in a network of defence and tolerance. *Carcinogenesis* 22(7):987-998.

106. Flaherty DM, Monick MM, Carter AB, Peterson MW, & Hunninghake GW (2002) Oxidant-mediated increases in redox factor-1 nuclear protein and activator protein-1 DNA binding in asbestos-treated macrophages. *J Immunol* 168(11):5675-5681.

107. Fromme JC, Banerjee A, & Verdine GL (2004) DNA glycosylase recognition and catalysis. *Curr Opin Struct Biol* 14(1):43-49.

108. Nishi T*, et al.* (2002) Spatial redox regulation of a critical cysteine residue of NF-kappa B in vivo. *The Journal of biological chemistry* 277(46):44548-44556.

109. Xanthoudakis S, Miao G, Wang F, Pan YC, & Curran T (1992) Redox activation of Fos-Jun DNA binding activity is mediated by a DNA repair enzyme. *EMBO J* 11(9):3323-3335.

110. Huang RP & Adamson ED (1993) Characterization of the DNA-binding properties of the early growth response-1 (Egr-1) transcription factor: evidence for modulation by a redox mechanism. *DNA Cell Biol* 12(3):265-273.

111. Gaiddon C, Moorthy NC, & Prives C (1999) Ref-1 regulates the transactivation and pro-apoptotic functions of p53 in vivo. *The EMBO journal* 18(20):5609-5621.

112. Huang LE, Arany Z, Livingston DM, & Bunn HF (1996) Activation of hypoxia-inducible transcription factor depends primarily upon redox-sensitive stabilization of its alpha subunit. *J Biol Chem* 271(50):32253-32259.

113. Tell G, *et al.* (2002) Redox effector factor-1 regulates the activity of thyroid transcription factor 1 by controlling the redox state of the N transcriptional activation domain. *J Biol Chem* 277(17):14564-14574.

114. Ando K, *et al.* (2008) A new APE1/Ref-1-dependent pathway leading to reduction of NF-kappaB and AP-1, and activation of their DNA-binding activity. *Nucleic Acids Research* 36(13):4327-4336.

115. Chung U, *et al.* (1996) The interaction between Ku antigen and REF1 protein mediates negative gene regulation by extracellular calcium. *J Biol Chem* 271(15):8593-8598.

116. Okazaki T, *et al.* (1994) A redox factor protein, ref1, is involved in negative gene regulation by extracellular calcium. *J Biol Chem* 269(45):27855-27862.

117. Fuchs S, Philippe J, Corvol P, & Pinet F (2003) Implication of Ref-1 in the repression of renin gene transcription by intracellular calcium. *Journal of hypertension* 21(2):327-335.

118. Bhakat KK, Izumi T, Yang SH, Hazra TK, & Mitra S (2003) Role of acetylated human AP-endonuclease (APE1/Ref-1) in regulation of the parathyroid hormone gene. *EMBO J* 22(23):6299-6309.

119. Barzilay G, Walker LJ, Robson CN, & Hickson ID (1995) Site-directed mutagenesis of the human DNA repair enzyme HAP1: identification of residues important for AP endonuclease and RNase H activity. *Nucleic Acids Res* 23(9):1544-1550.

120. Marenstein DR, Wilson DM, 3rd, & Teebor GW (2004) Human AP endonuclease (APE1) demonstrates endonucleolytic activity against AP sites in single-stranded DNA. *DNA Repair (Amst)* 3(5):527-533.

121. Berquist BR, McNeill DR, & Wilson DM, 3rd (2008) Characterization of abasic endonuclease activity of human Ape1 on alternative substrates, as well as effects of ATP and sequence context on AP site incision. *Journal of molecular biology* 379(1):17-27.

122. Tell G, Wilson DM, 3rd, & Lee CH (2010) Intrusion of a DNA repair protein in the RNome world: is this the beginning of a new era? *Mol Cell Biol* 30(2):366-371.

123. Fantini D*, et al.* (2008) APE1/Ref-1 regulates PTEN expression mediated by Egr-1. *Free radical research* 42(1):20-29.

124. Yacoub A, Kelley MR, & Deutsch WA (1997) The DNA repair activity of human redox/repair protein APE/Ref-1 is inactivated by phosphorylation. *Cancer research* 57(24):5457-5459.

125. Hsieh MM, Hegde V, Kelley MR, & Deutsch WA (2001) Activation of APE/Ref-1 redox activity is mediated by reactive oxygen species and PKC phosphorylation. *Nucleic Acids Research* 29(14):3116-3122.

126. Busso CS, Iwakuma T, & Izumi T (2009) Ubiquitination of mammalian AP endonuclease (APE1) regulated by the p53-MDM2 signaling pathway. *Oncogene* 28(13):1616-1625.

127. Qu J, Liu GH, Huang B, & Chen C (2007) Nitric oxide controls nuclear export of APE1/Ref-1 through S-nitrosation of cysteines 93 and 310. *Nucleic Acids Research* 35(8):2522-2532.

128. Fan Z*, et al.* (2003) Cleaving the oxidative repair protein Ape1 enhances cell death mediated by granzyme A. *Nature immunology* 4(2):145-153.

129. Izumi T*, et al.* (2003) Mammalian DNA base excision repair proteins: their interactions and role in repair of oxidative DNA damage. *Toxicology* 193(1-2):43-65.

130. Evans AR, Limp-Foster M, & Kelley MR (2000) Going APE over ref-1. *Mutation research* 461(2):83-108.

131. Barnes T*, et al.* (2009) Identification of Apurinic/apyrimidinic endonuclease 1 (APE1) as the endoribonuclease that cleaves c-myc mRNA. *Nucleic Acids Res* 37(12):3946-3958.

132. Young JJ, Patel A, & Rai P (2010) Suppression of thioredoxin-1 induces premature senescence in normal human fibroblasts. *Biochemical and biophysical research communications* 392(3):363-368.

133. Shatilla A & Ramotar D (2002) Embryonic extracts derived from the nematode Caenorhabditis elegans remove uracil from DNA by the sequential action of uracil-DNA glycosylase and AP (apurinic/apyrimidinic) endonuclease. *Biochem J* 365(Pt 2):547-553.

134. Nakatani Y & Ogryzko V (2003) Immunoaffinity purification of mammalian protein complexes. *Methods Enzymol* 370:430-444.

135. Wood ZA, Schroder E, Robin Harris J, & Poole LB (2003) Structure, mechanism and regulation of peroxiredoxins. *Trends Biochem Sci* 28(1):32-40.

136. Hofmann B, Hecht HJ, & Flohe L (2002) Peroxiredoxins. *Biological chemistry* 383(3-4):347-364.

137. Sato Y*, et al.* (2013) Synergistic cooperation of PDI family members in peroxiredoxin 4-driven oxidative protein folding. *Scientific reports* 3:2456.

138. Laboissiere MC, Sturley SL, & Raines RT (1995) The essential function of protein-disulfide isomerase is to unscramble non-native disulfide bonds. *J Biol Chem* 270(47):28006-28009.

139. Franceschini A*, et al.* (2013) STRING v9.1: protein-protein interaction networks, with increased coverage and integration. *Nucleic Acids Res* 41(Database issue):D808-815.

140. Rani V, Neumann CA, Shao C, & Tischfield JA (2012) Prdx1 deficiency in mice promotes tissue specific loss of heterozygosity mediated by deficiency in DNA repair and increased oxidative stress. *Mutation research* 735(1-2):39-45.

141. Richard D*, et al.* (2011) A genome-wide chromatin-associated nuclear peroxiredoxin from the malaria parasite Plasmodium falciparum. *The Journal of biological chemistry* 286(13):11746-11755.

142. Cesaratto L*, et al.* (2013) Specific inhibition of the redox activity of ape1/ref-1 by e3330 blocks tnf-alpha-induced activation of IL-8 production in liver cancer cell lines. *PLoS One* 8(8):e70909.

143. Hoffmann E, Dittrich-Breiholz O, Holtmann H, & Kracht M (2002) Multiple control of interleukin-8 gene expression. *J Leukoc Biol* 72(5):847-855.

144. Carper DA*, et al.* (1999) Oxidative stress induces differential gene expression in a human lens epithelial cell line. *Investigative ophthalmology & visual science* 40(2):400-406.

145. Sciacovelli M*, et al.* (2013) The mitochondrial chaperone TRAP1 promotes neoplastic growth by inhibiting succinate dehydrogenase. *Cell Metab* 17(6):988-999.

146. Sun Q*, et al.* (2011) Mammalian target of rapamycin up-regulation of pyruvate kinase isoenzyme type M2 is critical for aerobic glycolysis and tumor growth. *Proc Natl Acad Sci U S A* 108(10):4129-4134.

147. Iqbal MA, Gupta V, Gopinath P, Mazurek S, & Bamezai RN (2014) Pyruvate kinase M2 and cancer: an updated assessment. *FEBS Lett*.

148. Nakagawa T, Lomb DJ, Haigis MC, & Guarente L (2009) SIRT5 Deacetylates carbamoyl phosphate synthetase 1 and regulates the urea cycle. *Cell* 137(3):560-570.

149. Winter AD, McCormack G, & Page AP (2007) Protein disulfide isomerase activity is essential for viability and extracellular matrix formation in the nematode Caenorhabditis elegans. *Developmental biology* 308(2):449-461.

150. Friedman L*, et al.* (2000) Prolyl 4-hydroxylase is required for viability and morphogenesis in Caenorhabditis elegans. *Proc Natl Acad Sci U S A* 97(9):4736-4741.

151. Possemato R*, et al.* (2011) Functional genomics reveal that the serine synthesis pathway is essential in breast cancer. *Nature* 476(7360):346-350.

152. Mullarky E, Mattaini KR, Vander Heiden MG, Cantley LC, & Locasale JW (2011) PHGDH amplification and altered glucose metabolism in human melanoma. *Pigment cell & melanoma research* 24(6):1112-1115.

153. Wood ZA, Poole LB, & Karplus PA (2003) Peroxiredoxin evolution and the regulation of hydrogen peroxide signaling. *Science* 300(5619):650-653.

154. Kim YJ*, et al.* (2011) S-Glutathionylation of Cysteine 99 in the APE1 Protein Impairs Abasic Endonuclease Activity. *J Mol Biol*.

155. Waugh DJ & Wilson C (2008) The interleukin-8 pathway in cancer. *Clin Cancer Res* 14(21):6735-6741.

156. Dittmann LM*, et al.* (2012) Downregulation of PRDX1 by promoter hypermethylation is frequent in 1p/19q-deleted oligodendroglial tumours and increases radio- and chemosensitivity of Hs683 glioma cells in vitro. *Oncogene* 31(29):3409-3418.

157. O'Hara AM*, et al.* (2009) Tumor necrosis factor (TNF)-alpha-induced IL-8 expression in gastric epithelial cells: role of reactive oxygen species and AP endonuclease-1/redox factor (Ref)-1. *Cytokine* 46(3):359-369.

158. Nishiyama A*, et al.* (1999) Identification of thioredoxin-binding protein-2/vitamin D(3) up-regulated protein 1 as a negative regulator of thioredoxin function and expression. *J Biol Chem* 274(31):21645-21650.

159. Rhee SG (2006) Cell signaling. H2O2, a necessary evil for cell signaling. *Science* 312(5782):1882-1883.

160. Guo M*, et al.* (2011) The bZIP transcription factor MoAP1 mediates the oxidative stress response and is critical for pathogenicity of the rice blast fungus Magnaporthe oryzae. *PLoS Pathog* 7(2):e1001302.

161. Leal SM, Jr.*, et al.* (2012) Fungal antioxidant pathways promote survival against neutrophils during infection. *J Clin Invest* 122(7):2482-2498.

162. Sen CK & Packer L (1996) Antioxidant and redox regulation of gene transcription. *FASEB J* 10(7):709-720.

163. Rhee SG & Woo HA (2011) Multiple functions of peroxiredoxins: peroxidases, sensors and regulators of the intracellular messenger H(2)O(2), and protein chaperones. *Antioxid Redox Signal* 15(3):781-794.

164. Rhee SG, Chae HZ, & Kim K (2005) Peroxiredoxins: a historical overview and speculative preview of novel mechanisms and emerging concepts in cell signaling. *Free Radic Biol Med* 38(12):1543-1552.

165. Forman HJ, Maiorino M, & Ursini F (2010) Signaling functions of reactive oxygen species. *Biochemistry* 49(5):835-842.

166. Rhee SG, Woo HA, Kil IS, & Bae SH (2012) Peroxiredoxin functions as a peroxidase and a regulator and sensor of local peroxides. *J Biol Chem* 287(7):4403-4410.

167. Winterbourn CC (2008) Reconciling the chemistry and biology of reactive oxygen species. *Nat Chem Biol* 4(5):278-286.

168. Abate C, Patel L, Rauscher FJ, 3rd, & Curran T (1990) Redox regulation of fos and jun DNA-binding activity in vitro. *Science* 249(4973):1157-1161.

169. Walker LJ, Robson CN, Black E, Gillespie D, & Hickson ID (1993) Identification of residues in the human DNA repair enzyme HAP1 (Ref-1) that are essential for redox regulation of Jun DNA binding. *Mol Cell Biol* 13(9):5370-5376.

170. Angkeow P*, et al.* (2002) Redox factor-1: an extra-nuclear role in the regulation of endothelial oxidative stress and apoptosis. *Cell Death Differ* 9(7):717-725.

171. Kelley MR, Georgiadis MM, & Fishel ML (2012) APE1/Ref-1 role in redox signaling: translational applications of targeting the redox function of the DNA repair/redox protein APE1/Ref-1. *Curr Mol Pharmacol* 5(1):36-53.

172. Chaitanya GV, Steven AJ, & Babu PP (2010) PARP-1 cleavage fragments: signatures of cell-death proteases in neurodegeneration. *Cell communication and signaling : CCS* 8:31.

173. Lavrik IN, Golks A, & Krammer PH (2005) Caspases: pharmacological manipulation of cell death. *J Clin Invest* 115(10):2665-2672.

174. Fujii J & Ikeda Y (2002) Advances in our understanding of peroxiredoxin, a multifunctional, mammalian redox protein. *Redox report : communications in free radical research* 7(3):123-130.

175. Yang KS*, et al.* (2002) Inactivation of human peroxiredoxin I during catalysis as the result of the oxidation of the catalytic site cysteine to cysteine-sulfinic acid. *J Biol Chem* 277(41):38029-38036.

176. Shimizu N*, et al.* (2000) High-performance affinity beads for identifying drug receptors. *Nat Biotechnol* 18(8):877-881.

177. Kelley MR*, et al.* (2011) Functional analysis of novel analogues of E3330 that block the redox signaling activity of the multifunctional AP endonuclease/redox signaling enzyme APE1/Ref-1. *Antioxid Redox Signal* 14(8):1387-1401.

178. Sundaresan M, Yu ZX, Ferrans VJ, Irani K, & Finkel T (1995) Requirement for generation of H2O2 for platelet-derived growth factor signal transduction. *Science* 270(5234):296-299.

179. Tonks NK (2005) Redox redux: revisiting PTPs and the control of cell signaling. *Cell* 121(5):667-670.

180. Wei SJ*, et al.* (2000) Thioredoxin nuclear translocation and interaction with redox factor-1 activates the activator protein-1 transcription factor in response to ionizing radiation. *Cancer research* 60(23):6688-6695.

181. Brown JD*, et al.* (2013) A peroxiredoxin promotes H2O2 signaling and oxidative stress resistance by oxidizing a thioredoxin family protein. *Cell reports* 5(5):1425-1435.

182. Tuttle SW, Varnes ME, Mitchell JB, & Biaglow JE (1992) Sensitivity to chemical oxidants and radiation in CHO cell lines deficient in oxidative pentose cycle activity. *International journal of radiation oncology, biology, physics* 22(4):671-675.

183. Holmgren A*, et al.* (2005) Thiol redox control via thioredoxin and glutaredoxin systems. *Biochem Soc Trans* 33(Pt 6):1375-1377.

184. Izumi T*, et al.* (2005) Two essential but distinct functions of the mammalian abasic endonuclease. *Proc Natl Acad Sci U S A* 102(16):5739-5743.

185. Day AM*, et al.* (2012) Inactivation of a peroxiredoxin by hydrogen peroxide is critical for thioredoxin-mediated repair of oxidized proteins and cell survival. *Molecular cell* 45(3):398-408.

186. Woo HA*, et al.* (2010) Inactivation of peroxiredoxin I by phosphorylation allows localized H(2)O(2) accumulation for cell signaling. *Cell* 140(4):517-528.

Appendix A

The following manuscript has been submitted to the journal Gene

The long N-terminus of the *C. elegans* DNA repair enzyme APN-1 targets the protein to the nucleus of a heterologous system

Zhiqiang Wang[†], Xiaoming Yang[†], Abdelghani Mazouzi[†], and Dindial Ramotar[†]*

Running title: Functions of the N-terminus of *C. elegans* APN-1

[†]Maisonneuve-Rosemont Hospital, Research Center, Université de Montréal

5415 Boul. de l' Assomption, Montréal, Québec, Canada, H1T 2M4

* Corresponding author: Tel:(514) 252-3400 ext. 4684; Fax:(514) 252-3430;

Abstract

We previously isolated from a *Caenorhabditis elegans* cDNA library, designed for two-hybrid screening, a gene encoding the DNA repair enzyme APN-1 using cross-specie complementation analysis of the *Saccharomyces cerevisiae apn1*Δ *apn2*Δ *tpp1*Δ triple mutant deficient in the ability to repair several types of DNA lesions including apurinic/apyrimidinc (AP) sites. We subsequently purified the APN-1 from this yeast mutant and demonstrated that it possesses four distinct DNA repair activities. However, following the re-annotation of the *C. elegans* genome we discovered that the functionally active APN-1 encoded by the cDNA from the library lacked 108 amino acid residues from the N-terminal. We therefore synthesized the entire *C. elegans apn-1* gene encoding the full-length APN-1 and created several N-terminal deletion mutants lacking either 63, 83 or 118 amino acid residues. The full-length APN-1, APN-1 (1-63Δ) and APN-1 (1-83Δ), but not APN-1 (1-118Δ) were stably expressed in the yeast triple mutant and cleaved the AP site substrate. However, only the full-length APN-1 rescued the yeast mutant from the genotoxicity caused by methyl methane sulfonate, a DNA damaging agent that creates AP sites in the genome. The full-length APN-1 was localized to the yeast nucleus, while APN-1 (1-63Δ) and APN-1 (1-83Δ) retained a cytoplasmic distribution. Our data suggest that the N-terminal region has no direct role in the DNA repair functions of APN-1 other than to target the protein to the nucleus and possibly to maintain its stability. Thus, the truncated APN-1, isolated from the two-hybrid library, ability to complement the yeast triple mutant depends on the engineered SV40 nuclear localization signal.

Keywords: Keywords: AP endonuclease, DNA repair, nuclear localization signal, cross-specie complementation, *C. elegans*, yeast

1. Introduction

Caenorhabditis elegans APN-1 is a member of the endonuclease IV (Endo IV) family of DNA repair enzymes referred to as apurinic/apyrimidinic (AP) endonucleases/3'-diesterases and includes, for example, *Saccharomyces cerevisiae* Apn1 and *Escherichia coli* Endo IV [1]. These proteins possess at least four enzymatic activities (i) AP endonuclease that cleaves the DNA backbone 5' to an AP site producing a 3'-hydroxyl group and a 5'-deoxyribose phosphate [1,2], (ii) 3'-diesterase that removes a multitude of 3'-blocking groups such as 3'-phosphate present at DNA single strand breaks [2,3], (iii) 3'- to 5'-exonuclease capable of removing a few nucleotides at nicked DNA to create a gap, [3,4], and (iv) nucleotide incision repair activity that recognizes and removes certain oxidized bases by making an incision immediately 5' to the damaged base to create a 3'-hydroxyl group [5,6]. The members of the Endo IV family perform a role in the base-excision DNA repair pathway to eliminate specific types of mutagenic DNA lesions that would otherwise compromise genomic integrity [1].

We have shown that RNAi knockdown of the *C. elegans apn-1* gene caused the animals to accumulate 5-fold higher levels of spontaneous mutations [7]. The downregulation of the *apn-1* gene also sensitized *C. elegans* to DNA damaging agents such as methyl methane sulonate (MMS), which indirectly creates AP site lesions as a result of the removal of alkylated bases by DNA glycosylases [7]. Interestingly, these *apn-1* knockdown animals showed a delay in the progression of single cell embryo which has been ascribed to a defect in processing endogenous DNA lesions [7]. It is unlikely that the endogenous lesions are due to

the accumulation of AP sites or single strand breaks with blocked 3'-termini, as *C. elegans* embryos are proficient at processing these lesions due to the conservation of another highly active AP endonuclease/3'-diesterase, EXO-3, that belongs to the EXO III family of apurinic/apyrimidinic (AP) endonucleases/3'-diesterases [8,9]. As such, we postulated that APN-1 might be required to perform a distinct repair function that is uncommon to EXO-3 [7].

Although the *C. elegans apn-1* gene was identified and the predicted protein shares high identity with the Endo IV family members, the APN-1 enzyme could not be purified and functionally characterized from *C. elegans* because the expression level of APN-1 is extremely low and the protein was highly susceptible to proteolysis [9]. As such, we took advantage of the yeast heterologous model system to express and functionally characterized the *C. elegans* APN-1 [10,11]. This was achieved by the isolation of a plasmid, pGAL4-SV40(NLS)-apn-1, from a library containing *C. elegans* genes designed for two-hybrid screening in *S. cerevisiae*, which rescued the DNA repair defects of a yeast mutant strain YW778 (*apn1Δ apn2Δ tpp1Δ*) lacking Apn1, as well as two additional enzymes Apn2 (a member of the EXO III family) and Tpp1 (possessing a 3'-phosphodiesterase activity) that are involved in processing similar DNA lesions as Apn1 [12,13]. This yeast mutant YW778 exhibits exquisite sensitivities to various DNA damaging agents including MMS and hydrogen peroxide that produce AP sites and creates strand breaks terminated with 3'-phosphate, respectively [14]. The plasmid pGAL4-SV40(NLS)-apn-1 harboured the essential portion of the *apn-1* gene encoding a functional polypeptide that shared throughout its entire length 44 and 41 % identity at the amino acid level with *E. coli* endo IV and *S. cerevisiae* Apn1, respectively [15]. Subsequent analysis of the re-annotated *C. elegans* database

revealed that the cDNA harboured by the rescue plasmid was missing the N-terminal portion of the *apn-1* gene encoding residues 1 to 108. Thus, on the basis of the *C. elegans* database information and DNA sequence analysis, the complementing plasmid pGAL4-SV40(NLS)-apn-1 carried only the portion of the *apn-1* gene encoding residues 109 to 396 of the APN-1 protein.

We have established that the functional region of APN-1, which rescued the DNA repair defects of strain YW778, was located within residues 119 to 396 [16]. This finding strongly suggests that the N-terminal portion of the full-length APN-1 is unlikely to play a role in DNA repair. As such, this finding incites the question what is the purpose of the long N-terminal, that is, residues 1 to 118 of APN-1. Analysis of the missing portion of APN-1 from the plasmid pGAL4-SV40(NLS)-apn-1, that is, residues 1 to 108, for specific motifs revealed two segments that resemble nuclear localization signals (NLS), suggesting that the putative extended N-terminal may serve to at least target the protein to the nucleus in *C. elegans*. We have shown that APN-1 (119-396) carrying the SV40 NLS can rescue the DNA repair defects of strain YW778 [16]. However, this functional complementation does not occur if APN-1 (119-396) lacks the SV40 NLS [16]. This observation strongly suggests that the N-terminal portion of APN-1 could be involved in targeting the protein to the nucleus. Herein, we provide evidence that the full-length APN-1 (1-396) can confer MMS resistance to the yeast mutant YW778, but not if it is lacking the first 1-63 amino acid residues. This APN-1 (1-63Δ) variant retained full AP endonuclease activity, but lacked the ability to enter the nucleus and instead showed a cytoplasmic distribution as compared to the full-length APN-1.

2. Materials and Methods

2.1 Yeast and bacterial strains

Saccharomyces cerevisiae laboratory strain YW778 (*apn1*Δ*::HIS3 apn2*Δ*::KanMX4 tpp1*Δ*::MET15*) was generously provided by Dr. Tom Wilson (Ann Arbor, Michigan) and maintained on YPD agar and supplemented with adenine (20 μg/ml). *Escherichia coli* laboratory strain DH5α (used for amplification of plasmids) was maintained on Luria Broth (LB) agar.

2.2 Plasmid Construction

The full-length *C. elegans apn-1* cDNA gene encoding the entire open reading frame was synthesized and cloned into the vector pUC57 (Biobasic, Canada). This synthesized cDNA was fully sequenced and completely matched the sequence of the *C. elegans* genome. The full-length *apn-1* gene and three N-terminal deletions were amplified by PCR from the plasmid and cloned by gap-repair into the pYES2.0-GFP vector with the following primers:

PYES-GFP-CeAPN1-FL-F1:5'-GCTGCTGGGATTACACATGGCATGGATGAACTATA

CAAAGAATTCATG GCTAACAAAAAAGTAACA-3';

PYES-GFP-CeAPN1(Δ:1-63Nt)-F1:5'-GCTGCTGGGATTACACATGGCATGGA

TGAACTATACAAAGAATTCGAAACATTAACTGAAGAAAA-3';

PYES-GFP-CeAPN1(Δ:1-83Nt)-F1:5'-GCTGCTGGGATTACACATGGCATGGATGAACT

ATACAAAGAATTCAACAAACCGAAAAAAACAAG-3';

PYES-GFP-CeAPN1(Δ:1-118Nt)-F1: 5'- GCTGCTGGGATTACACATGGCATGGATGAA

CTATACAAAGAATTCATGTTGG GATTCCACGTGAG-3';

PYES-GFP-CeAPN1-R1 5'- GGGACCTAGACTTCAGGTTGTCTAACTCCTTCCTTTTCG

GTTAGAGCGTTATCTTTTATCCATATTGT-3' as previously described [8,17].

2.3 Extraction of Proteins, SDS-PAGE and Western Blot

These preparations and analyses were performed as previously described [8]. Briefly, cells were grown overnight in selective media lacking uracil, subcultured the next day and allowed to grow exponentially for an additional 4 h. Cells were harvested and stored at -80 ^{o}C overnight before preparation of the total protein extract using a bead beater. Total protein extracts were analyzed on SDS-PAGE followed by Western blot analysis using anti-GFP monoclonal antibody (Sigma) at a dilution of 1:2000 and anti-mouse secondary antibodies at a dilution of 1:2000.

2.4 Preparation of oligonucleotide AP site substrate and AP endonuclease assay

A synthetic 42-base pair 5'-end [^{32}P]-labeled oligonucleotide with a uracil at position 21 d(GCTGCATGCCTGCAGGTCGA**U**TCTAGAG GATCCCGGGTACCT) and complementary strand containing G opposite to U d(CGACGTACGGACGTCCAGCT**G**AGATCTCCTAGGG CCCATGGA) was prepared as previously described [9,18]. The uracil in the double-stranded DNA substrate was removed by uracil DNA glycosylase to create the resulting AP site [9,18].

The *in vitro* AP endonuclease assay was performed as previously described [19]. Briefly, 50 ng of the AP site substrate was incubated with the indicated amount of total protein extracts at 37ºC for 20 min in a final volume of 12.5 µl. Reactions were stopped with 5 µl formamide loading buffer (76% formamide, 0.3% bromophenol blue, 0.3% xylene

cyanole, 10 mM EDTA), and heated at 65ºC for 3-5 min. The reaction product was separated on denaturing 10% polyacrylamide-7 M urea gel, exposed to a Fugi FLA-3000 Phosphor Screen and analyzed using Image Gauge V3.12 software.

2.5 Fluorescent microscopy

Cells were grown to a density of 2×10^8 cells/ml and processed for fluorescent microscopy as previously described [20,21]. Briefly, expression of the GFP-APN-1 fusion proteins were induced for 4 h by addition of 0.5% galactose in the media, fixed in 1% formaldehyde, washed 4 times and resuspended in PBS. Cellular localization and nuclear staining were observed using 3 μl of cells in mounting media containing DAPI and mounted on microscope slides for fluorescent microscopy. Cells were photographed at 100 times magnification by imaging camera (Retiga GX 32-002TB-303) attached to a Leica DMRE immunofluorescent microscope and images were processed by the MacIntosh OpenLab program.

2.6 Spot test analysis

This assay was performed as previously described [17]

3. Results

***3.1 C. elegans* APN-1 lacking the N-terminal 118 amino acid residues is unstable**—To address the role of the extended N-terminal of *C. elegans* APN-1, we synthesized the full length cDNA of the *apn-1* gene encoding the entire open reading frame from amino acids residues 1 to 396. This was necessary, as we could not isolate the entire full-length cDNA from total mRNA derived from the worms harvested from different stages of its life cycle. In addition, the *C. elegans* library created for two-hybrid screening in yeast also did not contain the full-length cDNA [15]. The synthesized full-length *apn-1* cDNA was gap-repaired into the multicopy yeast expression plasmid pYES-GFP to create the fusion gene GFP-*apn-1* such that its expression could be driven by the galactose-inducible promoter *GAL1* [21]. We generated the N-terminal GFP-APN-1 fusion in order to monitor its expression and localization in the cell by epifluoresecent microscopy as yeast anti-APN1 and anti-Endo IV antibodies against the yeast Apn1 and *E. coli* Endo IV, respectively, have very weak cross-reactivity towards *C. elegans* APN-1 and therefore are not useful for indirect immunofluorescence analysis. In a similar manner, we created by gap repair various N-terminal deletion of the *apn-1* gene to create the following three fusion constructs pGFP-APN-1(1-63Δ), pGFP-APN-1(1-83Δ) and pGFP-APN-1(1-118Δ). The GFP-APN-1(1-63Δ) was created to eliminate the first putative NLS, the GFP-APN-1(1-83Δ) to retain the minimum sequences for a second putative NLS and the GFP-APN-1 (1-118Δ) to remove the entire N-terminal extension that shared no sequence homology with other members of the Endo IV family (Fig. 1). In addition to these GFP-tagged plasmid constructs, we also engineered an identical plasmid to express the entire full-length APN-1 without the GFP tag

to be used as control to monitor if GFP would interfere with APN-1 functional role in DNA repair.

The four plasmids carrying the full length APN-1 and the three N-terminal deletions fused to the C-terminal of GFP were introduced into the yeast strain YW778 lacking the DNA repair activities Apn1, Apn2 and Tpp1, required to process, e.g., MMS-induced AP sites. Total protein extracts were prepared from strain YW778 carrying the various APN-1 constructs and analyzed by Western blot using anti-GFP monoclonal antibody. Because the GAL1 promoter is leaky and the APN-1 constructs were engineered in a backbone that retained multicopies, there was no need to induce the expression level of the GFP-APN-1 and its derivatives with galactose. The plasmids pGFP-APN-1, pGFP-APN-1(1-63Δ) and pGFP-APN-1(1-83Δ) all expressed the expected size of the fusion proteins 73, 65, and 62 kDa (Fig. 2A), and distinctly resolved by 8 % SDS-PAGE (Fig. 2B). The expression level of GFP-APN-1(1-63Δ) and GFP-APN-1(1-83Δ) appeared to be higher than the full length GFP-APN-1 (Fig. 2A). The plasmid pGFP-APN-1(1-118Δ) did not express any detectable level of the GFP-APN-1(1-118Δ) fusion protein (Fig. 2A). The control plasmid pGFP carrying only GFP expressed the expected 26 kDa protein (Fig. 2A). Since the full-length APN-1 and its two N-terminal deletions APN-1(1-63Δ) and APN-1(1-83Δ) showed no major degradation product and that APN-1(1-118Δ) cannot be detected, it would suggest that residues 83 to 118 may play a role in stabilizing the protein in yeast. This is consistent with our previous findings that the GST-APN-1(1-118Δ) fusion is unstable unless it contains the SV40 NLS [16].

3.2 Amino acid residues 1 to 63 are involved in targeting APN-1 to the nucleus of yeast cells—We next monitored the localization of the GFP-APN-1 and the three N-terminal

deletions within strain YW778 using epifluorescent microscope. The GFP-APN-1 was found primarily in the nucleus of strain YW778 and coincided with staining of the nuclear DNA (Fig. 3). Removal of residues 1 to 63 blocked targeting of APN-1 to the nucleus and as a result the GFP-APN-1(1-63Δ) protein was distributed in the cytoplasm (Fig. 3). Similarly, removal of residues 1 to 83 also caused APN-1 to be localized to the cytoplasm (Fig. 3). In contrast, APN-1 lacking residues 1 to 118 was compartmentalized in the cytoplasm possibly in the vacuole and thus might provide an explanation for its lack of detection following extract preparation and Western blot analysis (Fig. 3 and 2A). These observations suggest that the N-terminal region, spanning residues 1 to 63, harbours a NLS that targets APN-1 into yeast nucleus. The findings also indicate that the NLS is likely conserved as it has the ability to function in a heterologous system. Moreover, residues 83-118 are important to prevent the protein from losing its stability.

3.3 APN-1(1-63Δ) and APN-1(1-83Δ) are active in processing AP site lesions—We checked if removing the N-terminal residues of APN-1 would interfere with its ability to process DNA lesions. Total protein extracts were prepared from strain YW778 expressing the native APN-1 and the three N-terminal deletions and examined for the ability to cleave an AP site substrate. The substrate is a 42-mer double-stranded oligonucleotide with a single synthetic AP site at position 21 and upon incision by AP endonuclease activity generates a 20-mer product [9]. Total protein extracts obtained from strain YW778 carrying either the APN-1(1-63Δ) or APN-1(1-83Δ) were proficient in cleaving the AP site substrate and to the same extend as the extract derived from YW778 carrying the full-length APN-1 (Fig. 4, lanes 7-9 and 10-12 vs. 4-6). Extracts from the YW778 harbouring the APN-1(1-118Δ) did not cleave the substrate (Fig. 4, lanes 13-15). We conclude that the N-terminal extension of APN-1

encompassing residues 1 to 83 has no direct role in processing DNA lesions, and that the inability of APN-1(1-118Δ) to process the DNA substrate is largely a result of its instability (Fig. 2A).

3.4 Targeting APN-1 to the nucleus is essential for rescuing the DNA repair defects of strain YW778—We examined whether APN-1 lacking the various N-terminal segments would retain the ability to rescue strain YW778 from the sensitivity of MMS. In this experiment, exponentially growing cultures of strain YW778 carrying the indicated plasmid were serially diluted and spotted onto solid minimal media plates without and with MMS (Fig. 5). While full-length GFP-APN-1 fully rescued the MMS sensitivity of strain YW778, none of the N-terminal deletion variants APN-1(1-63Δ), APN-1(1-83Δ) or APN-1(1-118Δ) retained the ability to complement the defect (Fig. 5). Although APN-1(1-63Δ) appeared to be expressed more than the full-length APN-1 (Fig. 2A), it still cannot enter the nucleus to rescue strain YW778 from the genotoxicity caused by MMS, suggesting that the N-terminal amino acid residues from 1 to 63 harbour a conserved and efficient NLS that can target APN-1 into the nucleus of yeast cells. Attachment of the SV40 NLS to replace residues 1 to 118 of APN-1 generated a functional NLS-APN-1(1-118Δ) protein that rescued the MMS sensitivity of strain YW778 (Fig. 5). Thus, targeting the APN-1(1-118Δ) protein to the nucleus maintains its stability and allows it to rescue the MMS sensitivity of strain YW778. Our data would also imply that the N-terminal portion of APN-1, that is, residues 1-118, performs no direct role in DNA repair. We note that tagging the native APN-1 on the N-terminal with either GFP or GST did not alter the protein ability to perform its role in processing DNA lesions *in vivo*, as the untagged native APN-1 rescued strain YW778 from MMS toxicity to the same extent as GFP-APN-1.

4 Discussion

In this study, we investigated the functional role associated with the long extended N-terminal, encompassing residues 1 to 118, of *C. elegans* APN-1. Because we have previously showed that expression of APN-1 lacking the N-terminal extension, but carrying a SV40 NLS can complement the DNA repair defects of the yeast strain YW778 [15,16], we reasoned that the entire N-terminal extension could be similarly tested in this well-studied and powerful heterologous yeast model system [10,22]. We provide evidence that within amino acid residues 1 to 63 there must be an essential stretch that constitutes an efficient NLS. We have not defined the exact sequence required for the NLS function, but it is likely to be within this basic stretch of residues RKLKQKLTPLKIKKGRGK which would be distinct from the *S. cerevisiae* Apn1 NLS (KKRKTKK) or the SV40 NLS (KKKRK) [23]. We have not tested further whether residues RKLKQKLTPLKIKKGRGK can function as an independent NLS or whether it acts as a bipartite NLS requiring two basic stretches of residues in order to constitute a functional NLS as in the case of yeast Apn1 [23]. In fact, residues ^{84}KPKKTRKTSGETIAQKKSR^{102} contain sequences that resemble NLS. However, this stretch alone cannot target APN-1 to the nucleus, as the APN-1(1-83Δ) variant remains predominantly in the cytosol. Thus, a combination of the basic amino acid stretches could constitute the functional NLS. It is noteworthy that despite the variation in the amino acid residues amongst the NLS from various species, it would appear that the NLS binding protein must be flexible to recognize diverse sequence context.

Our second observation relates to the stability of the APN-1(1-83Δ) *versus* APN-1(1-118Δ). While APN-1(1-83Δ) can be detected readily and retained a cytosolic distribution, APN-1 (1-118Δ) was undetectable in the extract by Western blot analysis and in the cell

appears to form aggregates presumably in the vacuoles (Fig. 3). We reasoned from this observation that residues 83 to 118 must play an important role in the stabilization of the protein. This region has a putative NLS sequence and it could likely compete for binding to the karyopherins, which may prevent APN-1(1-83Δ) from being targeted to the vacuoles for degradation [20].

5. Conclusions

We have shown that the long N-terminal extension of *C. elegans* APN-1 possesses at least one functional domain, which is involved in targeting the protein to the nucleus. There is no evidence that this N-terminal plays a direct role in DNA repair. Our data also reveal that the recognition apparatus for NLS in yeast is capable of recognizing variation in the sequences that mark protein for the nucleus.

Acknowledgements

This work was supported by research grants (MOP-93573 and RGPIN/202432-2012) to D. R. from the Canadian Institute of Health Research and the Natural Science and Engineering Research Council of Canada.

Conflict of Interest statement

The authors declare that there are no conflicts of interest.

References

[1] J.M. Daley, C. Zakaria, D. Ramotar, The endonuclease IV family of apurinic/apyrimidinic endonucleases, Mutat Res 705 (2010) 217-227.

[2] D. Ramotar, S.C. Popoff, E.B. Gralla, B. Demple, Cellular role of yeast Apn1 apurinic endonuclease/3'-diesterase: repair of oxidative and alkylation DNA damage and control of spontaneous mutation, Mol Cell Biol 11 (1991) 4537-4544.

[3] A.S. Karumbati, R.A. Deshpande, A. Jilani, J.R. Vance, D. Ramotar, T.E. Wilson, The role of yeast DNA 3'-phosphatase Tpp1 and rad1/Rad10 endonuclease in processing spontaneous and induced base lesions, J Biol Chem 278 (2003) 31434-31443.

[4] A.A. Ishchenko, X. Yang, D. Ramotar, M. Saparbaev, The 3'->5' exonuclease of Apn1 provides an alternative pathway to repair 7,8-dihydro-8-oxodeoxyguanosine in *Saccharomyces cerevisiae*, Mol Cell Biol 25 (2005) 6380-6390.

[5] L. Gros, A.A. Ishchenko, H. Ide, R.H. Elder, M.K. Saparbaev, The major human AP endonuclease (Ape1) is involved in the nucleotide incision repair pathway, Nucleic Acids Res 32 (2004) 73-81.

[6] A.A. Ischenko, M.K. Saparbaev, Alternative nucleotide incision repair pathway for oxidative DNA damage, Nature 415 (2002) 183-187.

[7] C. Zakaria, H. Kassahun, X. Yang, J.C. Labbe, H. Nilsen, D. Ramotar, Caenorhabditis elegans APN-1 plays a vital role in maintaining genome stability, DNA Repair (Amst) 9 (2010) 169-176.

[8] A. Shatilla, A.A. Ishchenko, M. Saparbaev, D. Ramotar, Characterization of Caenorhabditis elegans Exonuclease-3 and Evidence That a Mg(2+)-Dependent Variant Exhibits a Distinct Mode of Action on Damaged DNA, Biochemistry 44 (2005) 12835-12848.

[9] A. Shatilla, D. Ramotar, Embryonic extracts derived from the nematode Caenorhabditis elegans remove uracil from DNA by the sequential action of uracil-DNA glycosylase and AP (apurinic/apyrimidinic) endonuclease, Biochem J 365 (2002) 547-553.

[10] D. Ramotar, B. Demple, Functional expression of Escherichia coli endonuclease IV in apurinic endonuclease-deficient yeast, J Biol Chem 271 (1996) 7368-7374.

[11] D. Ramotar, S.C. Popoff, B. Demple, Complementation of DNA repair-deficient Escherichia coli by the yeast Apn1 apurinic/apyrimidinic endonuclease gene, Mol Microbiol 5 (1991) 149-155.

[12] J.R. Vance, T.E. Wilson, Repair of dna strand breaks by the overlapping functions of lesion-specific and non-lesion-specific dna 3' phosphatases, Mol Cell Biol 21 (2001) 7191-7198.

[13] B. Demple, L. Harrison, Repair of oxidative damage to DNA: enzymology and biology, Annu Rev Biochem 63 (1994) 915-948.

[14] J.R. Vance, T.E. Wilson, Uncoupling of 3'-phosphatase and 5'-kinase functions in budding yeast. Characterization of Saccharomyces cerevisiae DNA 3'-phosphatase (TPP1), J Biol Chem 276 (2001) 15073-15081.

[15] A. Shatilla, A. Leduc, X. Yang, D. Ramotar, Identification of two apurinic/apyrimidinic endonucleases from Caenorhabditis elegans by cross-species complementation, DNA Repair (Amst) 4 (2005) 655-670.

[16] X. Yang, J. Fan, A.A. Ishchenko, D. Patel, M.K. Saparbaev, D. Ramotar, Functional characterization of the Caenorhabditis elegans DNA repair enzyme APN-1, DNA Repair (Amst) 11 (2012) 811-822.

[17] M. Aouida, N. Page, A. Leduc, M. Peter, D. Ramotar, A genome-wide screen in Saccharomyces cerevisiae reveals altered transport as a mechanism of resistance to the anticancer drug bleomycin, Cancer Res 64 (2004) 1102-1109.

[18] J.Y. Masson, D. Ramotar, Normal processing of AP sites in Apn1-deficient Saccharomyces cerevisiae is restored by Escherichia coli genes expressing either exonuclease III or endonuclease III, Mol Microbiol 24 (1997) 711-721.

[19] A. Gelin, M. Redrejo-Rodriguez, J. Laval, O.S. Fedorova, M. Saparbaev, A.A. Ishchenko, Genetic and biochemical characterization of human AP endonuclease 1 mutants deficient in nucleotide incision repair activity, PLoS One 5 (2010) e12241.

[20] R. Vongsamphanh, P.K. Fortier, D. Ramotar, Pir1p mediates translocation of the yeast Apn1p endonuclease into the mitochondria to maintain genomic stability, Mol Cell Biol 21 (2001) 1647-1655.

[21] A. Jilani, R. Vongsamphanh, A. Leduc, L. Gros, M. Saparbaev, D. Ramotar, Characterization of two independent amino acid substitutions that disrupt the DNA repair functions of the yeast Apn1, Biochemistry 42 (2003) 6436-6445.

[22] D.M. Wilson, 3rd, R.A. Bennett, J.C. Marquis, P. Ansari, B. Demple, Trans-complementation by human apurinic endonuclease (Ape) of hypersensitivity to DNA damage and spontaneous mutator phenotype in apn1-yeast, Nucleic Acids Res 23 (1995) 5027-5033.

[23] D. Ramotar, C. Kim, R. Lillis, B. Demple, Intracellular localization of the Apn1 DNA repair enzyme of Saccharomyces cerevisiae. Nuclear transport signals and biological role, J Biol Chem 268 (1993) 20533-20539.

Legends

Figure 1. **Schematic representation of the full-length *C. elegans* APN-1 with its N-terminal deletion mutants and the region of homology shared by *S. cerevisiae* Apn1 and *E. coli* endo IV**. The vertical black bars in the N-terminal of *C. elegans* APN-1 are amino acid stretches that are putative nuclear localization signal (NLS). The vertical bars in the C-terminal of *S. cerevisiae* Apn1 constitute a bipartite NLS. The highlighted amino acid residues (bold underlined) indicate the location of the putative NLS within the N-terminal region of *C. elegans* APN-1.

Figure 2. Expression levels of APN-1 and its N-terminal deletion mutants as GFP fusion protein in yeast cells. A and C) Western blot analysis. The plasmids designed to express the indication GFP fusion APN-1 were introduced into strain YW778 and total extracts were prepared and analyzed by 12 % SDS-PAGE followed by Western blot analysis probed with anti-GFP monoclonal antibody. Panel A, Lanes 1, 3, 5, 7 and 9 and lanes 2, 4, 6, 8 and 10 contained 100 and 40 μg of total protein extracts, respectively. Panel C, lanes 1, 2 and 3 contained 60 μg of total protein extracts. **B)** Ponsceau staining of the membranes for panel A. **D)** Coomassie staining of the duplicate SDS-PAGE for panel C. Panels B and D were used for monitoring the amount of total protein extracts loaded.

Figure 3. Fluorescent microscopy showing the cellular distribution of GFP-APN-1 and its N-terminal deletions. Exponentially growing cultures of strain WY778 carrying the indicated plasmids were fixed and images captured by a Leica DMRE immunofluorescent

microscope and images were processed by the MacIntosh OpenLab program. The location of the nucleus was determined by staining the nuclear DNA with DAPI.

Figure 4. Cleavage of the AP site DNA substrate by APN-1 and the N-terminal deletion mutants. Increasing amounts of total extracts from Fig. 2 were incubated with the 5'-end [^{32}P]-labeled 42-mer AP site substrate for 20 min. The 20-mer product was detected by electrophoresis in denaturing 10 % (w/v) polyacrylamide gels (7 M Urea), exposed to a Fugi FLA-3000 Phosphor Screen and analyzed using Image Gauge V3.12 software. Lanes 4-6, 7-9, 10-12 and 13-15 each set of lanes contained 1000, 100 and 10 ng of total protein extracts.

Figure 5. MMS resistance of strain YW778 harboring plasmids carrying either APN-1 or its N-terminal deletion mutants without or with SV40-NLS. Exponentially growing cultures were serially diluted and spotted onto solid selective media without and with 0.015 mmol of methyl methane sulfonate (MMS). Picture was taken after two days of incubation at 30^{o}C.

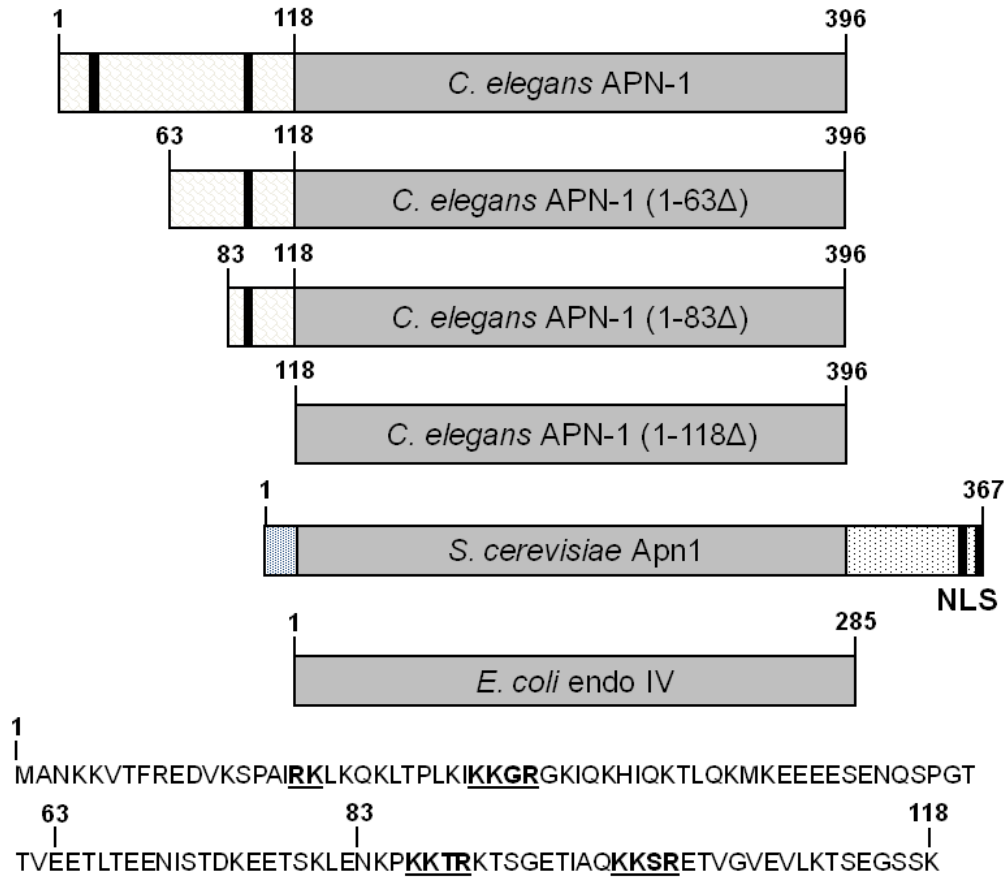

Fig. 1: Wang et al., 2014

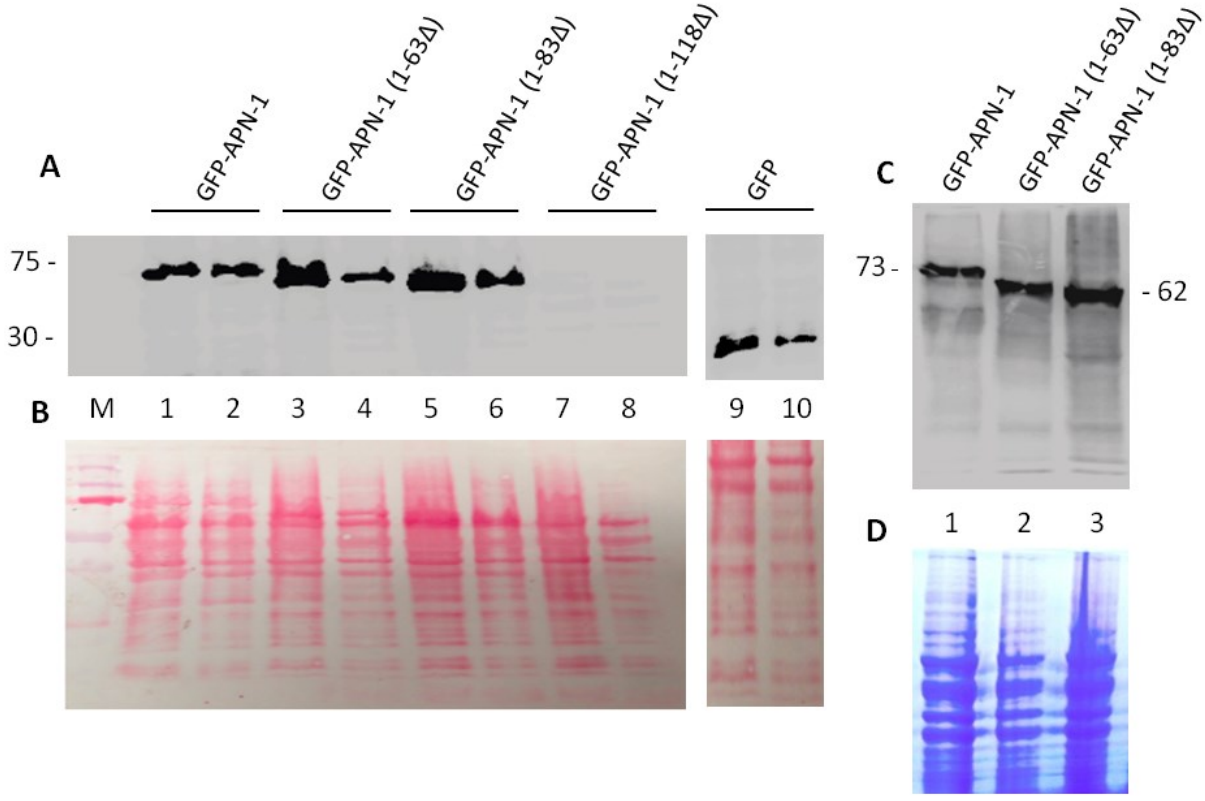

Fig. 2: Wang et al., 2014

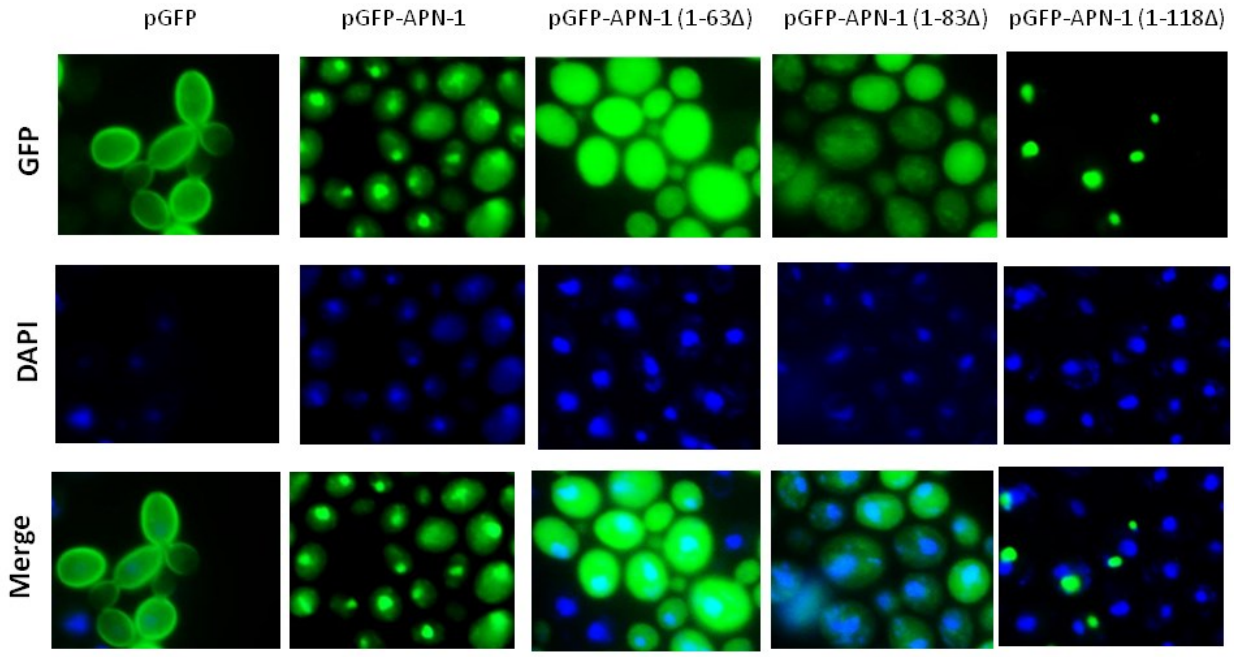

Fig. 3: Wang et al., 2014

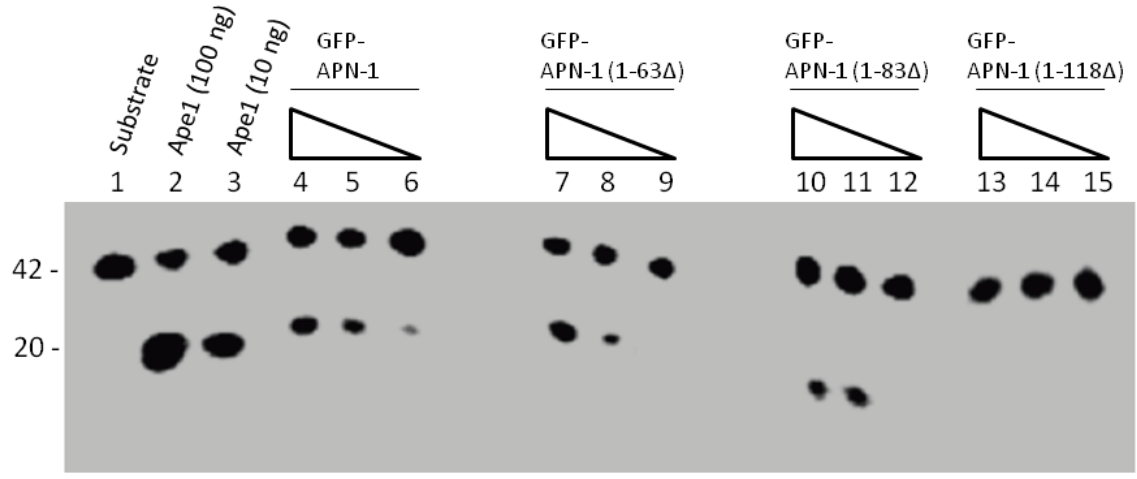

Fig. 4: Wang et al., 2014

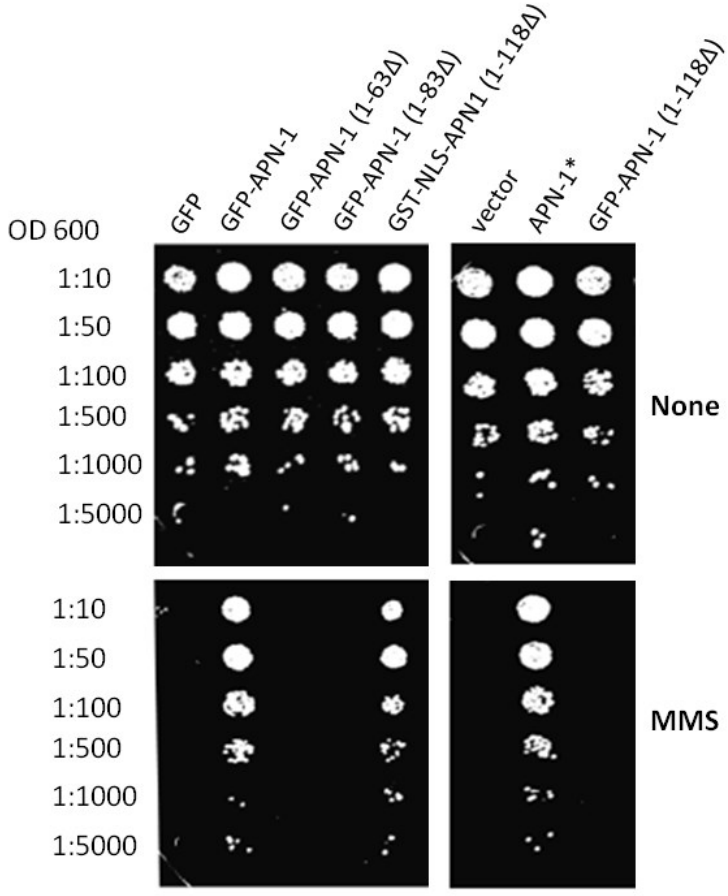

Fig. 5: Wang et al., 2014

Appendix B

The following is a paper reprint published in the journal DNA repair.

Functional variants of human APE1 rescue the DNA repair defects of the yeast AP endonuclease/3’-diesterase-deficient strain

DNA Repair 22 (2014) 53–66

Contents lists available at ScienceDirect

DNA Repair

journal homepage: www.elsevier.com/locate/dnarepair

Functional variants of human APE1 rescue the DNA repair defects of the yeast AP endonuclease/3′-diesterase-deficient strain

Zhiqiang Wang[a], Emily Ayoub[a], Abdelghani Mazouzi[a], Inga Grin[b,c], Alexander A. Ishchenko[b], Jinjiang Fan[d], Xiaoming Yang[a], Taramatti Harihar[a], Murat Saparbaev[b], Dindial Ramotar[a,*]

[a] Maisonneuve-Rosemont Hospital, Research Center, Université de Montréal 5415 Boul. de l' Assomption, Montréal, Québec, Canada H1T 2M4
[b] Groupe Réparation de l'ADN, Université Paris Sud, Laboratoire Stabilité Génétique et Oncogenèse CNRS, UMR 8200, Gustave-Roussy Cancer Center, F-94805 Villejuif Cedex, France
[c] SB RAS Institute of Chemical Biology and Fundamental Medicine, 8 Lavrentieva Ave. , Novosibirsk 630090, Russia
[d] Research Institute of the McGill University Health Centre and Department of Medicine, McGill University, 1650 Cedar Avenue, Montreal, QC H3G 1A4, Canada

ARTICLE INFO

Article history:
Received 24 March 2014
Received in revised form 2 July 2014
Accepted 17 July 2014

Keywords:
DNA repair
Oxidative DNA damage
Human AP endonuclease
Mutations
Base-excision repair
Yeast

ABSTRACT

Human APE1 is an essential enzyme performing functions in DNA repair and transcription. It possesses four distinct repair activities acting on a variety of base and sugar derived DNA lesions. APE1 has seven cysteine residues and Cys65, and to a lesser extent Cys93 and Cys99, is uniquely involved in maintaining a subset of transcription factors in the reduced and active state. Four of the cysteines Cys93, 99, 208 and 310 of APE1 are located proximal to its active site residues Glu96, Asp210 and His309 involved in processing damaged DNA, raising the possibility that missense mutation of these cysteines could alter the enzyme DNA repair functions. An earlier report documented that serine substitution of the individual cysteine residues did not affect APE1 ability to cleave an abasic site oligonucleotide substrate *in vitro*, except for Cys99Ser, although any consequences of these variants in the repair of *in vivo* DNA lesions were not tested. Herein, we mutated all seven cysteines of APE1, either singly or in combination, to alanine and show that none of the resulting variants interfered with the enzyme DNA repair functions. Cross-specie complementation analysis reveals that these APE1 cysteine variants fully rescued the yeast DNA repair deficient strain YW778, lacking AP endonucleases and 3′-diesterases, from toxicities caused by DNA damaging agents. Moreover, the elevated spontaneous mutations arising in strain YW778 from the lack of the DNA repair activities were completely suppressed by the APE1 cysteine variants. These findings suggest that the cysteine residues of APE1 are unlikely to play a role in the DNA repair functions of the enzyme *in vivo*. We also examine other APE1 missense mutations and provide the first evidence that the variant Asp308Ala with normal AP endonuclease, but devoid of 3′→5′ exonuclease, displays hypersensitivity to the anticancer drug bleomycin, and not to other agents, suggesting that it has a defect in processing unique DNA lesions. Molecular modeling reveals that Asp308Ala cannot make proper contact with Mg^{2+} and may alter the enzyme ability to cleave or disassociate from specific DNA lesions.

1. Introduction

Damaged DNA bases and apurinic/apyrimidinic (AP) sites are removed by the base-excision DNA repair pathway (BER) [1,2]. In this pathway, several well-conserved lesion-specific DNA glycosylases hydrolyze the *N*-glycosylic bond between an abnormal base and the deoxyribose sugar to produce an unmodified AP site as a secondary lesion [1,3]. The resulting AP site is cleaved by another highly conserved repair enzyme, AP endonuclease, which comprises of two distinct families, exemplified by *Escherichia coli* endonuclease IV (Endo IV, divalent cations-independent) and

Abbreviations: AP sites, apurinic/apyrimidinic sites; BLM, Bleomycin; H_2O_2, hydrogenperoixde; MMS, methyl methane sulfonate; DTT, dithiothreitol; UDG, uracil DNA glycosylase; THF, tetrahydrofuran; dHU, 5,6-dihydrouracil; 5-ohU, 5-hydroxyuracil; 8oxoG, 8-oxoguanine; αdN, alpha-anomeric 2′-deoxynucleosides; PCR, polymerase chain reaction; PMSF, phenyl methyl sulfonylflouride; SDS, sodium dodecyl sulphate.

* Corresponding author. Tel.: +1 514 252 3400x4684; fax: +1 514 252 3430.
E-mail address: dindial.ramotar@umontreal.ca (D. Ramotar).

http://dx.doi.org/10.1016/j.dnarep.2014.07.010
1568-7864/

exonuclease III (Exo III, Mg^{2+}-dependent) [1,2]. Both Endo IV and Exo III homologues are present in several organisms, including *Saccharomyces cerevisiae* and *Caenorhabditis elegans* [2,4]. However, in humans, homology searches and immuno-detection approaches failed to identify the Endo IV counterpart, and so far only the Exo III members APE1 and APE2 have been found [1,2].

APE1 is an essential enzyme that executes three known functions one in DNA/RNA repair and two others in transcriptional regulation, while APE2 has been recently shown to play a role in ATR-Chk1 checkpoint signaling caused by oxidative stress [5,6]. In DNA repair, APE1 functions in the BER pathway to process spontaneous and exogenous agent-induced AP sites [1,7]. APE1 initiates the repair by cleaving the phosphodiester bond immediately 5′ to the AP site to produce a nick containing a free 3′-hydroxyl group and a 5′-deoxyribose phosphate (5′-dRP) residue. The 5′-dRP is removed by the DNA polymerase β (Polβ) catalyzed 5′-lyase activity, which then concomitantly fills in the single nucleotide gap followed by the action of DNA ligase III-XRCC1 complex to seal the nick [8]. APE1 is also endowed with three additional activities including (*i*) 3′-phosphodieterase to clean up the DNA strand breaks with 3′-blocked termini such as 3′-phosphoglycolate and 3′-phosphate [1], (*ii*) non-specific 3′→5′ exonuclease capable of removing a few nucleotides at nicked DNA duplex to create a single-stranded gap and which may be involved in the proof-reading function during DNA synthesis to prevent the misincorporation of damaged nucleotides such as 8-oxoguanine by DNA polymerases [9,10], and (*iii*) nucleotide incision repair (NIR) activity that removes a variety of oxidized DNA bases by making an incision immediately 5′ to the damaged nucleotide to create a 3′-hydroxyl group and 5′-dangling base [11,12]. Thus, APE1 can process several types of DNA lesions and it is believed to employ a common active site mechanism by using the amino acid residues Glu96, Asp210 and His309 to coordinate Mg^{2+} binding and the cleavage of the phosphodiester bond [13,14]. Downregulation of the APE1 protein level increases cellular sensitivity to DNA-damaging agents including the alkylating agent methyl methane sulfonate (MMS) and the anticancer drug bleomycin, which are known to create DNA lesions that are repairable by APE1 [15,16]. APE1-depleted cells also accumulate high levels of AP sites, which if left unrepaired are mutagenic and can trigger apoptosis [7].

Besides its role in DNA repair, APE1 uses its N-terminal non-conserved domain to perform two distinct transcriptional regulatory functions: (*i*) it uses cysteine 65 to regulate the redox state of many transcriptional factors such as p53, AP-1, c-Jun, c-Fos, and NFkB [17–19], and (*ii*) it acts as a *trans*-acting factor that binds to the negative Ca^{2+}-response element to modulate expression of various genes [20–22]. How APE1 is being recruited to execute these non-DNA repair functions remains a challenge, although this could be directly related to its ability to interact with multiple different partners as well as to undergo several types of post-translational modifications that include acetylation, deacetylation, phosphorylation, and ubiquitination [22–27]. More recent studies showed that in addition to Cys65, Cys93 and Cys99 are also redox active, but not the remaining four cysteines of APE1, that is, Cys138, Cys208, Cys296 and Cys310 [28]. We have shown that APE1 is sensitive to oxidation and that total extracts or purified fractions of APE1 contain various oxidized species that can be reduced to its native state by β-mercaptoethanol [29], raising the possibility that the oxidized forms are driven by disulfide bond formation. It has been a longstanding interest to determine if any of the cysteine residues of APE1 undergoes oxidation *in vivo* leading to inactivation of the enzyme. Although the crystal structure of APE1 suggests that the cysteines do not participate in the catalytic reaction [13,28,30], four of these, i.e., Cys93, Cys99, Cys208 and Cys310, are located proximal to the amino acid residues Glu96, Arg210 and His309 that are critical for Mg^{2+} coordination and the catalytic activity of APE1. A few studies were therefore undertaken to test if substitution of the cysteine residues of APE1 has any consequences on the enzyme ability to process AP sites *in vitro*. The study by Mantha et al. created variants of APE1 by substituting the cysteines for serine and then measured the AP endonuclease activity of the purified proteins [31]. The authors reported that the cysteine variants behave like native APE1, except for Cys99Ser (C99S) whose AP endonuclease activity was regulated by Mg^{2+} concentration [31]. At high Mg^{2+} concentration (10 mM), the C99S variant lost its activity towards the AP site substrate, but showed normal activity at 2 mM Mg^{2+} [31]. In the absence of Mg^{2+}, C99S lacks the ability to bind the AP site DNA substrate providing evidence that Cys99, and not the other cysteine residues, is involved in making contact with the substrate AP site [31]. However, it is not known whether C99S substitution of APE1 has a similar defect in repairing AP sites *in vivo*, although it has been shown that C99 can be S-glutathionylated causing the enzyme to have reduced AP endonuclease activity as a consequence of impaired binding to DNA [32]. A more recent study by Vascotto et al. examined the effects of two of these cysteine mutants, namely C65S and C310S in HeLa cells upon silencing the endogenous APE1 and scored for various phenotypes [33]. Only C65S had a profound effect, whereby it lacks the ability to promote cell growth or suppress apoptosis when APE1 was silenced [33]. The defects of the C65S variant were unrelated to its ability to repair AP sites, but due to improper folding that prevented its accumulation in the mitochondria [33]. These defects are believed to be caused by the redox function played by Cys65, although no effects were observed when the equivalent cysteine Cys64 was mutated to Cys64Ala in the mouse model [33,34]. In contrast, the C310S variant showed no major defects in rescuing the endogenous APE1 [33].

In this study, we replaced the cysteine residues with alanine, either singly or in combination, and investigate for the first time whether the resulting variants of APE1 would alter the ability of the enzyme to repair damaged DNA using an *in vivo* model system based on cross-specie complementation analysis. In this analysis, we check if the expressed APE1 variants can rescue the DNA repair-deficient *S. cerevisiae apn1Δ apn2Δ tpp1Δ* triple mutant strain, that is completely devoid of AP endonuclease and 3′-diesterase activities [9,35,36], from (*i*) drug-induced DNA damage and (*ii*) enhanced genomic instability. This yeast mutant strain YW778 exhibits exquisite sensitivities to various DNA damaging agents including methyl methane sulfonate (MMS) and bleomycin (BLM) that produce AP sites and DNA strand breaks with blocked 3′-termini, respectively [9,35,36]. Importantly, this strain has been used in cross-species complementation analysis to test *in vivo* the DNA repair function of many AP endonuclease/3′-diesterase, independent of their interacting partners, from various organisms including *E. coli*, *S. pombe*, *C. elegans* and mammalian cells [9,35–37].

It is noteworthy that the classic DNA glycosylase-initiated BER pathway raises theoretical problems for the efficient removal of DNA base damage because it generates highly genotoxic intermediates such as AP sites and/or blocked 3′-termini that must be eliminated by additional steps before initiating the repair synthesis. In the alternative NIR pathway, an AP endonuclease cleaves 5′ to a damaged nucleotide, resulting in a free 3′-OH group proper for DNA polymerases and a 5′-dangling damaged nucleotide [12]. The NIR endonucleases including *Escherichia coli* Nfo, *S. cerevisae* Apn1 and human APE1 can directly cleave DNA duplexes containing α-anomeric 2′-deoxynucleosides (αdN) and various oxidized pyrimidines to initiate their removal *via* strand displacement

synthesis coupled to the cleavage of the 5′-flap by a specific endonuclease [11,12,38,39]. Importantly, DNA repair activities of *E. coli* Nfo and human APE1 involved in the AP site repair and NIR pathways can be separated by constructing mutants deficient in the NIR activity but still capable of performing the AP endonuclease and 3′-repair phosphodiesterase functions [40,41]. Previously, we attempted to separate various DNA repair functions of APE1 by constructing point mutants. Using structural and genetic data we have isolated and characterized the APE1 protein mutants carrying single K98A, R185A, D308A and double K98A/R185A amino acid substitutions [41]. Purified APE1 mutant proteins exhibit a dramatic reduction in NIR and 3′→5′ exonuclease activities, while retaining BER functions and the ability to reduce sensitivity to alkylation DNA damage when expressed in the AP endonuclease-deficient *E. coli* strain [41]. Among these proteins the D308A APE1 mutant completely lacks NIR activity on αdA-containing DNA and exhibits dramatic decrease in 3′→5′ exonuclease function, but shows virtually normal AP endonuclease and 3′-phosphodiesterase activities, revealing the crucial role of this residue in NIR and exonuclease functions [41]. Interestingly, at very low Mg^{2+} concentrations, APE1 D308A exhibited a dramatic reduction in the AP endonuclease and 5,6-dihydrouracil-incision activities, as compared to wild type APE1. In fact, D308A was previously shown to possess normal DNA binding affinity for the AP site substrate, but displayed higher AP endonuclease activity and dissociated more rapidly from the cleaved DNA product as compared to the wild type APE1 [42–44]. In addition, others have shown that the D308A variant either had only a minor effect on APE1 incision activity or exhibited a 10-fold decrease in the turnover number as compared to the wild type APE1 [44,45]. It is suggested that D308 may contribute to metal ion coordination to promote conformational change that maintains the integrity of the active site [43–45].

The single K98A and R185A APE1 mutants exhibited a stronger decrease in NIR activity on αdA•T (220 and 52-fold, respectively) compared to the reduction in AP endonuclease (17 and 1.1-fold, respectively) and 3′-phosphoglycolate diesterase (1.7 and 1.4-fold, respectively) activities [41]. Whereas, the double APE1 K98A/R185A mutant was completely devoid of all NIR and 3′→5′ exonuclease activities, but still retained reduce BER activities. Despite the weaker than normal BER function and low expression level, the K98A/R185A APE1 mutant can still reduce the sensitivity of BER-deficient *E. coli xth nfo* strain to an alkylating agent [41]. As such, we also tested in this study if these missense APE1 variants with striking defects in the NIR and 3′→5′ exonuclease activities would affect the enzyme ability to confer drug resistance and prevent the genomic instability of strain YW778. We show that the APE1 variant D308A located next to the active site residue H309 rescued cells from MMS-, but not from BLM-induced toxicity. On the basis of our data, we propose that the inability of D308A to confer resistance to BLM is related to the lack of 3′→5′ exonuclease and not the NIR activity. We provide modeling structures to show that D308A is unable to make proper contact with Mg^{2+} required for efficient substrate cleavage.

2. Materials and methods

2.1. Yeast and bacterial strains, growth media and transformation

Saccharomyces cerevisiae laboratory strains YW465 (*MATalpha ade2Δ0 his3Δ-200 leu2Δ-1 met15Δ0 trp1Δ-63 ura3Δ0*), which is wild-type for AP endonuclease, 3′-diesterase and 3′-phosphatase activities and its isogenic triple mutant derivative YW778 (*apn1Δ::HIS3 apn2Δ::KanMX4 tpp1Δ::MET15*) were generously provided by Dr. Tom Wilson (Ann Arbor, Michigan). Strain YW465 and YW778 were maintained on YPD agar supplemented with adenine (20 μg/mL). *Escherichia coli* laboratory strain DH5α (used for amplification of plasmids) was maintained on Luria Broth (LB) agar. Yeast cells were transformed by the lithium acetate method [46].

2.2. Site-directed mutagenesis

Site-directed mutagenesis (QuikChange® II XL kit, Stratagene) was used according to the manufacturer's instructions to create the various APE1 variants using native HIS-APE1 in pET-14b as the template [29]. Briefly, the primers used for site-directed mutagenesis and verification of the mutated DNA sequence are listed in the Table S1. PCR was done for 20 cycles with one cycle at 95 °C for 2 min; 18 cycles at 95 °C for 20 s coupled with annealing at 60 °C for 10 s and synthesis at 68 °C for 8 min; and final cycle at 68 °C for 5 min. The *Dpn* I-treated PCR product was transformed into the *E. coli* cells XL10-Gold® (Ultracompetent, Stratagene) and plasmid extracted using DNA extraction columns (Qiagen Qiaprep® spin Miniprep kit) and checked for the desired point mutation by DNA sequencing analysis.

2.3. Construction of the yeast expression plasmids

Plasmid pTW438 [47] was used as the backbone to insert the native APE1 gene and its variants that were amplified from the pET14b-HIS-APE1 using the primers

PTW438-APE1-F: 5′-GCACAATATTTCAAGCTATACCAAGCATACAATAAGCTTCTCAC CATGCCGAAGCGTGGGAAAAA-3′ and PTW438-APE1-R: 5′-TATGTAACGTTATAG

ATATGAAGGATTTCATTCGTCTGTCGACCCTCACAGTGCTAGGTATAGGGTGAT-3′ (In Vitrogen) and placed next to the *ADH* promoter using gap-repair. Following the gap-repair, the plasmid DNA carrying the APE1 gene under the expression of the *ADH* promoter was recovered from the yeast cells by glass bead extraction. It was then transformed into *E. coli* cells to recover, amplify and verify the plasmid construct by DNA sequence analysis [47].

2.4. Spot test

These assays were done as previously described [48,49]. All agents for the spot tests were purchased from Sigma–Aldrich Chemical Co. (USA), except bleomycin-A5 (Cat. 55658-47-4, product ID B4517), which was from LKT Laboratories Inc., St. Paul, MN 55130, USA.

2.5. Survival curves

Yeast overnight cell suspensions were subcultured into selective media and incubated at 30 °C for 4 h. Prior to treatment, the $O.D._{(600)}$ of each culture was adjusted to 1.0 and then cultures were aliquoted into one milliliter portions, treated (or not) with increasing concentrations of either hydrogen peroxide (H_2O_2) or bleomycin and incubated for 1 h in an orbital shaker (150 rpm) at 30 °C. Cells were serially diluted into 20 mM potassium phosphate buffer (pH 7.0) and 100 μl of 10^{-3} or 10^{-4} dilution was plated onto 10-cm solid media agar Petri plates. Colonies were counted after 2–3 days incubation at 30 °C.

2.6. Expression and purification of APE1 and its variants from E. coli

His-APE1 native (WT) and its variants were cloned in pET14-b vector under a T7 promoter and expressed in BL21 (DE3) pLysS strain and purified using Talon Metal Affinity column (Clonetech) according to manufacturer instructions with some modifications. Briefly, BL21 pLysS *E.coli* cells expressing His-APE1 (WT or variants) were streaked out on Luria Broth (LB) agar plates containing

Ampicillin (100 μg/mL), a single colony was inoculated in 20 mL of LB containing Ampicillin (100 μg/mL) for overnight incubation at 37 °C with shaking (180 rpm). Next morning, 10 mL of the overnight culture was subcultured in 1 L of LB and grown up to O.D. = 0.5. IPTG (0.4 mM) was added to the culture and left for 2 h at 37 °C with shaking. Cells were harvested by centrifugation at 6000 rpm for 15 min at 4 °C. Cell pellet was resuspended in the washing buffer (50 mM sodium phosphate pH 7.0, 300 mM NaCl) containing protease inhibitors (Invitrogen) and is subjected to sonication for short bursts on ice at 50% amplitude (Branson Digital Sonifier ®) to lyse the cells. Cell lysate was then centrifuged at 13,000 rpm (eppendorf centrifuge) for 20 min at 4 °C. The purification steps were done at 4 °C. The supernatant was loaded onto a column made of 1 mL of Talon metal affinity resin (Clonetech) and the flow through was collected and passed again on the column to maximize the amount of binding proteins. The column was washed with the washing buffer containing protease inhibitors. His-tagged bound proteins were eluted by elution buffer (50 mM sodium phosphate pH 7.0, 300 mM NaCl, 150 mM imidazole), and collected as fractions of 500 μL each. Protein concentration and purity were estimated by Bradford assay and subsequently by SDS-PAGE. The purified proteins were dialyzed against 1 L of the storage buffer (20 mM HEPES pH 7.6, 100 mM NaCl, 1 mM EDTA, 10% Glycerol) at 4 °C. The untagged native APE1 was expressed and purified from *E. coli* BH110 (DE3) strain to avoid cross contamination of bacterial AP endonucleases as described elsewhere [50].

2.7. Yeast extract preparation

Total protein extracts were prepared as previously described [48].

2.8. Western blot analysis

Western blot analysis was performed as previously described with either purified His-APE1 or total yeast protein extracts that were quantified using the Bradford analysis [48]. Briefly, proteins were loaded onto a 10% SDS polyacrylamide gel, which was run at 100 V. The proteins were then transferred to a nitrocellulose membrane at 100 V for 1 h. The membrane was blocked with 5% of skim milk in TBST and then probed overnight at 4 °C with monoclonal anti-APE1 antibody (Cat. 2851-1, Eptomics) at a concentration of 1:1000 in PBS. Three successive washes (10 min each) with TBST were then performed to wash all excess of the primary antibody. After the last wash, the membrane was incubated for 1 h with the anti-mouse IgG antibody (Cat. ADI-SAB-300-J, ENZO) at 1:5000 dilution and was followed by 3 washes of 10 min each with TBST. Finally, the membrane was incubated for 1 min in chemiluminescence reagent and developed using a FujiFilm Intelligent Dark Box and images were acquired with a LAS-3000 camera and the Image Reader LAS-3000 Lite software.

2.9. Oligonucleotides

All other oligodeoxyribonucleotides containing modified residues, and their complementary oligonucleotides were purchased from Eurogentec (Seraing, Belgium), including the following: 30mer for kinetic studies d(TGACTGCATAXGCATGTAGACGATGTGCAT) where X is either alpha-anomeric 2′-deoxyadenosine (αdA), 5,6-dihydrouridine (DHU) or tetrahydrofuranyl (THF); and complementary oligonucleotides, containing either dA, dG, dC or T opposite the adduct. Oligonucleotides were either 5′-end labeled by T4 polynucleotide kinase (New England Biolabs, OZYME France) in the presence of [γ-^{32}P]-ATP (3000 Ci•mmol^{-1}) (PerkinElmer SAS, France), or 3′-end labeled by terminal transferase (New England Biolabs) in the presence of [α-^{32}P]-3′-dATP (Cordycepin 5′-triphosphate, 5000 Ci•mmol^{-1}) (PerkinElmer) as recommended by the manufacturers. The [^{32}P]-labelled oligonucleotides were annealed to their appropriate complementary oligonucleotides in a buffer containing 50 mM NaCl, 10 mM HEPES–KOH (pH 7.2) at 65 °C for 3 min with following slow cooling, as previously described [51]. The resulting duplex oligonucleotides are referred to as X•C (G,A,T), respectively, where X is a modified residue.

The following oligonucleotides were used to measure 3′→5′ exonuclease and 3′-repair diesterase activities: Exo20, d(GTGGCGCGGAGACTTAGAGA); Exo20^{THF}, d(GTGGCGCGGAGACTTAGAGAX), where X is 3′-terminal THF; 5P-Exo19, d(pATTTGGCGCGGGGAATTCC), where p is 5′-terminal phosphate; and complementary Rex-G, d(GGAATTCCCCGCGCCAAATGTCTCTAAGTCTCCGCGCCAC). The nicked/gapped duplexes, Exo20•G and Exo20^{THF}•G were comprised of 5P-Exo19 and Rec-G, and Exo20, or Exo20^{THF}, respectively [41].

2.10. DNA repair assays in vitro

APE1 assay conditions vary depending on the DNA repair pathways studied. The standard AP endonuclease (BER) assay was performed under high Mg^{2+} concentration (≥5 mM): the reaction mixture (20 μL) for APE1 protein contained 5 nM [^{32}P]-labeled THF•T duplex oligonucleotide, 5 mM $MgCl_2$, 50 mM KCl, 20 mM HEPES–KOH (pH 7.6), 0.1 mg mL^{-1} BSA and 10 pM of the enzyme, unless specified otherwise. The standard nucleotide incision assay was performed at a low Mg^{2+} concentration (≤1 mM) and acidic/neutral pH (≤7): the reaction mixture (20 μL) contained 5 nM [^{32}P]-labeled αdA•T or DHU•G duplex oligonucleotide, 0.5 mM $MgCl_2$, 50 mM KCl, 20 mM HEPES-KOH (pH 6.8), 0.1 mg mL^{-1} BSA and 0.2 nM APE1, unless specified otherwise. The standard exonuclease and 3′-repair diesterase assays were also performed at low Mg^{2+} concentrations (≤1 mM) and acidic/neutral pH (≤7): the reaction mixture (20 μL) for APE1 protein contained 5 nM [^{32}P]-labeled Exo20•G, or Exo20^{THF}•T, or Exo20^{P}•T nicked/gapped duplex oligonucleotide, 1 mM $MgCl_2$, 50 mM KCl, 20 mM HEPES-KOH (pH 6.8), 0.1 mg mL^{-1} BSA, and 0.2 nM of the enzyme, unless specified otherwise. The assays were performed at 37 °C for 10 min, unless specified otherwise. Reactions were stopped by adding 10 μL of a solution containing 0.5% SDS and 20 mM EDTA, then desalted in hand-made spin-down columns filled with Sephadex G25 (Amersham Biosciences) equilibrated in 7 M urea. Purified reaction products were heated at 65 °C for 3 min and separated by electrophoresis in denaturing 20% (w/v) polyacrylamide gels (7 M urea, 0.5 X TBE). Gels were exposed to Phosphor Screen and analyzed using Typhoon FLA 9500 GE Healthcare and ImageQuant TL software.

2.11. Modeling of APE1 and its D308A variants with AP site substrate

Comparative modeling of APE1 wild-type and its D308A mutant with AP site substrate and molecular docking of the AP site substrate was done according to Macindoe et al. The three-dimensional coordinates of the APE1 are from Protein Data Bank (PDB: 4IEM; http://www.pdb.org) [52]. The D308A mutant protein of APE1 was derived from the wild-type protein via virtual mutation using Swiss-PdbViewer, V4.1 [53]. Protein–DNA docking between APE1 and AP site substrate was performed with HEX V 6.3 (http://hex.loria.fr) [54]. All graphics of proteins and DNA structures and docking results were presented either in Swiss-PdbViewer (V4.1) or in PyMOL Molecular Graphics System (http://pymol.org).

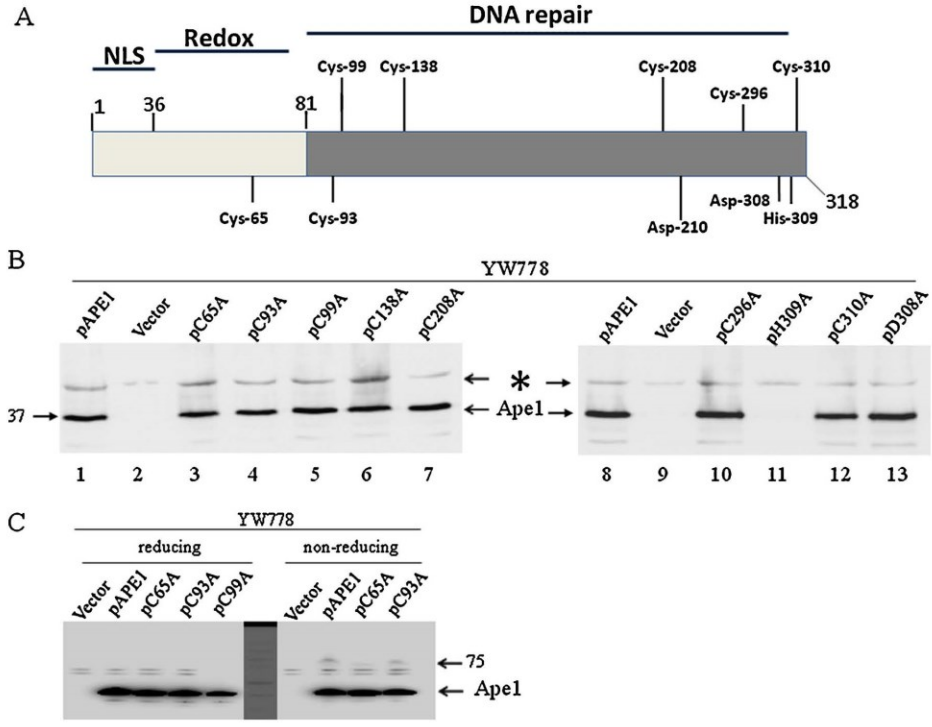

Fig. 1. Location of functional domains of APE1 and expression in the yeast DNA repair deficient strain YW778. (A) Linear structure of APE1 showing the regions harbouring the nuclear localization signal (NLS), the redox and DNA repair functions. (B) Western blot analysis showing expression of native APE1 and the indicated variants. Total protein extracts was derived from exponentially growing cultures of strain YW778 carrying the indicated plasmids or empty vector and subjected to Western blot analysis probed with monoclonal anti-APE1. The asterisk indicates the existence of a non-specific polypeptide. (C) Western blot detection of a 75-kDa APE1 related protein under non-reducing conditions. Total protein extracts were prepared as in panel B, but in the presence of 6 M guanidine-HCl and 50 mM iodoacetamide followed by TCA precipitation. The samples were analyzed by Western blots under reducing or non-reducing conditions and probed with monoclonal anti-APE1 antibody.

3. Results

3.1. APE1 cysteine variants are stably expressed in the yeast DNA repair deficient strain YW778

Previous studies created APE1 cysteine variants by replacing the cysteine residue with serine and monitored the expressed mutant proteins purified from *E. coli* for *in vitro* enzymatic activities [31]. However, no analysis was done to check Cys→Ala variants of APE1 for *in vivo* defects, except for the replacement of the native murine APEX with its variant C64A [34]. To examine for functional defects of the Cys→Ala variants of APE1, we placed the APE1 cDNA next to the constitutive *ADH1* promoter in the yeast expression vector pTW438 and the resulting construct pAPE1 was used to create mutations in the APE1 gene by replacing each cysteine codon for alanine using site-directed mutagenesis (Fig. 1A). This resulted in seven plasmids pC65A, pC93A, pC99A, pC138A, pC208A, pC296A and pC310A each carrying mutations leading to the indicated cysteine to alanine substitutions of APE1. The same strategy was used to produce three additional plasmids each carrying either double C65A/C296A and C65A/C93A or the triple C65A/C93A/C99A mutations. We chose to create alanine instead of the previous substitutions with serine [31], as alanine is not expected to cause any major distortion in the structure of APE1. The empty vector or the plasmids carrying either the native APE1 or the various cysteine mutations were introduced into the yeast DNA repair deficient strain YW778, which lacks the three base-excision repair proteins, Apn1, Apn2 and Tpp1 and display marked hypersensitivity to various DNA damaging agents [36]. Total protein extracts derived from the indicated yeast strains were assessed for expression of native APE1 and its variants using Western blot analysis probed with monoclonal antibody against the N-terminal region of APE1 (Fig. 1B). Native APE1, as well as the cysteine variants were readily expressed and to the same extent in the yeast strain, indicating that the cysteine to alanine substitutions did not cause any severe structural defect to APE1 to make the protein susceptible to proteolysis or subjected to any visible post-translational modification (Fig. 1B). The upper protein band marked by an asterisk was present in all samples including extract from the strain carrying the empty vector indicating that it is a non-specific polypeptide recognized by the antibody (Fig. 1B). For this part of the study, we also replaced one of the active site residues His309 with alanine, however, this variant was not detected in the total yeast extract and only weakly if the whole cells were boiled (i.e., without making extracts) and directly analyzed by PAGE (Fig. 1B) (see below), suggesting that this variant is unstable.

It is noteworthy that under non-reducing conditions, the native APE1, but not the C65A, contained a weak amount of an apparent dimeric form of APE1 (Fig. 1C). This data suggest that C65 is involved in the formation of an intermolecular disulfide bond to yield the apparent dimeric form.

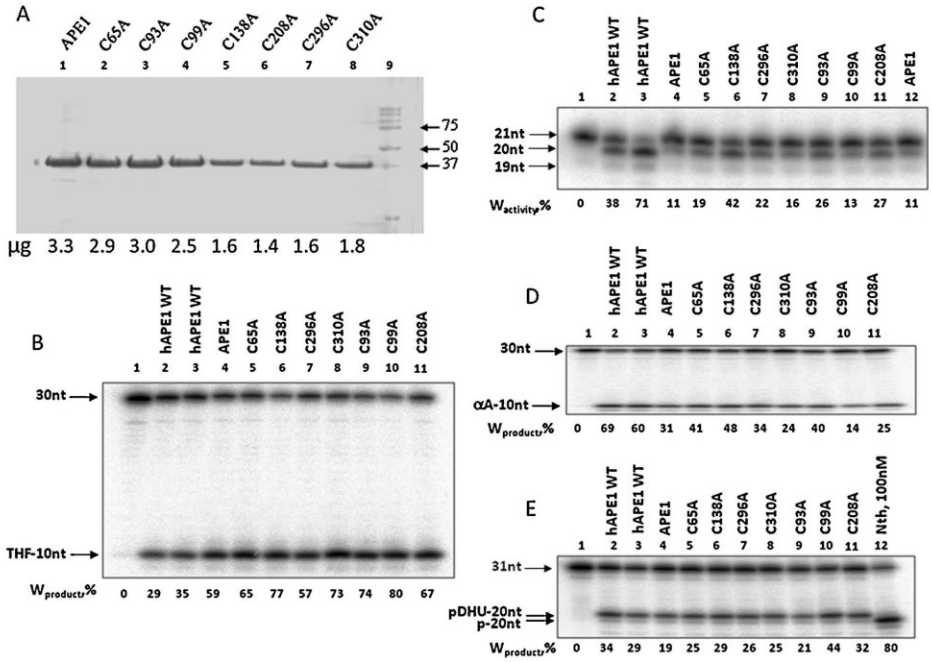

Fig. 2. Processing of [^{32}P]-labelled oligonucleotide duplex substrates containing either THF•G, Exo-THF•G, αdA•T and DHU•G. (A) Coomassie stained gel of purified native APE1 and the indicated Cys variants. APE1 and the variants were expressed as N-terminal His-tag fusion proteins using an *E. coli* expression system, purified to homogeneity and analyzed by SDS-PAGE stained with Coomassie (lanes 1–8; the total amount of proteins (μg) in each lane is indicated at the bottom of the panel). Lane 9, molecular weight markers. (B) Cleaving of the AP site lesion TFH•G by the AP endonuclease activity of purified native APE1 and its Cys mutant variants. Lane 1, substrate alone; lanes 2 and 3, two independent batches of purified native APE1 without the His-tag (hAPE1 WT); lanes 4-11, His-tag purified APE1 and its variants. (C) Removal of the blocked 3′-THF and 3′-nucleotides of Exo-THF•G substrate by the 3′-diesterase and 3′→5′ exonuclease activities, respectively, of purified native APE1 and its Cys mutants. Lane 1, substrate alone; lanes 2 and 3, as in panel B; lanes 4-12, His-tag purified APE1 and its variants. (D) Incision of the αdA•T substrate by the NIR activity of purified native APE1 and its Cys mutants. Lane 1, substrate alone; lanes 2 and 3, as in panel B; lanes 4-11, His-tag purified APE1 and its variants. (E) Incision of the DHU•G substrate by the NIR activity of purified native APE1 and its Cys mutants. Lane 1, substrate alone; lanes 2 and 3, as in panel B; lanes 4–11, His-tag purified APE1 and its mutant variants; and lane 12, purified *E. coli* Nth (100 nM). For the THF•G, Exo-THF•G and αdA•T substrates, the proteins were used at 3 nM, except C93A and C99A were used at 7.5 nM, the substrate at 10 nM and the reactions were incubated at 37 °C for 10 min. In the case of the DHU•G substrate all proteins were used at 5 nM, except C93A and C99A used at 12.5 nM. The hAPE1 WT from two independent purification preparations were used to check if there were potential variations in protein activities from one preparation to another.

3.2. *APE1 cysteine variants are proficient in processing DNA lesions in vitro*

We examined whether the different cysteine substitutions would interfere with the enzymatic functions of APE1. Although the Cys to Ser substitution mutants were examined previously for effect on AP endonuclease activity, these mutants were not tested for activity against other DNA substrates [31]. To do this, we purified the native APE1 and its cysteine variants as HIS tag fusion proteins using an *E. coli* system that drives expression from a T7 promoter (Fig. 2A). We also used the native untagged APE1 (hAPE WT) obtained from two independent preparations of purified protein. The purified proteins were examined for the AP endonuclease, 3′-phosphodiesterase, 3′→5′ exonuclease and NIR activities that are associated with native APE1 under the appropriate optimal reaction conditions [11]. The AP endonuclease activity was monitored by following the cleavage of a 30-mer labeled duplex oligonucleotide substrate bearing a single synthetic AP site, a tetrahydrofuran located at nucleotide position 11 (Fig. 2B, lane 1). The native non-tagged APE1s from two different preparations (lanes 2 and 3), His-tagged APE1 (lane 4) and the various cysteine variants (lanes 5–11) were all proficient in cleaving the AP site substrate to produce the 10-mer product. In contrast to the previous study reported by Mantha et al., showing that C99S has a defect in processing the AP site substrate depending on the Mg^{2+} concentrations, we found no noticeable defect in the ability of the C99A variant to cleave the substrate under our standard assay conditions that include 5 mM Mg^{2+} [31]. We note that this difference was not the result of the type of substitution, as Mantha et al., found similar defect whether Cys99 was replaced by either Ser, Ala or Thr [31].

To monitor for the 3′-repair phosphodiesterase activity, we used a 39-mer oligonucleotide duplex substrate mimicking a 1 nt gap with a single THF lesion at the 3′-end at position 21, Exo20THF•G [41]. As shown in Fig. 2C, the native non-tagged APE1s (lanes 2 and 3), His-tagged APE1 (lane 4) and the Cys variants (lanes 5–11) removed the 3′-blocking THF lesion to produce the 20-nt product. Following removal of the THF lesion, the Cys variants were capable of removing the next nucleotide by the 3′→5′ exonuclease activity to generate the 19-nt fragment in a manner similar to the native APE1 (Fig. 2C). The exonuclease activity was allowed to proceed for only 10 min thereby limiting the appearance of additional reaction products such as the 18-nt fragment (Fig. 2C). In a similar manner, we assessed the APE1 Cys variants for the NIR activity by monitoring the cleavage of two separate substrates: αdA•T carrying the purine alpha-anomeric 2′-deoxyadenosine and DHU•G carrying the pyrimidine 5,6-dihydrouridine, as APE1 is believed to recognize these substrates using different mechanisms [41]. As in the case of the WT his-tagged APE1 (Fig. 2D and E, lane 4), the

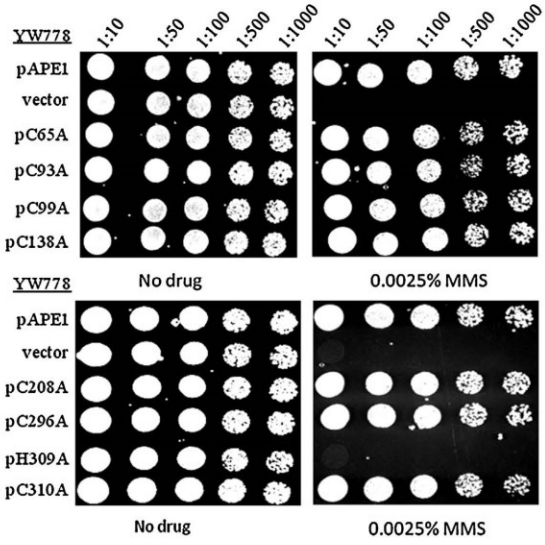

Fig. 3. Expression of Cys variants of APE1 protect strain YW778 from the genotoxicity of MMS. Exponentially growing cultures of strain YW778 carrying the vector or the indicated plasmids expressing either native APE1 or its Cys variants were grown in selective liquid media, serially diluted and spotted on solid YPD agar plates containing the indicated concentration of MMS. Plates were photographed after 48 h of incubation. The result is representative of two independent experiments.

cysteine variants were all active at nicking the αdA•T and DHU•G, although C99A may appear to possess a weaker activity toward αdA•T (Fig. 2D, lane 10). If oxidation of the cysteine residues of APE1 led to disulfide bridges that would reduce the activity of the protein, then preventing formation of these bonds by alanine substitution should increase the enzymatic activity of APE1. However, there was no Cys variant with enhanced DNA repair activities. Thus, it is unlikely that APE1 activities are influenced by disulfide bridges. On the basis of our *in vitro* findings, it would appear that none of the cysteine residues when mutated individually interfere with the ability of APE1 to cleave AP sites, remove blocked 3′-ends or incise oxidized base lesions.

3.3. APE1 cysteine variants rescue the MMS and H_2O_2 sensitivities of strain YW778

While the Cys substitutions did not alter APE1 ability to repair DNA lesions *in vitro*, we cannot exclude the possibility that these mutants may exhibit structural defects that compromise their ability to access and repair DNA lesions *in vivo*. To assess this, exponentially growing cultures of the YW778 strain expressing the indicated APE1 variants were serially diluted and spotted onto solid YPD media containing the DNA damaging agent methyl methane sulfonate (MMS) (Fig. 3). MMS alkylates bases which are removed by DNA glycosylases to generate AP sites. All of the Cys variants of APE1 conferred upon strain YW778 full resistance to MMS, when compared to the native APE1 (Fig. 3). Strain YW778 carrying only the empty vector showed extreme sensitivity to very low concentrations of MMS (Fig. 3). We interpret this observation to suggest that the expressed APE1 variants possess the ability to repair MMS-induced AP sites *in vivo* and therefore prevent strain YW778 from accumulating the genotoxic lesions that lead to cell death. Using the same approach, we tested if variants with multiple cysteine substitutions would alter APE1 ability to rescue strain YW778 from the genotoxicity of MMS. APE1 variants bearing the double mutations either C65A/C93A or C65A/C296A, or the triple mutations C65A/C93A/C99A were expressed normally as the native APE1 (Fig. 4A) and retained full ability to protect strain YW778 from MMS-induced DNA lesions (Fig. 4B). This latter finding is in agreement with the notion that the cysteine residues do not participate in the enzymatic reaction that allows APE1 to process damaged DNA. Thus, substituting multiple cysteine residues of APE1 with alanine is not likely to cause any significant impediment on the enzyme ability to repair AP sites *in vivo*.

We next examined if these APE1 Cys variants would interfere with the ability of the enzyme to repair other types of DNA lesions such as DNA strand breaks with blocked 3′-termini. In this experiment, exponentially growing cultures were treated in phosphate buffer with the chemical oxidant H_2O_2, which is known to create DNA strand breaks with blocked 3′-phosphate, as well as other types of oxidized base lesions such as 8-oxo-guanine [55], and then examined these treated cells for the surviving fractions. The YW778 strain is hypersensitive to H_2O_2 as it lacks the ability to process DNA strand breaks with blocked 3′-phosphate, but which showed parental resistance to the oxidant upon expression of the native APE1 that has the ability to remove blocked 3′-phosphate groups (Fig. 5) [56]. Likewise, all of the APE1 Cys variants fully rescued the sensitivity of strain YW778 towards H_2O_2 (Fig. 5). Similar results were obtained if cells were treated with the anticancer agent bleomycin, which is known to create at least four types of DNA lesions that include oxidized AP sites and DNA strand breaks terminated with 3′-phosphoglycolate (suppl. Fig. S1 and shown for C65A and C310A). Collectively, it would appear that none of the cysteine residues of APE1 plays a critical role in the mechanism by which the enzyme processes drug-induced DNA lesions.

3.4. APE1 cysteine variants prevent the genomic instability of strain YW778

We have previously shown that strain YW778 exhibits a high spontaneous mutation rate, which arises as a result of multiple types of DNA lesions including AP sites and oxidized base lesions generated during normal aerobic metabolism [10]. We tested if the APE1 Cys variants could suppress the spontaneous mutations exhibited by strainYW778 by scoring for canavanine resistant colonies (Can^{R+}) [10]. These colonies arise as a result of mutation in the *CAN1* gene encoding the arginine permease, which permits entry of the arginine analog canavanine into the cell. Expression of any of the APE1 Cys variants, whether carrying a single or multiple cysteine substitutions, completely reduced the mutation frequency of strain YW778 to the level observed when the strain expressed the native APE1 (Table 1). As expected, the active site variant H309A or the empty vector did not suppress the high mutation frequency of strain YW778 (Table 1). Since the elevated spontaneous mutations in YW778 were completely suppressed by the APE1 Cys variants, it would appear that these cysteine substitutions also do not interfere with APE1 ability to process endogenous DNA lesions. Thus, it is unlikely that the cysteine residues would be directly involved in any of the DNA repair functions of APE1 *in vivo*.

3.5. The NIR-deficient APE1 D308A mutant confers differential resistance to the oxidants, H_2O_2 and bleomycin, but fully suppresses the genomic instability of strain YW778

Several separation-of-function missense APE1 variants that have nearly normal AP endonuclease, but with severely compromised NIR activity, were previously characterized [41]. However, attempts to show that these mutants are defective in repairing oxidative DNA lesions *in vivo* have been difficult [57,58]. In the *E. coli* model system, native APE1 can substitute for the repair of AP sites in mutants lacking the two AP endonucleases and 3′-repair

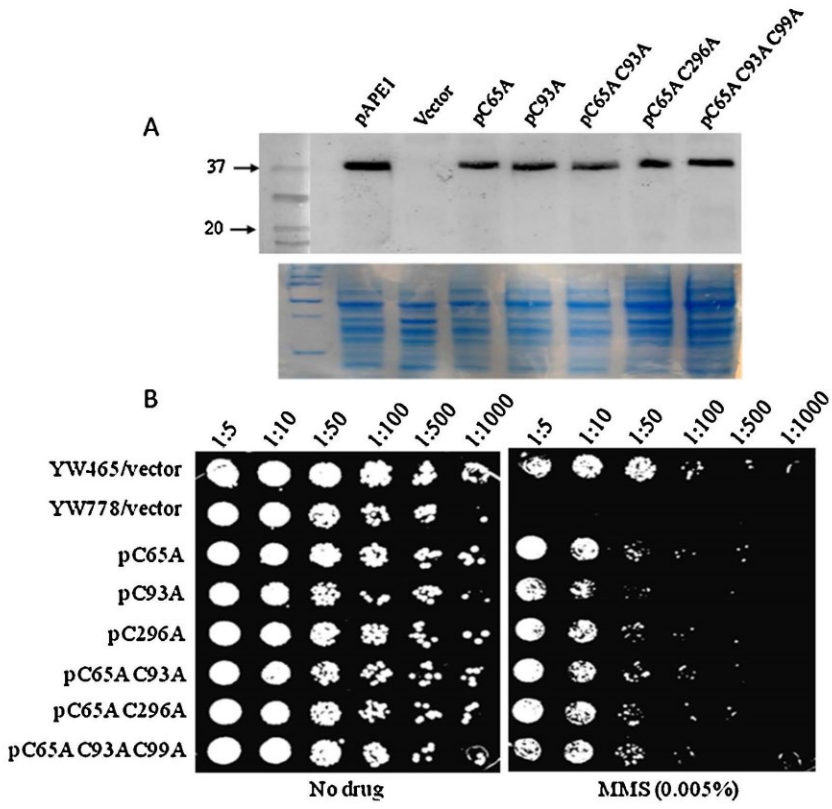

Fig. 4. APE1 variants with double or triple cysteine substitutions are stable and rescue the MMS-sensitivity of strain YW778. (A) Western blot analysis showing expression levels of APE1 variants with double or triple cysteine substitutions. Total protein extracts was prepared and analyzed as in Fig. 1B. The lower panel stained with Coomassie indicates the level of protein loaded in each lane for the Western blot analysis. (B) Spot test analysis. Cells were grown in-ura drop-out liquid media, serially diluted and spotted onto-ura drop-out solid media containing MMS. Plates were photographed after 48 h of incubation. The result is representative of two independent experiments.

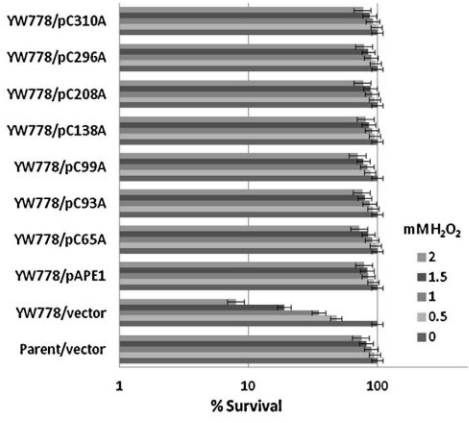

Fig. 5. H_2O_2-sensitivity of strain YW778 carrying the native APE1 or the Cys variants. Exponentially growing cultures were washed, resuspended in potassium phosphate buffer and treated with the indicated concentration of H_2O_2 for 30 min. Cells were diluted and plated on-ura drop-out solid media to score for the percentage of survivors with respect to the parent strain. The data are averages of three independent experiments.

Table 1
Frequency of spontaneous Can^R mutations.

Strains	Mutation frequency can^R (10^{-8})	Fold increase relative to YW465/vector
YW465(Parent)/vector	4.2 ± 1.1	1.0
YW778/vector	39.8 ± 4.8	9.5
YW778/pAPE1	4.6 ± 0.9	1.1
YW778/pC65A	5.1 ± 1.7	1.2
YW778/pC93A	3.9 ± 1.6	0.9
YW778/pC99A	4.8 ± 1.4	1.1
YW778/pC138A	3.5 ± 1.2	0.8
YW778/pC208A	4.7 ± 1.6	1.1
YW778/pC296A	5.4 ± 2.2	1.3
YW778/pC310A	4.5 ± 0.9	1.1
YW778/pC65A/C93A	5.2 ± 1.8	1.2
YW778/pC65A/C296A	4.8 ± 1.7	1.1
YW778/pC65A/C93A/C99A	7.1 ± 2.5	1.7
YW778/pD308A	4.3 ± 1.1	1.0
YW778/pH309A	43.3 ± 5.2	10.3
YW778/pK98A	31.7 ± 3.7	7.5
YW778/pR185A	6.1 ± 2.6	1.5
YW778/pK98A/R185A	5.5 ± 1.5	1.3
YW778/pendo IV	5.3 ± 1.7	1.3
YW778/pCeEXO-3	4.9 ± 0.9	1.2
YW778/pCeAPN-1	5.1 ± 1.9	1.2

diesterases, Nfo and Xth [57,58]. However, it cannot substitute for the repair of oxidative DNA lesions accumulated by Nfo and Xth deficiency [41,57,58]. In contrast, in the yeast model system native APE1 can substitute for the repair of both AP sites and oxidative DNA lesions caused by H_2O_2 and bleomycin (Figs. 3 and 5, and suppl. Fig. S1), although the exact reason for the difference between the two model systems is not known. Because of the advantage of the yeast system, we were prompted to test whether APE1 mutants deficient in the NIR function would rescue strain YW778 from agents that produce oxidative DNA lesions. Thus, we examined whether the APE1 missense mutations K98A, R185A, K98A/R185A and D308A that possess either weak (52- and 220-fold less for K98A and R185A, respectively) or virtually no NIR (K98A/R185A and D308A) activity towards αdA•T would interfere with the enzyme ability to confer drug resistance and suppress the genomic instability exhibited by strain YW778 [41]. Both R185A and the double variant K98A/R185A were shown to exhibit reduced AP endonuclease activity (i.e., 17- and 44-fold less than native APE1, respectively), while K98A and D308A display nearly comparable levels of the activity as the native APE1 enzyme [41]. In addition, the K98A/R185A double mutant and D308A that completely lacked NIR activity also displayed greatly diminished 3′→5′ exonuclease activity [41].

These four APE1 variants K98A, R185A, K98A/R185A and D308A were constructed in the identical yeast expression plasmid pTW438 as the APE1 cysteine variants and introduced into strain YW778. Total protein extracts prepared from these cells using the standard approach with glass beads revealed that YW778 carrying pK98A or pH309A did not express any detectable APE1 variant protein (data not shown), suggesting that these proteins might be unstable to the extraction procedure. However, if these cells were harvested and heated for 5 min at 95 °C in the gel loading buffer following SDS-PAGE analysis, both the K98A and H309A variants were found to be weakly expressed as compared to the native APE1 (Fig. 6A). In contrast, the APE1 variants R185A and D308A were present at the same level as the native APE1, while the double mutant K98A/R185A was expressed at a 2- to 3-fold higher level (Fig. 6A). Thus, it would appear that the instability of the K98A variant might be suppressed by substituting the Arg185 residue with alanine.

Based on the previous report on the functional characterization of these four variants K98A, R185A, K98A/R185A and D308A, we predict that K98A (because of its instability), R185A and K98A/R185A (because of their reduced AP endonuclease activity) would be unable to rescue strain YW778 from the genotoxicity caused by MMS. While K98A did not confer MMS resistance to YW778 as expected, the surprising observation was that both R185A and K98A/R185A provided full resistance to the drug even though these two variants possess significantly reduced AP endonuclease activity as compared to the native APE1 or the D308A variant (Fig. 6B). We interpret this finding to suggest that although R185A and K98A/R185A have reduced AP endonuclease activity, the ability to complement strain YW778 in the repair of AP sites might be compensated by the overproduction of these variants from the constitutive and highly expressed *ADH* promoter.

To test if the NIR activity of APE1 plays a significant role in the repair of oxidative DNA lesions in our *in vivo* model, we examined if these variant would rescue strain YW778 from agents that produce oxidative DNA lesions. When exponentially growing cells expressing the indicated APE1 variants were treated with the chemical oxidant H_2O_2, which is known to create a variety of oxidized DNA lesions including 8-oxoguanine and DNA single-strand breaks with 3′-phosphate blocking groups, all three expressed variants provided to strain YW778 full resistance to the chemical oxidant H_2O_2 (Fig. 6C). It is possible that H_2O_2 might not produce sufficient level of oxidized base lesions to cause toxicity in the absence of functional NIR activity. We therefore tested another oxidant, namely the anticancer drug bleomycin, which creates oxidized AP sites, strand breaks with blocked 3′-termini and bi-stranded DNA lesions [59]. Interestingly, the K98A/R185A and D308A, but not R185A, variants were unable to protect strain YW778 from the genotoxicity caused by bleomycin as compared to the native APE1 when cells were treated in liquid cultures with the drug (Fig. 6D). Since all three variants are severely compromised for NIR activity on α-anomers of 2′-deoxynucleosides, but only the K98A/R185A and D308A variants lacked 3′→5′ exonuclease activity, we suggest that bleomycin might generate strand breaks that cannot be processed by these two latter variants (see Section 4).

We next tested if the high levels of spontaneous mutations exhibited by strain YW778 could be a contribution also from unrepaired oxidized base lesions that require the function of the NIR activity on α-anomers or 3′→5′ exonuclease activity. The APE1 R185A, K98A/R185A and D308A variants completely suppressed the high spontaneous mutations of strain YW778 to the basal levels observed by the expression of the native APE1 (Table 1). Thus, it would appear that under normal aerobic growth conditions, the lesions causing mutations at the *CAN1* gene are not likely to be the α-anomers of 2′-deoxynucleosides or those that require 3′→5′ exonuclease activity of APE1. Whether NIR serves to repair the oxidized base lesions in β-conformation produced during normal aerobic metabolism cannot be assessed by these assays.

3.6. Molecular modeling reveals that D308A is unable to make proper contact with DNA

Since D308A is the only single amino acid substitution mutant exhibiting a clear separation of the APE1 repair functions, i.e., possessing normal AP endonuclease while completely lacking the NIR and 3′→5′ exonuclease activities, we exploited computer modeling to understand how this variant might alter APE1 ability to repair damaged DNA. We used the coordinates from the 3D crystal structure of the enzyme from the protein data base (PDB: 4IEM; http://www.pdb.org) to model the interaction of the native APE1 residue D308 with an oligonucleotide substrate carrying an AP site and compared it with the alanine substitution of the D308A variant (Suppl. Fig. S2). The ribbon structure of APE1 revealed that the D308A substitution did not alter the active site structure of the enzyme nor the overall globular structure of the enzyme (Suppl. Fig. S2). However, the D308A mutation slightly enlarged the hydrophobic pocket of the active site when compared to the native APE1 (Suppl. Fig. S3). In addition, the electrostatic surface potential map revealed that the negative charge within the active site was reduced, as compared to the native enzyme (Suppl. Fig. S3). We next docked the native APE1 and the D308A variant onto the AP site substrate and calculate the free energy of binding (Suppl. Fig. S4). While the free energy of binding of native APE1 onto the AP site was calculated to be −1141.23 kcal/mol, it was −1157.28 for the D308A variant (Suppl. Fig. S4). Thus, the 16.05 kcal/mol difference of free energy of binding for the D308A variant suggests that its wider active site pocket may reduce proper contact and impede recognition and/or cleavage of the substrate (Suppl. Fig. S4), although this could be more severe for some substrates. A close-up view of the active site residues E96, Y171, D210, N212 and H309 and their bond distances to the AP site were compared between the native APE1 and the D308A variant (Fig. 7A vs. B). The analysis revealed that the AP site substrate was pushed closer to residues D210 and H309 of the D308A variant, although this did not cause any severe impediment in the enzyme ability to cleave the AP site substrate since it has normal level of AP endonuclease activity (Fig. 7A vs. B) [41]. However, the close-up view showed that while the three residues E96, D70 and D308 of the native APE1 enzyme made contact with the Mg^{2+} metal ion in the active site [14], only E96 and D70, and not the substitution D308A, remained associated with Mg^{2+} in the D308A

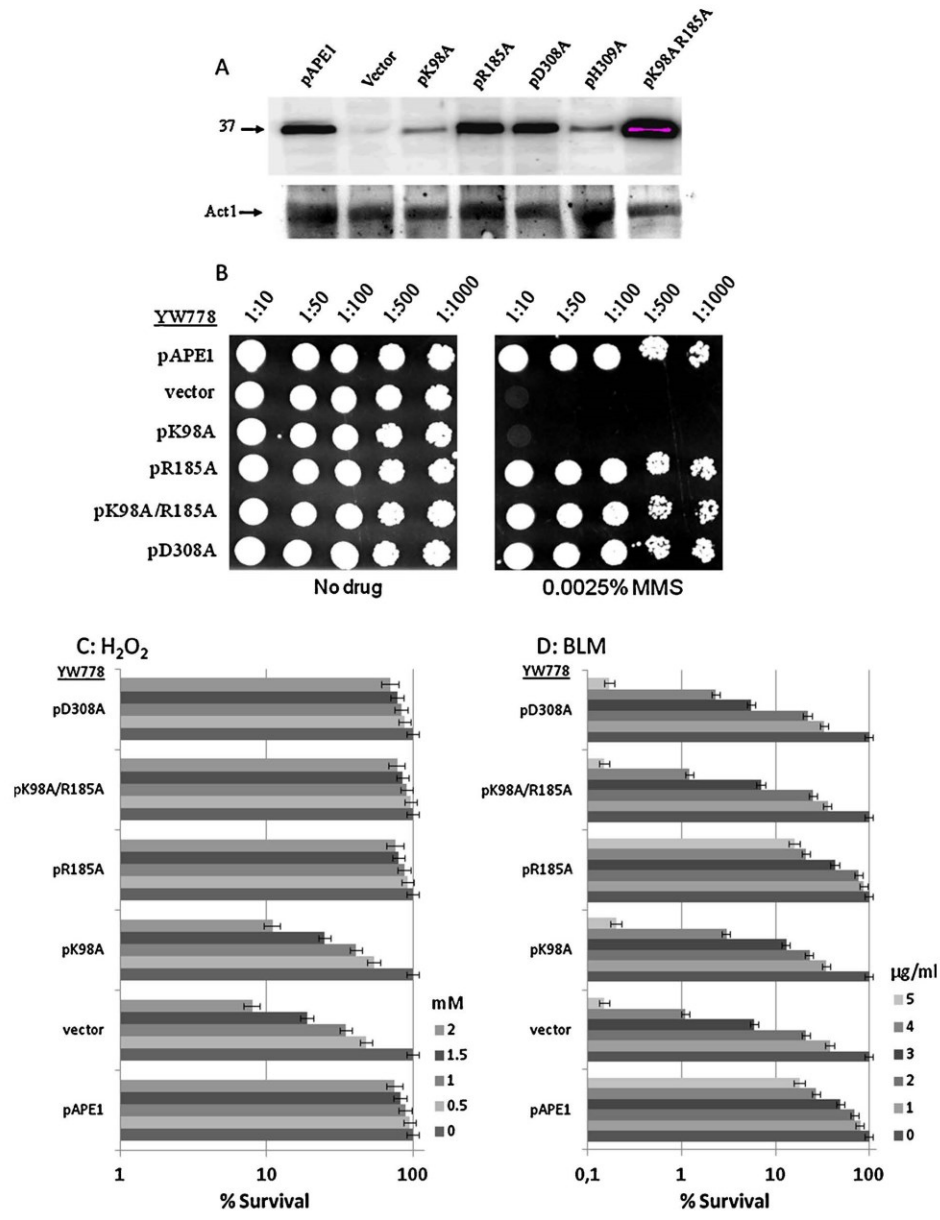

Fig. 6. Expression and complementation analyses of strain YW778 with APE1 variants lacking distinct functional activities. (A) Western blot analysis of strain YW778 expressing the indicated APE1 variants. Exponentially growing cultures in-ura liquid media were harvested, heated in loading buffer without reducing agents and analyzed on SDS-PAGE. The membrane was probed with monoclonal anti-APE1 and subsequently with anti-Act1 antibodies. (B) Spot test analysis. Cells were grown in-ura drop-out liquid media, serially diluted and spotted onto-ura drop-out solid media containing the indicated concentrations of MMS. Plates were photographed after 48 h of incubation. The result is representative of two independent experiments. (C and D) H_2O_2- and bleomycin (BLM)-sensitivity of strain YW778 carrying the APE1 variants. Exponentially growing cultures in selective media were treated with the indicated concentration of H_2O_2 for 30 min or BLM for 1 h. Cells were diluted and plated on-ura drop-out solid media to score for the percentage of survivors with respect to the YW778 strain carrying pAPE1. The data are averages of three independent experiments.

variant (Fig. 7C vs. D). Thus, a likely explanation for the APE1 variant D308A inability to prevent bleomycin toxicity could be due to altered Mg^{2+} concentration requirements for the particular damage repair.

4. Discussion

One of the aims of this study was to determine whether substitution of the cysteine amino acid residues of APE1 would interfere

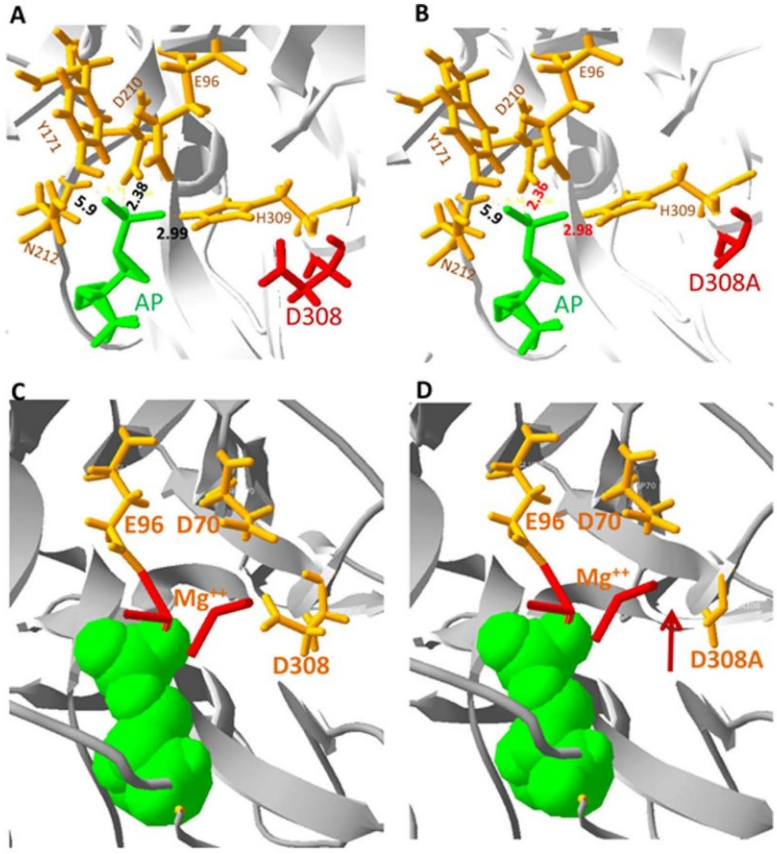

Fig. 7. Close-up views of the active site residues E96, Y171, D210, N212 and H309 and D308/A binding to Mg^{2+} with respect to the bound AP site. (A and B) The AP site substrate is closer within the hydrophobic binding pocket of the variant D308A in comparison to the native APE1. All residues are highlighted in stick mode, where the color brown is for active site residues; the red is for D308 or D308A; and the green is for AP site. (C and D) The amino acid residues making contact with Mg^{2+} in the native APE1 and the variant D308A. The three Mg^{2+} binding sites are in brown color, the Mg^{2+} ion is in red and the AP side is in green. The red arrow indicates the lost interaction of D308A with the Mg^{2+} metal ion.

with its ability to repair damaged DNA in an *in vivo* heterologous model system. Although APE1 is associated with multiple interacting partners involved in DNA repair in human cells and that its cysteine variants could influence these interactions, our approach assessed whether the cysteine substitutions directly affect APE1 DNA repair activities independent of its partners in the yeast model system. Moreover, since *ape1*$^{-/-}$ human cells are not viable it is justifiable to use a heterologous expression system to study APE1-catalyzed DNA repair functions *in vivo*. We show that APE1 variants with single, double or triple cysteine substitutions retained full capability to act and process drug-induced AP sites and DNA strand breaks with blocked 3′-terimini in a yeast strain YW778 that is deficient in these DNA repair functions. In addition, these APE1 Cys variants can act to repair spontaneously occurring DNA lesions and thus suppress the genomic instability exhibited by strain YW778. Our data are consistent with a previous study by Mantha et al., showing that all of the APE1 Cys to Ser variants, for the exception of C99S, retained full ability to cleave AP sites *in vitro* [31]. However, in their studies the authors did not examine whether the Cys to Ser variants affected the 3′-diesterase, 3′→5′ exonuclease, the NIR activity of APE1 or whether these variants influence the repair functions *in vivo*. On the basis of our findings, we suggest that the cysteine residues of APE1 do not appear to participate in the catalytic mechanism of enzyme-mediated repair activities, and thus, are dispensable for repairing damaged DNA *in vitro* and *in vivo*. The unexpected finding by Mantha et al. that C99S impairs the ability of APE1 to cleave the AP site analog tetrahydrofuran at high (10 mM), but not at low Mg^{2+} concentration (0.5 or 2 mM) and independently of whether the cysteine substitution is by serine, alanine or threonine, could not be validated herein [31]. In our study, we did not detect any difference with C99A in cleaving any of the substrates as the reaction mixture contains 0.5–5 mM Mg^{2+}. Since C99A showed no defect in rescuing strain YW778 from MMS toxicity, it seems that the intracellular concentration of Mg^{2+} in yeast cells is sufficient to maintain optimal function of this variant. Thus, the assumption that the residue C99 that is ~16 Å from the active site of APE1 could be involved in the catalytic mechanism is not supported by our experimental data from the yeast *in vivo* model using the C99A variant, although this is unlikely to be related to the type of substitutions [31].

Another aim of our study was to examine whether APE1 variants lacking the NIR activity has any biological consequences with

respect to repairing damaged DNA *in vivo*. We focused on a previously reported variant D308A, which has normal AP endonuclease but completely lacks NIR activity [41,44]. As expected, D308A fully rescued strain YW778 from the genotoxic lesions caused by MMS. Likewise, the D308A fully rescue the H_2O_2 sensitivity of strain YW778 suggesting that this variant has a functional 3′-phosphodiesterase activity to repair the H_2O_2-induced single strand breaks with blocked 3′-termini such as 3′-phosphate [9]. Moreover, the D308A variant also completely suppressed the elevated spontaneous mutations observed in strain YW778 that are caused by the accumulation of endogenous DNA lesions including unrepaired AP sites and oxidized base lesions. Since D308A lacks NIR activity specifically towards the *alpha-anomeric dA, a classic NIR lesion* substrate, the mutations this variant suppresses cannot arise as a result of these unrepaired oxidized base lesions. Similarly, the APE1 variant with a double mutation K98A/R185A, which completely lacks NIR activity against all types of oxidized DNA bases including alpha- and beta-anomers, also fully suppressed the increase of spontaneous mutations exhibited by strain YW778 (Table 1), again suggesting that these mutations occur independently of the NIR repair function of APE1. We believe that the main source of spontaneous mutations in YW778 strain is due to unrepaired AP sites. We propose that our APE1 mutants contain sufficient AP endonuclease activity to repair the majority of AP sites *in vivo*. However, the possibility remains that our two *in vivo* functional assays, survival and mutation analysis, might not be sufficiently sensitive to detect the small fraction of oxidized base lesions that depends on the NIR function. Thus, we cannot address the issue of whether APE1 variants completely lacking NIR function has any biological consequences at the level of maintaining genomic stability by using either of the model organisms *E. coli* or yeast.

The observation that the APE1 variant D308A is unable to rescue the BLM-sensitivity of strain YW778 highlights for the first time an *in vivo* defect associated with this variant in repairing a specific class of DNA lesion(s). Importantly, APE1 depletion by siRNA renders human TK6 lymphoblastoid cells and HCT116 colorectal carcinoma cells extremely sensitive to BLM, but to much lesser extent to ionizing radiation exposure thus suggesting that APE1-catalyzed DNA repair activities are essential for the removal of BLM-induced DNA lesions [16]. However, it is unlikely that the D308A defect in repairing BLM-induced lesions is linked to the deficiency of the NIR function. In support of this notion, we have shown in our earlier studies that the functional expression of the *C. elegans* CeEXO-3, which lacks NIR activity, fully rescues strain YW778 against the genotoxicity caused by either H_2O_2 or BLM, raising the possibility that these agents do not produce substantial levels of oxidized base lesions to warrant repair by the NIR activity [60].

So what is the underlying cause for the sensitivity of the APE1 D308A variant towards BLM? The mechanistic action of BLM first involves the binding of the drug to the reduced form of iron (Fe II) and in the presence of molecular oxygen it becomes activated to form the BLM-Fe(II)-O_2 complex [59]. This activated complex abstracts a hydrogen atom from the 4′-carbon of deoxyribose to produce an unstable sugar carbon-radical, which can be rearranged to generate at least four types of oxidative DNA lesions [59]. One of the lesions include DNA single strand breaks where the 3′-end is terminated with a portion of the deoxyribose ring to form 3′-phosphoglycolate, which effectively blocks DNA synthesis by DNA polymerase [59]. Interestingly, in our previous work the structural modeling of APE1 in complex with nicked duplex oligonucleotide containing 3′-terminal dC residue showed that D308 interacts with 3′-dC and stabilize the enzyme:substrate complex in order to maintain the 3′-terminal nucleotide in a position favorable for 3′→5′ exonuclease activity of APE1 [61]. In agreement with this, we showed that APE1 D308A lacks 3′→5′ exonuclease function and is not able to perform 3′-cleansing function and remove damaged bases located at 3′ side in close proximity to DNA strand breaks [41]. Another highly toxic lesion produced by BLM is bi-stranded DNA lesions that can form at certain specific sequences, such as CGCC, which are generated when the Fe–BLM complex creates an oxidized AP site on one strand, and a directly opposed single-strand break on the complementary strand [59]. The spontaneous cleavage of the AP site by primary amines (e.g., histone amine) *in vivo* converts the bi-stranded lesion into a double strand break such that both strands contain blocked 3′-ends [59]. Since the D308A variant completely lacks the 3′→5′ exonuclease activity, it is possible that these blocked 3′-termini derived from the bi-stranded lesions cannot be processed into free 3′-hydroxyl groups to be channelled into the homologous recombination DNA repair pathway and as a result caused sensitivity to BLM [59]. The dependence of AP endonuclease with 3′-end repair activity to process lesions with blocked 3′-termini is underscored by the fact that yeast mutants lacking Apn1 and Apn2 display a BLM-hypersensitive phenotype upon deleting a key gene *RAD52* in the homologous recombination pathway [9]. Accordingly, the native APE1 and not the D308A variant would rescue strain YW778 from BLM toxicity.

In short, our data conclusively indicate that Cys→Ala mutations do not perturb various DNA repair functions of the APE1 protein *in vitro*. Furthermore, the heterologous expression of human repair enzyme in yeast deficient for AP endonucleases showed that the native and the Cys→Ala mutants of APE1 can rescue cells from genotoxic treatments, suggesting that the cysteine residues do not have significant role in DNA repair. The inability of APE1 D308A NIR-deficient mutant to rescue YW778 strain from BLM genotoxicity suggest that BLM generates specific types of DNA lesions that may require processing by the 3′→5′ exonuclease function of the enzyme. Molecular modelings performed in the previous study showed that the APE1 D308A variant make improper contacts with base moiety of 3′-terminal nucleotide and also with AP site suggesting that this mutant may be unable to repair BLM-induced damage such as oxidized base lesions at 3′-end of DNA strand break.

Conflict of interest

The authors declare that there are no conflicts of interest.

Acknowledgements

We thank Imane Moutalibi for technical assistance with the spot test assays. This work was supported by a research grant to D.R. from the Canadian Institute of Health Research and the Natural Science and Engineering Research Council of Canada, and by the Agence Nationale pour la Recherche (http://www.agence-nationale-recherche.fr) [ANR Blanc 2010 Projet ANR- 10-BLAN-1617 to M.S.], Electricité de France RB 2014-26 (http://www.edf.fr) to M.S., Science Committee of the Ministry of Education and Science of the Republic of Kazakhstan to M.S. (http://www.nu.edu.kz), and by the Fondation de France (http://www.fondationdefrance.org) [#2012 00029161 to A.A.I.]; I.G. was supported by postdoctoral fellowships from the Fondation ARC PDF20101202141 (http://www.recherche-cancer.net).

Appendix A. Supplementary data

Supplementary data associated with this article can be found, in the online version, at http://dx.doi.org/10.1016/j.dnarep.2014.07.010.

References

[1] B. Demple, L. Harrison, Repair of oxidative damage to DNA: enzymology and biology, Annu. Rev. Biochem. 63 (1994) 915–948.
[2] J.M. Daley, C. Zakaria, D. Ramotar, The endonuclease IV family of apurinic/apyrimidinic endonucleases, Mutat. Res. 705 (2010) 217–227.
[3] K. Sakumi, M. Sekiguchi, Structures and functions of DNA glycosylases, Mutat. Res. 236 (1990) 161–172.
[4] G. Barzilay, I.D. Hickson, Structure and function of apurinic/apyrimidinic endonucleases, Bioessays 17 (1995) 713–719.
[5] G. Tell, D. Fantini, F. Quadrifoglio, Understanding different functions of mammalian AP endonuclease (APE1) as a promising tool for cancer treatment, Cell. Mol. Life Sci. 67 (2010) 3589–3608.
[6] J. Willis, Y. Patel, B.L. Lentz, S. Yan, APE2 is required for ATR-Chk1 checkpoint activation in response to oxidative stress, Proc. Natl. Acad. Sci. U.S.A. 110 (2013) 10592–10597.
[7] H. Fung, B. Demple, A vital role for Ape1/Ref1 protein in repairing spontaneous DNA damage in human cells, Mol. Cell 17 (2005) 463–470.
[8] L. Balakrishnan, P.D. Brandt, L.A. Lindsey-Boltz, A. Sancar, R.A. Bambara, Long patch base excision repair proceeds via coordinated stimulation of the multienzyme DNA repair complex, J. Biol. Chem. 284 (2009) 15158–15172.
[9] A.S. Karumbati, R.A. Deshpande, A. Jilani, J.R. Vance, D. Ramotar, T.E. Wilson, The role of yeast DNA 3′-phosphatase Tpp1 and rad1/Rad10 endonuclease in processing spontaneous and induced base lesions, J. Biol. Chem. 278 (2003) 31434–31443.
[10] A.A. Ishchenko, X. Yang, D. Ramotar, M. Saparbaev, The 3′→5′ exonuclease of Apn1 provides an alternative pathway to repair 7,8-dihydro-8-oxodeoxyguanosine in *Saccharomyces cerevisiae*, Mol. Cell. Biol. 25 (2005) 6380–6390.
[11] L. Gros, A.A. Ishchenko, H. Ide, R.H. Elder, M.K. Saparbaev, The major human AP endonuclease (Ape1) is involved in the nucleotide incision repair pathway, Nucl. Acids Res. 32 (2004) 73–81.
[12] A.A. Ischenko, M.K. Saparbaev, Alternative nucleotide incision repair pathway for oxidative DNA damage, Nature 415 (2002) 183–187.
[13] C.D. Mol, T. Izumi, S. Mitra, J.A. Tainer, DNA-bound structures and mutants reveal abasic DNA binding by APE1 and DNA repair coordination [corrected], Nature 403 (2000) 451–456.
[14] L.H. Nguyen, D. Barsky, J.P. Erzberger, D.M.3rd Wilson, Mapping the protein–DNA interface and the metal-binding site of the major human apurinic/apyrimidinic endonuclease, J. Mol. Biol. 298 (2000) 447–459.
[15] L.J. Walker, R.B. Craig, A.L. Harris, I.D. Hickson, A role for the human DNA repair enzyme HAP1 in cellular protection against DNA damaging agents and hypoxic stress, Nucl. Acids Res. 22 (1994) 4884–4889.
[16] H. Fung, B. Demple, Distinct roles of Ape1 protein in the repair of DNA damage induced by ionizing radiation or bleomycin, J. Biol. Chem. 286 (2011) 4968–4977.
[17] S. Xanthoudakis, T. Curran, Identification and characterization of Ref-1, a nuclear protein that facilitates AP-1 DNA-binding activity, EMBO J. 11 (1992) 653–665.
[18] L.J. Walker, C.N. Robson, E. Black, D. Gillespie, I.D. Hickson, Identification of residues in the human DNA repair enzyme HAP1 (Ref-1) that are essential for redox regulation of Jun DNA binding, Mol. Cell. Biol. 13 (1993) 5370–5376.
[19] L. Jayaraman, K.G. Murthy, C. Zhu, T. Curran, S. Xanthoudakis, C. Prives, Identification of redox/repair protein Ref-1 as a potent activator of p53, Genes Dev. 11 (1997) 558–570.
[20] T. Okazaki, U. Chung, T. Nishishita, S. Ebisu, S. Usuda, S. Mishiro, S. Xanthoudakis, T. Igarashi, E. Ogata, A redox factor protein, ref1, is involved in negative gene regulation by extracellular calcium, J. Biol. Chem. 269 (1994) 27855–27862.
[21] S. Fuchs, J. Philippe, P. Corvol, F. Pinet, Implication of Ref-1 in the repression of renin gene transcription by intracellular calcium, J. Hypertens. 21 (2003) 327–335.
[22] K.K. Bhakat, A.K. Mantha, S. Mitra, Transcriptional regulatory functions of mammalian AP-endonuclease (APE1/Ref-1), an essential multifunctional protein, Antioxid. Redox Signal. 11 (2009) 621–638.
[23] S. Sengupta, A.K. Mantha, S. Mitra, K.K. Bhakat, A.P. Human, endonuclease (APE1/Ref-1) and its acetylation regulate YB-1-p300 recruitment and RNA polymerase II loading in the drug-induced activation of multidrug resistance gene MDR1, Oncogene 30 (2011) 482–493.
[24] T. Yamamori, J. DeRicco, A. Naqvi, T.A. Hoffman, I. Mattagajasingh, K. Kasuno, S.B. Jung, C.S. Kim, K. Irani, SIRT1 deacetylates APE1 and regulates cellular base excision repair, Nucl. Acids Res. 38 (2010) 832–845.
[25] E. Huang, D. Qu, Y. Zhang, K. Venderova, M.E. Haque, M.W. Rousseaux, R.S. Slack, J.M. Woulfe, D.S. Park, The role of Cdk5-mediated apurinic/apyrimidinic endonuclease 1 phosphorylation in neuronal death, Nat. Cell. Biol. 12 (2010) 563–571.
[26] C.S. Busso, T. Iwakuma, T. Izumi, Ubiquitination of mammalian AP endonuclease (APE1) regulated by the p53-MDM2 signaling pathway, Oncogene 28 (2009) 1616–1625.
[27] C.S. Busso, C.M. Wedgeworth, T. Izumi, Ubiquitination of human AP-endonuclease 1 (APE1) enhanced by T233E substitution and by CDK5, Nucl. Acids Res. (2011).
[28] M. Luo, J. Zhang, H. He, D. Su, Q. Chen, M.L. Gross, M.R. Kelley, M.M. Georgiadis, Characterization of the redox activity and disulfide bond formation in apurinic/apyrimidinic endonuclease, Biochemistry 51 (2012) 695–705.
[29] S. Azam, N. Jouvet, A. Jilani, R. Vongsamphanh, X. Yang, S. Yang, D. Ramotar, Human glyceraldehyde-3-phosphate dehydrogenase plays a direct role in reactivating oxidized forms of the DNA repair enzyme APE1, J. Biol. Chem. 283 (2008) 30632–30641.
[30] C.D. Mol, D.J. Hosfield, J.A. Tainer, Abasic site recognition by two apurinic/apyrimidinic endonuclease families in DNA base excision repair: the 3′ ends justify the means, Mutat. Res. 460 (2000) 211–229.
[31] A.K. Mantha, N. Oezguen, K.K. Bhakat, T. Izumi, W. Braun, S. Mitra, Unusual role of a cysteine residue in substrate binding and activity of human AP-endonuclease 1, J. Mol. Biol. 379 (2008) 28–37.
[32] Y.J. Kim, D. Kim, J.L. Illuzzi, S. Delaplane, D. Su, M. Bernier, M.L. Gross, M.M. Georgiadis, D.M.3rd Wilson, S-glutathionylation of cysteine 99 in the APE1 protein impairs abasic endonuclease activity, J. Mol. Biol. 414 (2011) 313–326.
[33] C. Vascotto, E. Bisetto, M. Li, L.A. Zeef, C. D'Ambrosio, R. Domenis, M. Comelli, D. Delneri, A. Scaloni, F. Altieri, I. Mavelli, F. Quadrifoglio, M.R. Kelley, G. Tell, Knock-in reconstitution studies reveal an unexpected role of Cys-65 in regulating APE1/Ref-1 subcellular trafficking and function, Mol. Biol. Cell 22 (2011) 3887–3901.
[34] J.M. Ordway, D. Eberhart, T. Curran, Cysteine 64 of Ref-1 is not essential for redox regulation of AP-1 DNA binding, Mol. Cell. Biol. 23 (2003) 4257–4266.
[35] A. Shatilla, A. Leduc, X. Yang, D. Ramotar, Identification of two apurinic/apyrimidinic endonucleases from *Caenorhabditis elegans* by cross-species complementation, DNA Rep. (Amst.) 4 (2005) 655–670.
[36] J.R. Vance, T.E. Wilson, Uncoupling of 3′-phosphatase and 5′-kinase functions in budding yeast. Characterization of *Saccharomyces cerevisiae* DNA 3′-phosphatase (TPP1), J. Biol. Chem. 276 (2001) 15073–15081.
[37] D.M.3rd Wilson, R.A. Bennett, J.C. Marquis, P. Ansari, B. Demple, Trans-complementation by human apurinic endonuclease (Ape) of hypersensitivity to DNA damage and spontaneous mutator phenotype in apn1-yeast, Nucl. Acids Res. 23 (1995) 5027–5033.
[38] A.A. Ishchenko, H. Ide, D. Ramotar, G. Nevinsky, M. Saparbaev, Alpha-anomeric deoxynucleotides, anoxic products of ionizing radiation, are substrates for the endonuclease IV-type AP endonucleases, Biochemistry 43 (2004) 15210–15216.
[39] L. Gros, A.V. Maksimenko, C.V. Privezentzev, J. Laval, M.K. Saparbaev, Hijacking of the human alkyl-*N*-purine-DNA glycosylase by 3,N4-ethenocytosine, a lipid peroxidation-induced DNA adduct, J. Biol. Chem. 279 (2004) 17723–17730.
[40] A.A. Ishchenko, E. Deprez, A. Maksimenko, J.C. Brochon, P. Tauc, M.K. Saparbaev, Uncoupling of the base excision and nucleotide incision repair pathways reveals their respective biological roles, Proc. Natl. Acad. Sci. U.S.A. 103 (2006) 2564–2569.
[41] A. Gelin, M. Redrejo-Rodriguez, J. Laval, O.S. Fedorova, M. Saparbaev, A.A. Ishchenko, Genetic and biochemical characterization of human AP endonuclease 1 mutants deficient in nucleotide incision repair activity, PLoS One 5 (2010) e12241.
[42] Y. Masuda, R.A. Bennett, B. Demple, Rapid dissociation of human apurinic endonuclease (Ape1) from incised DNA induced by magnesium, J. Biol. Chem. 273 (1998) 30360–30365.
[43] Y. Masuda, R.A. Bennett, B. Demple, Dynamics of the interaction of human apurinic endonuclease (Ape1) with its substrate and product, J. Biol. Chem. 273 (1998) 30352–30359.
[44] J.P. Erzberger, D.M.3rd Wilson, The role of Mg^{2+} and specific amino acid residues in the catalytic reaction of the major human abasic endonuclease: new insights from EDTA-resistant incision of acyclic abasic site analogs and site-directed mutagenesis, J. Mol. Biol. 290 (1999) 447–457.
[45] J.A. Lucas, Y. Masuda, R.A. Bennett, N.S. Strauss, P.R. Strauss, Single-turnover analysis of mutant human apurinic/apyrimidinic endonuclease, Biochemistry 38 (1999) 4958–4964.
[46] R.D. Gietz, R.H. Schiestl, A.R. Willems, R.A. Woods, Studies on the transformation of intact yeast cells by the LiAc/SS-DNA/PEG procedure, Yeast 11 (1995) 355–360.
[47] J.M. Daley, T.E. Wilson, D. Ramotar, Genetic interactions between HNT3/Aprataxin and RAD27/FEN1 suggest parallel pathways for 5′ end processing during base excision repair, DNA Rep. (Amst.) 9 (2010) 690–699.
[48] J. Poschmann, S. Drouin, P.E. Jacques, K. El Fadili, M. Newmarch, F. Robert, D. Ramotar, The peptidyl prolyl isomerase Rrd1 regulates the elongation of RNA polymerase II during transcriptional stresses, PLoS One 6 (2011) e23159.
[49] M. Aouida, A. Leduc, R. Poulin, D. Ramotar, AGP2 encodes the major permease for high affinity polyamine import in *Saccharomyces cerevisiae*, J. Biol. Chem. 280 (2005) 24267–24276.
[50] S. Daviet, S. Couve-Privat, L. Gros, K. Shinozuka, H. Ide, M. Saparbaev, A.A. Ishchenko, Major oxidative products of cytosine are substrates for the nucleotide incision repair pathway, DNA Rep. (Amst.) 6 (2007) 8–18.
[51] A.A. Ishchenko, G. Sanz, C.V. Privezentzev, A.V. Maksimenko, M. Saparbaev, Characterisation of new substrate specificities of *Escherichia coli* and *Saccharomyces cerevisiae* AP endonucleases, Nucl. Acids Res. 31 (2003) 6344–6353.
[52] S.E. Tsutakawa, D.S. Shin, C.D. Mol, T. Izumi, A.S. Arvai, A.K. Mantha, B. Szczesny, I.N. Ivanov, D.J. Hosfield, B. Maiti, M.E. Pique, K.A. Frankel, K. Hitomi, R.P. Cunningham, S. Mitra, J.A. Tainer, Conserved structural chemistry for incision activity in structurally non-homologous apurinic/apyrimidinic endonuclease APE1 and endonuclease IV DNA repair enzymes, J. Biol. Chem. 288 (2013) 8445–8455.
[53] N. Guex, A. Diemand, M.C. Peitsch, Protein modelling for all, Trends Biochem. Sci. 24 (1999) 364–367.

[54] G. Macindoe, L. Mavridis, V. Venkatraman, M.D. Devignes, D.W. Ritchie, HexServer: an FFT-based protein docking server powered by graphics processors, Nucl. Acids Res. 38 (2010) W445–W449.
[55] E.S. Henle, S. Linn, Formation, prevention, and repair of DNA damage by iron/hydrogen peroxide, J. Biol. Chem. 272 (1997) 19095–19098.
[56] G. Barzilay, L.J. Walker, C.N. Robson, I.D. Hickson, Site-directed mutagenesis of the human DNA repair enzyme HAP1: identification of residues important for AP endonuclease and RNase H activity, Nucl. Acids Res. 23 (1995) 1544–1550.
[57] C.N. Robson, I.D. Hickson, Isolation of cDNA clones encoding a human apurinic/apyrimidinic endonuclease that corrects DNA repair and mutagenesis defects in E. coli xth (exonuclease III) mutants, Nucl. Acids Res. 19 (1991) 5519–5523.
[58] Y.J. Xu, E.Y. Kim, B. Demple, Excision of C-4′-oxidized deoxyribose lesions from double-stranded DNA by human apurinic/apyrimidinic endonuclease (Ape1 protein) and DNA polymerase beta, J. Biol. Chem. 273 (1998) 28837–28844.
[59] D. Ramotar, H. Wang, Protective mechanisms against the antitumor agent bleomycin: lessons from *Saccharomyces cerevisiae*, Curr. Genet. 43 (2003) 213–224.
[60] A. Shatilla, A.A. Ishchenko, M. Saparbaev, D. Ramotar, Characterization of *Caenorhabditis elegans* exonuclease-3 and evidence that a $Mg^{(2+)}$-dependent variant exhibits a distinct mode of action on damaged DNA, Biochemistry 44 (2005) 12835–12848.
[61] A. Mazouzi, A. Vigouroux, B. Aikeshev, P.J. Brooks, M.K. Saparbaev, S. Morera, A.A. Ishchenko, Insight into mechanisms of 3′-5′ exonuclease activity and removal of bulky 8,5′-cyclopurine adducts by apurinic/apyrimidinic endonucleases, Proc. Natl. Acad. Sci. U.S.A. 110 (2013) E3071–E3080.